

INFLUENCE OF QUENCHING PROCESS ON MUNICIPAL SOLID WASTE INCINERATION BOTTOM ASH CHARACTERIZATION

カナウツト, インカエウ

<https://doi.org/10.15017/1654856>

出版情報：九州大学, 2015, 博士（工学）, 課程博士
バージョン：
権利関係：全文ファイル公表済

**INFLUENCE OF QUENCHING PROCESS ON
MUNICIPAL SOLID WASTE INCINERATION
BOTTOM ASH CHARACTERIZATION**

Kanawut Inkaew

February, 2016

**INFLUENCE OF QUENCHING PROCESS ON MUNICIPAL
SOLID WASTE INCINERATION BOTTOM ASH
CHARACTERIZATION**

A Thesis Submitted
In Partial Fulfillment of the Requirements
For the Degree of
Doctor of Engineering

By
Kanawut Inkaew



to the
DEPARTMENT OF URBAN AND ENVIRONMENTAL ENGINEERING
GRADUATE SCHOOL OF ENGINEERING
KYUSHU UNIVERSITY
Fukuoka, Japan
February, 2016

DEPARTMENT OF URBAN AND ENVIRONMENTAL ENGINEERING
GRADUATE SCHOOL OF ENGINEERING
KYUSHU UNIVERSITY
Fukuoka, Japan

CERTIFICATE

The undersigned hereby certify that they have read and recommended to the Graduate School of Engineering for the acceptance of this thesis entitled, “*Influence of Quenching Process on Municipal Solid Waste Incineration Bottom Ash Characterization*” by **Kanawut Inkaew** in partial fulfillment of the requirements for the degree of **Doctor of Engineering**.

Dated :February, 2016

Thesis Supervisor:

Prof .Takayuki Shimaoka, Dr. Eng.

Examining Committee:

Prof .Takayuki Shimaoka, Dr. Eng.

Prof. Hidenori Hamada, Dr. Eng.

Prof. Koichiro Watanabe, Dr. Sci.

ABSTRACT

The management of municipal solid waste incineration (MSWI) bottom ash is a topic of growing importance in the field of waste management in the world. Since incineration technology has been introduced as a viable alternative for processing municipal solid waste (MSW), the bottom ash as the most significant remained residues requires for a safe and sound handling. Bottom ash is a heterogeneity admixture of multi-component such as slag, glass, ceramic, metal, mineral, or else that remained after combustion. Nature of this material is active in the exposure condition. Thus, it could be considered either as the hazardous material or the raw material depending upon the standpoint of management.

As the active material, bottom ash will be altered under weathering process until it reaches the equilibrium with the exposure condition. Besides, although the utilization of bottom ash can play an important role as a new resource for several purposes such as use in construction or cement production, only few could be used in present situation due to its property that contains some encumbrance substances like heavy metal or chloride. The prominent key that would enable the appropriate management is characterization.

Many efforts have been undertaken in past decades to characterize municipal solid waste incineration bottom ash. However, the investigation in this field still challenges due to the bottom ash from place to place is different, particularly in terms of both composition quantity and quality. In this study, the main focus is paid to the influence of quenching process, and the formation of the quench product on the bottom ash which details are existed in less information. Quenching process could influence the characteristic of the ash directly and this could affect to its management due to the proper ash management should be practiced based on its characterization. Therefore, quenching process is important in the sense of waste management and material recycle.

With the goal to obtain a better understanding the quenching process and the formation of the quench product on the bottom ash, two approaches have been used in this study; 1) the intensive investigation on the representative samples obtained from the incineration plants, and 2) the simulative investigation on lab-scale quenching experiment . Details of research are divided into six chapters.

In Chapter 1, the background of this research as well as objectives and research flow were introduced with the review of literature regarding to MSW generation and

treatment strategy in Japan, incineration technology, ash discharge technology/quenching system, MSWI residue generations, bottom ash characterization, and its disposal strategy.

In Chapter 2, the details of the investigation on physical, chemical and mineralogical characterization of materials involved in quenching system namely grate sifting, unquenched bottom ash and freshly quenched bottom ash were presented. The investigations were implemented utilizing various methods to determine the characteristics of specimen, namely visual observation, analysis of particle size distribution, particle thin section analysis, measurement of pH, moisture content, and loss on ignition, bulk chemical analysis, and mineral composition analysis. Results showed that the pH of all samples was in the range of 11.7-12.7. Approximately 70-80 % of samples consisted of CaO, SiO₂, Al₂O₃, and Fe₂O₃. All samples were also enriched with Zn, Cu, Ba, Pb, and Cr, with concentrations higher than 500 mg/kg. Major minerals found in all samples included calcite, quartz, gehlenite, hematite, plagioclase feldspar and mayenite. However, physical, chemical, and mineral characteristics of the samples were different in details. Grate sifting was slightly similar to the unquenched bottom ash in terms of physical appearance that did not contain the quench product. It was dominant with the characteristic of high concentration of Al and heavy metals. The unquenched bottom ash was dominated by the melt product which contains amorphous glass, minerals and refractory. The mineral that could be found only in the grate sifting and the unquenched bottom ash was lime. In the opposition, the freshly quenched bottom ash was dominant by the existence of the quench product on its surface and the presence of Friedel's salt.

In Chapter 3, the influence of water quenching on the characterization of the bottom ash from two incineration plants (Kamitsu and Nishiyodo) with the different quenching system; drag chain conveyor tank and hydraulic ram discharger were investigated. The observation was based on the comparative study between the unquenched samples and freshly quenched samples. The particle size distribution analysis, thin section analysis, intact particle analysis, specific surface area analysis, pH and bulk chemical composition analysis, and mineralogical analysis were conducted to evaluate the impacts of water quenching on the characterization of bottom ash product. The result showed that water quenching was considerable influence on the bottom ash characterization by changing particle size, increasing specific surface area, changing its morphology by forming the quench product, reducing pH, altering the chemical composition, and enhancing portlandite,

hydrocalumite and Friedel's salt formation.

In Chapter 4, the characterization of the quench product on the bottom ash was performed with the aim of describing this material in terms of microstructure and mineralogy. A variety of microscopic and spectroscopic analyses were carried out in both intact particles, thin section, and bulk particles. In addition, the relationship between the existence of Friedel's salt and the quench product was evaluated. Microstructure characterization revealed that the quench product commonly distributes on the surface of the melt product. The thickness is variable from 10 μm to 1 mm. The quench product mainly exhibits by amorphous and microcrystalline of hydrate phases. Minerals such as quartz and iron-oxide was embedding in the matrix of amorphous hydrate as well as refractory glass, relics, metal, and organic matter. The experimental data showed that the characteristic of the quench product from the simulate quenching experiment was similar to the reference samples that obtained from the large-scale quenching.

In Chapter 5, the quenching experiment were performed with the different scenarios to observe the formation mechanisms of the quench product on the surface of bottom ash. In the experiments, the unquenched bottom ash was heated to 300 °C, immediately quenched by warm water, filtered, and dried. Particle size distribution analysis, intact particle and thin-section observation, X-ray diffractometry, and scanning electron microscope/energy dispersive X-ray spectroscopy were conducted on the freshly quenched bottom ash samples. The results indicated that after quenching, the morphology and mineralogy of the bottom ash changed significantly. The freshly quenched bottom ash was dominated by a quench product that was characterized by amorphous and microcrystalline calcium-silicate-hydrate phases which bounded as a layer. The layer also enclosed tiny minerals, glasses, ceramics, metals, and organic materials as unburned residues. The dominant mineral phases produced by quenching process and detected by XRD were calcite, Friedel's salt, hydrocalumite and portlandite. The formation of quench product on the surface of the bottom ash was controlled by moisture/quenching water, fine fraction of the ash with a diameter less than 0.425 mm, and physiochemical changes during discharging. It was also found that the formation of the quench product may be defined into two steps; 1) chemical alteration of the particles with a diameter less than 0.425 mm to be the quench product during quenching, and 2) the attachment of the quench product on to the surface of the melt product which perceived as the core particle. From the

observations, a conceptual model of the ash-water reactions and formation of the quench product in the bottom ash was proposed.

In Chapter 6, the key finding of the research was summarized. The main conclusion was that water quenching influenced the characteristics of the bottom ash drastically, particularly enhancing the formation of the quench product on the surface of the bottom ash. The existence of the quench product provided the additional active surface to the bottom ash and also enhanced the formation of the Friedel's salt which is a drawback in both environment and engineering point of view. Since the formation of the quench product is controlled by the ash particle smaller than 0.425 mm, the results suggest that separation of this fraction prior to quenching would help to prevent the formation of the quench product and Friedel's salt in the bottom ash. The separation might be applied in both grate sifting and the grate ash which would enable for materials recovery and effectively management.

ACKNOWLEDGEMENTS

The successful of this dissertation would not be accomplished without supporting from all those who has contributed to me during study in the international special course on Environmental Systems Engineering, Graduate School of Engineering, Kyushu University, I am greatly indebted. Here, I would like to take this opportunity to express my heartfelt gratitude to all those contributors.

First and foremost, I would like to sincere thank Professor Takayuki Shimaoka for his supervision and professional instruction during my study. The extend gratitude is also due to Professor Hidenori Hamada and Professor Koichiro Watanabe, the examiner of this thesis, who spent precious time on reviewing and gave me a lot of valuable comments and suggestions.

I wish to thanks Dr. Amirhomayoun Saffarzadeh who gave me technical suggestions and constructive guidances during the investigation, Dr. Yoshihiro Hayata, Dr. Munchara Fujikawa, Dr. Yoshitada Kakuta and Dr. Takashi Kawano for useful comments and discussions, Dr. Teppei Komiya for his obligingly assistances during sampling at the incineration facilities, Ms. Shoko Arizono and Ms. Setsuko Shigemasu for the kindly mutual and administrative supports during study, Ms. Mu Yue and Miss Kyoko Kimura for documents translation, Mr. Fumihiro Kashima for data searching, Dr. Shue Yang, Ms. Reika Sou, Mr. Yuya Ogusu and Mr. Yuki Kajino for laboratory supports.

I am deeply grateful to Associate Professor Hirofumi Nakayama, who inspired me to study at the Laboratory of Environmental System Analysis and Control Engineering (Shimaoka Lab.), Department of Urban and Environmental Engineering, Kyushu University. Additionally, I would also extend my gratitude to Associate Professor Mami Shinozaki for her encouragement in both studying and daily life. Thanks should also mention to staffs of the Research Institute of East Asia Environment (RIEAE), and my colleagues at Shimaoka Lab. for their mutual support during the past three years.

It should be noted here that the research samples used in this study were provided by Takuma CO.LTD. All permissions and supports from the company at the sampling sites are appreciated. Besides, special acknowledgement is regard to Rajamangala University of Technology Phra Nakorn Scholarship Foundation, Thailand, for granting all tuition fee and living expenses throughout my doctoral course.

Finally, I would like to thank my younger brother, Khomkrich Inkaew, for graphical assistance, my parents, Kaung and Wannee Inkaew, for their unwavering support and encouragement throughout my life.

TABLE OF CONTENTS

CERTIFICATE	ii
ABSTRACT	iii
ACKNOWLEDGEMENTS	vii
TABLE OF CONTENTS	ix
LIST OF FIGURES.....	xiv
LIST OF TABLES	xviii

CHAPTER 1 INTRODUCTION

1.1 BACKGROUND.....	2
1.1.1 MUNICIPAL SOLID WASTE AND TREATMENT STRATEGY IN JAPAN	2
1.1.2 INCINERATION TECHNOLOGY FOR MUNICIPAL SOLID WASTE TREATMENT	4
1.1.3 MSWI RESIDUES AND BOTTOM ASH GENERATION	7
1.1.4 ASH DISCHARGER AND QUENCHING TECHNOLOGY	9
1.1.5 BOTTOM ASH CHARACTERIZATION IN ENVIRONMENTAL ENGINEERING FIELD	12
1.1.5.1 BOTTOM ASH CHARACTERIZATION	12
1.1.5.2 FACTOR CONTROLLING THE CHARACTERISTIC OF BOTTOM ASH	14
1.1.5.3 BOTTOM ASH COMPOSITION AND CLASSIFICATION	15
1.1.5.4 BOTTOM ASH CHEMICAL CHARACTERISTIC.....	17
1.1.5.5 BOTTOM ASH MINERAL CHARACTERISTIC	19
1.1.5.6 CHLORIDE AND FRIEDEL'S SALT IN BOTTOM ASH	20
1.1.6 ALTERATION OF BOTTOM ASH UNDER WEATHERING AND ITS ENVIRONMENTAL CONCERNS	21

1.1.7 BOTTOM ASH DISPOSAL STRATEGY.....	22
1.2 RESEARCH OBJECTIVES.....	23
1.3 SIGNIFICANCE OF THIS STUDY.....	23
1.4 RESEARCH FLOW AND THESIS STRUCTURE.....	24
REFERENCES.....	26
CHAPTER 2 PHYSICAL, CHEMICAL AND MINERALOGICAL CHARACTERISTICS OF MSWI BOTTOM ASH	
2.1 ABSTRACT.....	32
2.2 INTRODUCTION.....	32
2.3 MATERIALS AND METHODS.....	34
2.3.1 PLANT DESCRIPTION.....	34
2.3.2 SAMPLING.....	34
2.3.3 ANALYSIS.....	35
2.4 RESULTS AND DISCUSSION.....	36
2.4.1 GRATE SIFTINGS.....	36
2.4.1.1 PHYSICAL CHARACTERISTICS.....	36
2.4.1.2 CHEMICAL CHARACTERISTICS.....	39
2.4.1.3 MINERALOGICAL CHARACTERISTICS.....	41
2.4.2 UNQUENCHED BOTTOM ASH.....	42
2.4.2.1 PHYSICAL CHARACTERISTICS.....	42
2.4.2.2 CHEMICAL CHARACTERISTICS.....	44
2.4.2.3 MINERALOGICAL CHARACTERISTICS.....	46
2.4.3 QUENCHED BOTTOM ASH.....	47
2.4.3.1 PHYSICAL CHARACTERISTICS.....	47
2.4.3.2 CHEMICAL CHARACTERISTICS.....	50
2.4.3.3 MINERALOGICAL CHARACTERISTICS.....	51
2.5 FINDING SYNTHESIS AND DISCUSSION.....	52

2.6 CONCLUSIONS	55
REFERENCES.....	56
CHAPTER 3 INFLUENCE OF WATER QUENCHING ON THE MSWI BOTTOM ASH CHARACTERIZATION	
3.1 ABSTRACT	60
3.2 INTRODUCTION	60
3.3 MATERIALS AND METHODS	62
3.3.1 PLANT DESCRIPTION.....	62
3.3.2 SAMPLING	62
3.3.3 ANALYTICAL METHODS	63
3.4 RESULTS	63
3.4.1 CHARACTERIZATION OF SAMPLES.....	63
3.4.1.1 MSWI BOTTOM ASH.....	63
3.4.1.2 QUENCHING WATER.....	64
3.4.2 IMPACT OF WATER QUENCHING PROCESS ON MSWI BOTTOM ASH.....	65
3.4.2.1 PARTICLE SIZE DISTRIBUTION	65
3.4.2.2 BOTTOM ASH SURFACE MORPHOLOGY.....	67
3.4.2.3 SPECIFIC SURFACE AREA.....	69
3.4.2.4 MINERALOGICAL COMPOSITION	70
3.4.2.5 BOTTOM ASH pH.....	72
3.4.2.6 CHLORINE DISTRIBUTION.....	73
3.5 GENERAL DISCUSSION	75
3.6 CONCLUSIONS	77
REFERENCES.....	78

CHAPTER 4 MICROSTRUCTURE AND MINERALOGICAL CHARACTERIZATION
OF THE QUENCH PRODUCTS ON MSWI BOTTOM ASH

4.1 ABSTRACT	81
4.2 INTRODUCTION	81
4.3 MATERIALS AND METHODS	83
4.3.1 SAMPLING	83
4.3.2 INVESTIGATION AND ANALYTICAL METHODS	83
4.4 RESULTS AND DISCUSSION.....	84
4.4.1 THE EXISTENCE AND APPEARANCE OF THE QUENCH PRODUCT.....	84
4.4.2 MICROSTRUCTURE OF THE QUENCH PRODUCT	86
4.4.3 HYDRATE PHASE IN THE QUENCH PRODUCT	88
4.4.4 DISTRIBUTION OF THE QUENCH PRODUCT ON BOTTOM ASH SURFACE	89
4.4.5 ORIGIN OF THE QUENCH PRODUCT	91
4.4.6 SUSPENDED SOLID ANALYSIS AND ITS ROLE ON THE QUENCH PRODUCT FORMATION	93
4.4.7 DISTRIBUTION OF CHLORINE AND OTHER ELEMENTS ON THE QUENCH PRODUCT	94
4.4.8 MINERAL COMPOSITION ON THE BOTTOM ASH WITH REGARD TO PARTICLE SIZE DISTRIBUTION	96
4.4.9 FORMATION OF FRIEDEL'S SALT IN THE FRESHLY QUENCHED BOTTOM ASH	97
4.5 CONCLUSIONS	98
REFERENCES.....	99

CHAPTER 5 MODELING THE FORMATION MECHANISM OF
THE QUENCH PRODUCT ON THE SURFACE OF MSWI BOTTOM ASH

5.1 ABSTRACT	102
5.2 INTRODUCTION	102
5.3 MATERIALS AND METHODS	104
5.3.1 MATERIALS.....	104
5.3.2 EXPERIMENTS	105
5.3.3 ANALYTICAL METHODOLOGIES AND APPARATUS	105
5.4 RESULTS	107
5.4.1 CHARACTERIZATION OF BOTTOM ASH BEFORE QUENCHING	107
5.4.2 CHARACTERIZATION OF QUENCHING WATER.....	111
5.4.3 ALTERATION OF BOTTOM ASH DURING QUENCHING	112
5.4.4 CHARACTERIZATION OF THE QUENCHED BOTTOM ASH	115
5.4.4.1 MORPHOLOGY.....	115
5.4.4.2 MINERAL COMPOSITION	118
5.4.5 FACTOR CONTROLLING THE FORMATION OF THE QUENCH PRODUCT.....	121
5.4.6 PROPOSED MODEL FOR FORMATION MECHANISM OF THE QUENCH PRODUCT ON BOTTOM ASH	124
5.5 CONCLUSIONS	125
REFERENCES.....	127
CHAPTER 6 CONCLUSIONS	
6.1 CONCLUSIONS	131
6.2 OUTLOOK AND RECOMMENDATION.....	133
REFERENCES.....	135

LIST OF FIGURES

Figure	Caption	Page No.
Figure 1.1	The amounts of waste generated in Japan during 1995 to 2013	5
Figure 1.2	Vision of a sound material-cycle-society in the Basic Act for Establishing a Sound Material-Cycle Society (Basic Framework Act) that was enacted in 2000	5
Figure 1.3	Generic mass-burn incineration plant with energy recovery system	6
Figure 1.4	Schematic of Martin dry discharger system operated without water.....	10
Figure 1.5	Schematic of KEZO semi-dry discharger system operated with spray water	10
Figure 1.6	Schematic of quenching tank equipped with a drag-chain conveyer discharger	11
Figure 1.7	Schematic of hydraulic ram (Martin) wet discharger	11
Figure 1.8	The dissertation structure that divided into six chapters.....	25
Figure 2.1	A schematic overview of a typical mass burn waste-to-energy plant, showing the four material sampling locations	35
Figure 2.2	Physical appearance of grate siftings	37
Figure 2.3	Particle size distributions of grate siftings	38
Figure 2.4	Grate siftings with particles larger than 4.75 mm obtained after sieving by mesh	38
Figure 2.5	Morphological characteristic of the grate siftings' thin sections under plane polarized light mode of petrographic light microscope.....	39
Figure 2.6	Total heavy metals concentrations in grate siftings.....	41
Figure 2.7	X-ray diffraction data of grate siftings	42
Figure 2.8	Physical appearance of unquenched bottom ash.....	43
Figure 2.9	Particle size distribution of the unquenched bottom ash	43

Figure 2.10	The thin section of unquenched bottom ash particles under plane polarized light mode of petrographic microscope.....	44
Figure 2.11	Heavy metals concentration in the unquenched bottom ash.....	46
Figure 2.12	X-ray diffraction data of unquenched bottom ash.....	46
Figure 2.13	Physical appearance of the quenched bottom ash.....	48
Figure 2.14	Particle size distribution of the quenched bottom ash	48
Figure 2.15	The thin-cross section of quenched bottom ash particles under plane polarized light mode of petrographic microscope	49
Figure 2.16	Heavy metals content in the bottom ash.	51
Figure 2.17	X-ray diffraction data of quenched bottom ash.....	52
Figure 3.1	The cumulative particle size distribution of samples.....	66
Figure 3.2	Unquenched bottom ash and quenched bottom ash morphology under different microscopic observation	68
Figure 3.3	Hydrate phase microcrystals at the surface of quenched bottom ash which represent the alteration of bottom ash as a function of water-quenching	69
Figure 3.4	X-ray diffractogram of bulk samples	71
Figure 3.5	The pH value of unquenched bottom ash and water quenched bottom ash.....	72
Figure 3.6	Photomicrograph of a bottom ash particle showing the designated points of EDX analyses and the distribution of hydrate microcrystals on the quenched product	74
Figure 4.1	The quenched bottom ash under scanning electron microscope shows a rough texture containing the quench product at the outer surface.....	85
Figure 4.2	The photomicrograph of the cross-thin section of the quenched bottom ash showing the precipitated quench product at the concave of the melt glass particle	86

Figure 4.3	Photomicrograph of the quench products with heterogeneous admixture of various materials.....	87
Figure 4.4	Morphologies of hydrate phases observed under petrographic thin section	89
Figure 4.5	Distribution pattern of the quench product	90
Figure 4.6	Photomicrograph of the fine fraction of ash samples a) unquenched bottom ash and b) quenched bottom ash.....	91
Figure 4.7	The newly-formed microcrystalline of C-S-H phases on the surface layer of the quenched bottom ash.....	92
Figure 4.8	X-ray diffraction data with SEM photomicrograph of suspended solid obtained from quenching tank	93
Figure 4.9	Distribution of elements in freshly quenched MSWI bottom ash particle.....	95
Figure 4.10	The diffraction data of mineral in the MSWI bottom ash with different size fractions ranging from less 0.075 mm to 4.75 mm.....	96
Figure 5.1	Schematic diagram of the experimental quenching setup.....	106
Figure 5.2	Particle size distribution of unquenched bottom ash before quenching.....	108
Figure 5.3	Interaction between bottom ash and water during quenching experiment.....	112
Figure 5.4	Accumulation of calcite scum on the side-wall of the quenching tank in the real incineration facility	114
Figure 5.5	Photomicrographs of quenched bottom ash with different quenching scenarios.....	116
Figure 5.6.	The quench product with heterogeneous admixture under different light modes	117
Figure 5.7	X-ray diffraction data of sample after quenching experiment compared to unquenched bottom ash and reference freshly quenched bottom ash from the same incineration plant.....	119

Figure 5.8	X-ray diffraction data of samples after quenching with different liquid/solid ratio.....	120
Figure 5.9	X-ray diffraction data of samples after quenching with different residence time	120
Figure 5.10	Percentage weight of bottom ash particles retained on sieve before and after quenching comparing between 2 drying method.....	122
Figure 5.11	X-ray diffractogram of bottom ash particles with diameter smaller than 0.425 mm comparing before and after quenching.....	123
Figure 5.12	Backscattered electron images show Ca-rich dendritic hydrate phases that precipitated near a) the vicinity of the melt product and b) an aluminum relic.....	123
Figure 5.13	A schematic conceptual model describing various stages in the formation of the quench products in bottom ash particles.....	125

LIST OF TABLES

Tables	Title	Page No.
Table 1.1	Generation points and percent portions of MSWI residues	8
Table 1.2	The terminology used for MSWI residues recommended by the international ash working group	8
Table 1.3	Examples of characterization method of bottom ash.....	13
Table 1.4	Ranges of total content of elements in MSWI residues.....	18
Table 2.1	Chemical compositions, LOI, moisture contents and pH of grate siftings.....	40
Table 2.2	Chemical compositions, LOI, moisture contents and pH of unquenched bottom ash.....	45
Table 2.3	Chemical compositions, LOI, moisture contents and pH of quenched bottom ash.....	50
Table 3.1	The major and minor constituents in bulk samples measured by XRF.....	64
Table 3.2	The concentration of cation and anion in liquid samples	65
Table 3.3	Specific surface area and pore size of representative samples	70
Table 3.4	Chemical compositions of the designated in Figure 3.6 measured by SEM/EDX.....	75
Table 4.1	Chemical composition of the points designated on the quench product	88
Table 5.1	Experimental condition and treatment	106
Table 5.2	Chemical composition of the unquenched bottom ash determined by XRF.....	109
Table 5.3	Mineral composition in the unquenched bottom ash identified by XRD	110
Table 5.4	Basic characteristic of liquid samples used in this study.....	111

CHAPTER 1
INTRODUCTION

CHAPTER 1

INTRODUCTION

1.1 BACKGROUND

Incineration is one of the effective technologies for municipal solid waste (MSW) management that applied dominantly in many industrialized countries included Japan. This technology provides considerable advantages that could be a benefit society in both social, environmental and economic aspect. One of the interesting features is that municipal solid waste incineration (MSWI) bottom ash, the main byproduct generated after thermal treatment by incineration, could be either the hazardous material that needs to paid attention in disposal or the resource that could be recycled or be utilized in many options. According to the information obtained from literature reviews, bottom ash is the heterogeneous material contained chemical elements and minerals that remain active. If the bottom ash is exposed to the environment, the subsequent alteration will occur under weathering process. The changing behavior of bottom ash basically concerns to the original characteristic of the ash itself as well as the exposure condition. Therefore, knowing about bottom ash characterization is essential for appropriate handling strategy selection. As most of the incineration plant used quenching system to discharge the bottom ash to date, this study attempts to describe the influence of quenching process on bottom ash characterization. Following this chapter is the inside literature of MSW treatment strategy by incineration, MSWI residues generation, robust ash discharge technology, bottom ash characterization, and ash handling strategy options. At the end of chapter, research objective and thesis structure are also presented.

1.1.1 MUNICIPAL SOLID WASTE AND TREATMENT STRATEGY IN JAPAN

Municipal solid waste (MSW), or commonly known as rubbish, trash or garbage, consists of everyday items that were used and thrown away from residential, commercial, or institutional segment. The composition of MSW may vary from place to place and times to times depending on culture, consumption behavior, economics and regulation of

each country (Diaz et al., 2005). However, generally it may contain product packaging, grass, clippings, furniture, clothing, bottles, food scraps, newspaper, appliances, paint and batteries (US EPA, 2013).

In the present year, immerging of MSW crisis has been recognized worldwide. As of 2012, it was estimated that approximately 1.4 billion tons of MSW generated each year, and this volume will be increased to 2.4 billion tons by 2025 (Hoornweg and Bhada-Tata, 2012). Increasing of MSW generation requires an effective management strategy because the failure of MSW management incurs a severe penalty at a later time in the form of resources needlessly lost and a staggering adverse impact on the environment and on public health and safety (Diaz et al., 2005). In addition, MSW management via collection, treatment, and final disposal is also varied throughout the world, from no organized collection at all to systematic classification and advanced system handling. Therefore, MSW management becomes more and more important activity in society. It is a great challenge for each country to develop a system that could manage MSW effectively in both social, environmental and economic aspect.

In Japan, as other industrialized countries, economic development led to the large amount of MSW generation. According to the statistical data by Ministry of the Environment (2015), approximately 44.9 million tons of MSW was generated in the fiscal year of 2013. This amount is equivalent to the generation of waste 958 g per capita per day. By comparison the previous data since 1955 as shown in Figure 1.1, the amount of MSW in Japan continued to increase over time until around 2000. After that, there is a slightly decrease trend from 53.7 million tons per annum to current generation rate. This decreasing is regarding to the effectiveness of waste management policy (Ministry of the Environment, 2013).

Although the current stage of MSW generation in Japan trends to decrease, a large portion of annual generation still requires treatment. Based on the experience, to cope with MSW problem, Japanese government has enacted, revised laws and worked in cooperation with all involved sectors, including local government, private company and household to promote the proper waste management, the effective use of resources as well as the steady development of a sound material-cycle society (Ministry of the Environment, 2014). Since 1990s, the basic measures taken to control waste management in Japan are included: 1) pollution prevention, 2) reuse and recycling, and 3) waste incineration with pollution control (Ministry of the Environment, 2014; Sakai, 1996). This measurement led to the implication

of a sound-material-cycle society, the intensive MSW separation system and MSWI facility along with landfill overall country. The vision of a sound material-cycle society is presented as [Figure 1.2](#). Regardless to the material recycling scheme, the incineration process has been considered the main treatment system for burnable MSW, while landfill is the final disposal for settling incineration residues ([Ministry of the Environment, 2014](#); [Tanaka et al., 2005](#)). As the most prevalent means of waste disposal, about 75 % of MSW in Japan is being treated by incineration ([Mahajan, 2015](#)).

1.1.2 INCINERATION TECHNOLOGY FOR MUNICIPAL SOLID WASTE TREATMENT

As a result of increasing concern about environment and difficulties in constructing a new landfill, achieving a reduction in quantity of waste to be land filled become a priority goal in Japan waste management for both national and local government ([Tanaka et al., 2005](#)). Incineration, the waste treatment process that destroys combustible material by burning, were applied as the principal method for MSW disposal in Japan due to its capacity to reduce a large volume of waste that preferential for final disposal at the landfill site ([Ministry of the Environment, 2014](#); [Sakai, 1996](#); [Tanaka et al., 2005](#)). Incineration process does not completely eliminate the waste but reduce it volume and mass by oxidation reaction. By incineration, the mass and the volume of original waste could be reduced by up to 70 % and 90 % respectively, depending on composition and the degree of material's recovery before being combusted ([Chandler et al., 1997](#); [Lam et al., 2010](#)). Besides, this method also offers attractive several advantages included: 1) reduce the cost of waste transportation, 2) air pollutions from the incineration could be controlled to the level of emission regulation, 3) heat from incineration could be used to generate electricity ([Bayuseno and Schmahl, 2010](#)). Currently, there are 1,172 incinerators operated in Japan. Among this number, 778 plants use residual heat, and 328 facilities are adopted to generated electricity ([Ministry of the Environment, 2013](#)).

There are a number of types of the incinerator for MSW management including, stoker furnace, fluidized bed furnace, rotary kiln furnace, gasification fusion resource furnace, combustion chamber, and multi-hearth furnace. Details of these incinerators are described by many authors ([Chandler et al., 1997](#); [Chang and Wey, 2006](#); [Diaz et al., 2005](#)).

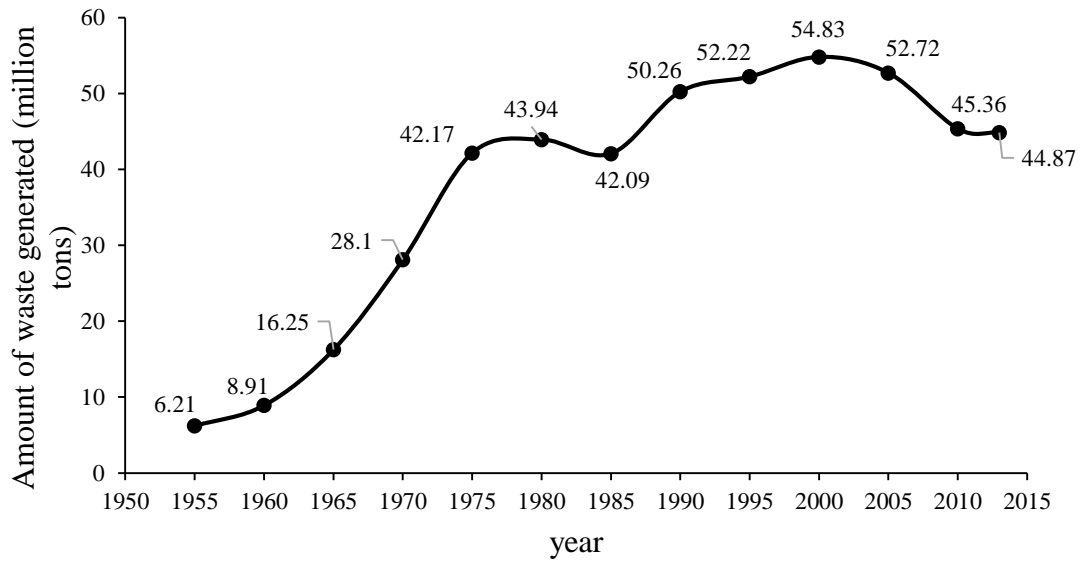


Figure 1.1 The amounts of waste generated in Japan during 1995 to 2013 (adopted from Ministry of the Environment, 2015, 2014).

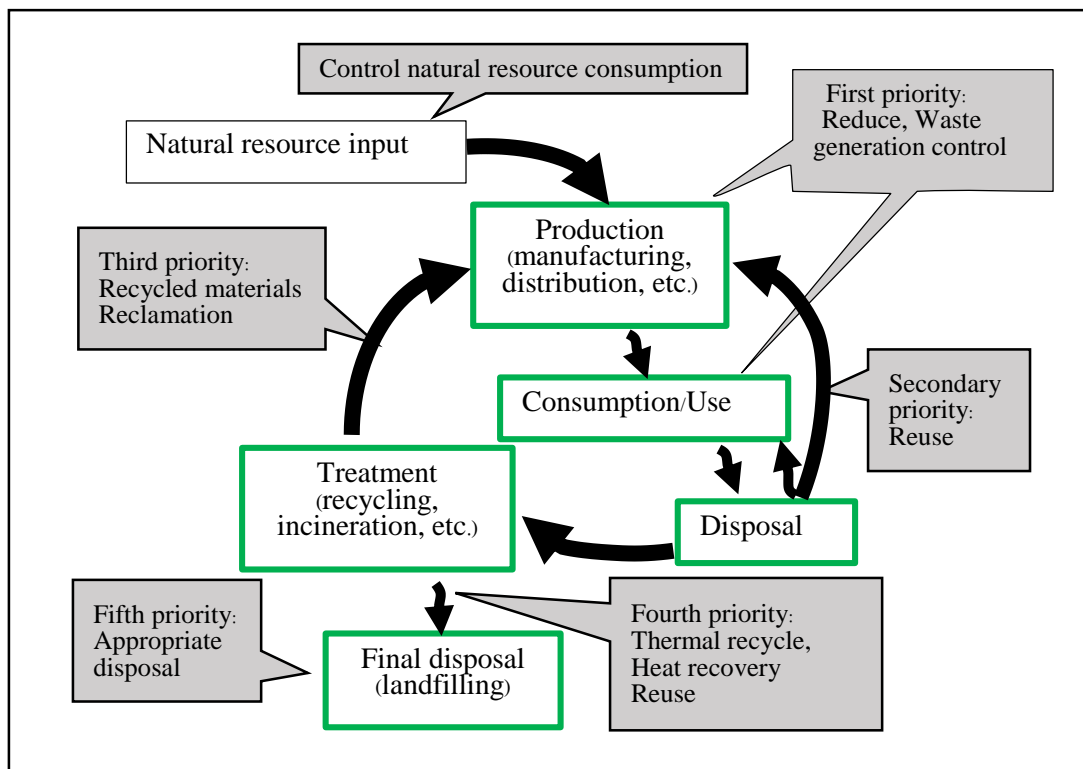
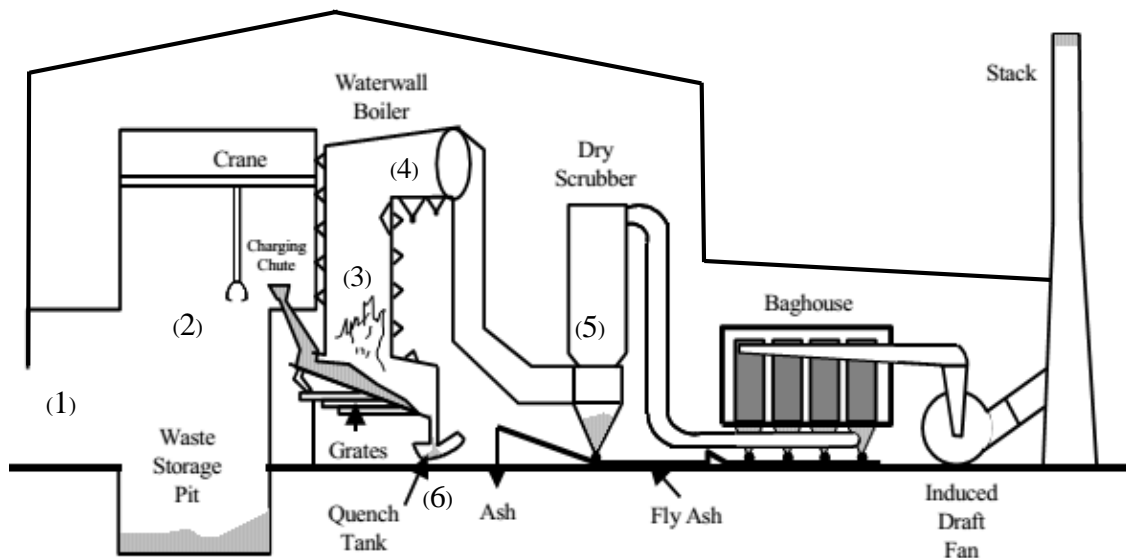


Figure 1.2 Vision of a sound material-cycle-society in the Basic Act for Establishing a Sound Material-Cycle Society (Basic Framework Act) that was enacted in 2000 (adopted from Ministry of the Environment, 2014).

However, in Japan, stoker furnaces, fluidized bed furnace, and gasification fusion resource furnaces were used, of which the most common technology is the mass-burn stoker which is also known as a grate system (Ministry of the Environment, 2012; Sabbas et al., 2003).

Figure 1.3 shows schematic diagram of typical mass-burn incineration plant, which incorporate the following operational sections: 1) a waste receiving and storage area, 2) a processing to prepare waste and waste feeding system, 3) a combustion system, 4) a boiler to convert the heat of combustion to useable energy, 5) an air-pollution control system, and 6) a residues (ash) handling system. In operation, the mass-burn stoker furnace equipped with a three-step movable grate system (involving pre-combustion, combustion and post-combustion section grate). The temperature in the combustion chamber was controlled at 850-1,100 °C to complete the combustion (Chandler et al., 1997; Chang and Wey, 2006).



- | | |
|---------------------------------------|---|
| 1) a waste receiving and storage area | 2) a processing to prepare waste and waste feeding system |
| 3) a combustion system, | 4) a boiler to convert the heat of combustion to useable energy |
| 5) an air-pollution control system | 6) a residues (ash) handling system |

Figure 1.3 Generic mass-burn incineration plant with energy recovery system (adopted from Diaz et al., 2005).

1.1.3 MSWI RESIDUES AND BOTTOM ASH GENERATION

Municipal solid waste incineration (MSWI) is a viable management strategy for treating burnable MSW that cannot be recycled. During incineration, organic material is oxidized. The volume of materials is reduced while exothermic energy could be recovered (Eighmy et al., 1994). Although the incineration process can reduce a large volume of waste as above mention, a significant amount of combustion residues still remains in various forms. The less-volatile inorganic substances persist in the ash on the grate, while the more volatile inorganic substances are in flue dust and also captured in the air pollution control system.

Since incineration facility combines several process sections as described in previous section, each part of the system has a unique function and generates a different kind of residual steam. Typical residues of MSWI by grate combustion are bottom ash (BA) or grate ash, grate sifting, boiler and economizer ash, fly ash (FA) and air-pollution control (APC) residues as shown in Table 1.1. These residues are produced by the different temperature regimes which led to the diverse characteristics on the residues collected from the various individual generation points within MSWI facility (Chandler et al., 1997; Sabbas et al., 2003; Sawell et al., 1995).

From Table 1.1, the bottom ash consists primarily of coarser non-combustible and unburned organic matter collected at the outlet of the combustion chamber. If the wet discharger (quenching/cooling tank) is used, the bottom ash could be collected at the exit end of quenching tank. Bottom ash is the most significant residue generated, which account for up to 20-30 % by mass of the original waste on a wet basis. Grate siftings is included relatively fine materials passing through the grate and collected at the bottom of the combustion chamber (Sabbas et al., 2003). In practice, grate siftings are usually combined with bottom ash in the ash discharger. Boiler and economizer ash represent the coarse fraction of the particulate carried over by flue gases from the combustion chamber and collected at the heat recovery section. This stream may constitute up to 10 % by mass of the original waste on a wet basis (Sabbas et al., 2003). Fly ash is the fine particulate matter in the flue gases downstream of the heat recovery units. It is removed before any further treatment of the gaseous effluents. Air pollution control residues refers to the particulate material captured after reagent injection in the acid gas treatment units prior to emission

gases discharged into the atmosphere. These residues may be in a solid, liquid or sludge form, depending on whether dry, semi-dry or wet processes are adopted for air pollution control over the facility.

To avoid any potential confusion, the international ash working group (Sawell et al., 1995) recommended the terminology used for these different ash streams based on the specific area from which the residue is collected as shown in Table 1.2.

Table 1.1 Generation points and percent portions of MSWI residues.

MSWI residues	Generation point	Percent portion
Bottom ash/ grate ash	Grate in the combustion chamber	20-30%**
Grate siftings	Bottom of the combustion chamber	1-3%*
Boiler and economizer ash	Boiler and economizer	10%**
Fly ash	Combustion chamber	1-3%**
Air-pollution control residues/ Scrubber residues	Air-pollution control system	2-5%**

Remark; *(Chimenos et al., 1999), ** (Sabbas et al., 2003)

Table 1.2 The terminology used for MSWI residues recommended by the international ash working group (Sawell et al., 1995).

Term	Definition
Grate ash	is the ash collected from the grate
Grate siftings	is the material collected from the hoppers underneath the grate
Bottom ash	is the material combined grate ash and grate siftings, and sometimes heat recovery ash
Heat recovery ash	is the ash collected from the boiler, economizer and super heater
Fly ash	is a raw particulate matter entrained in the flue gas stream prior to the addition of scrubbing reagents
Air pollution control residue	is all particulate material captured downstream of any reagent injection and prior to discharge of gases to the stack

In this study, due to the main focus is about the influence of quenching process on bottom ash characterization, the term “unquenched bottom ash” is used instead of grate ash in order to depict the characteristic of the materials. Additionally, the term “quenched bottom ash” is also used to represent the bottom ash that was generated by the wet discharger which will be discussed in the following section.

1.1.4 ASH DISCHARGER AND QUENCHING TECHNOLOGY

At the end of the combustion chamber, the ash is transferred to the ash discharge system. This system serves to cool down the hot ash that was already burnt, and it is a major design difference between various facilities regardless of the combustion system (Chandler et al., 1997). Since this system processes the bottom ash after combustion, it plays a vital role in the characteristic of the discharged ash. Currently, there are two major types of the ash discharge system; dry or wet system. The dry discharge system is a new technology, operate without water (Figure 1.4) or a little water as a semi-dry system (Figure 1.5). Whereas, the wet system is combined the water reservoir to help cooling down the hot ash, this system is the dominant technology used world-wide as well as in Japan (Bourtsalas, 2013). The wet system sometimes refers as quenching tank. There are three optional designs available namely drag-chain conveyer, plate conveyor, and hydraulic ram. In case of Japan, the drag-chain conveyer (Figure 1.6) and the hydraulic ram discharger (Figure 1.7) are popular. The drag-chain conveyor consists of a series of scrapers attached to a chain. This scarpers covers the width of the quench tank and move along the floor of the tank before riding up a slope to the discharge point. The hot ash transfers to the tank settle to the bottom ash and the scraper move it as it passes through the tank (Chandler et al., 1997). In the hydraulic ram, the unit connected to the discharge of the furnace by vertical inlet chute that is partially filled with water, consists of a curved bottom plate and inclined discharge chute. The ram inside the discharger continuously reciprocates along the bottom plate pushing the ash out of the discharger. The ash is compressed through the discharge chute, facilitating de-watering and reducing the size of any large compressible materials (Chandler et al., 1997).

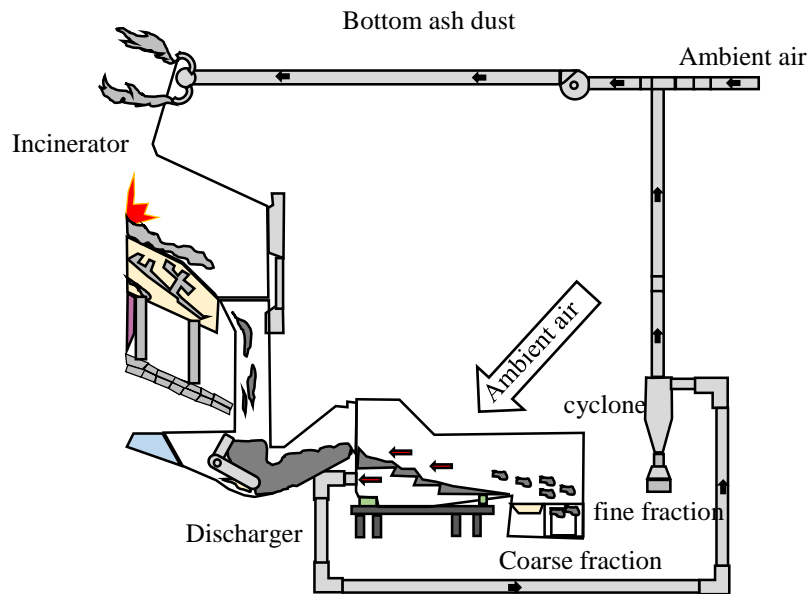


Figure 1.4 Schematic of Martin dry discharger system operated without water (adopted from Bourtsalas, 2013).

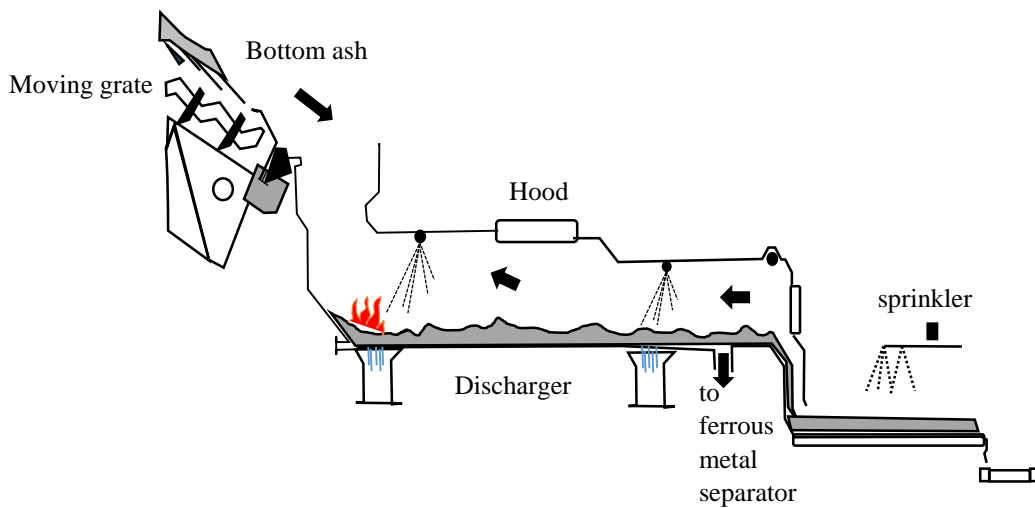


Figure 1.5 Schematic of KEZO semi-dry discharger system operated with spray water (adopted from Bourtsalas, 2013).

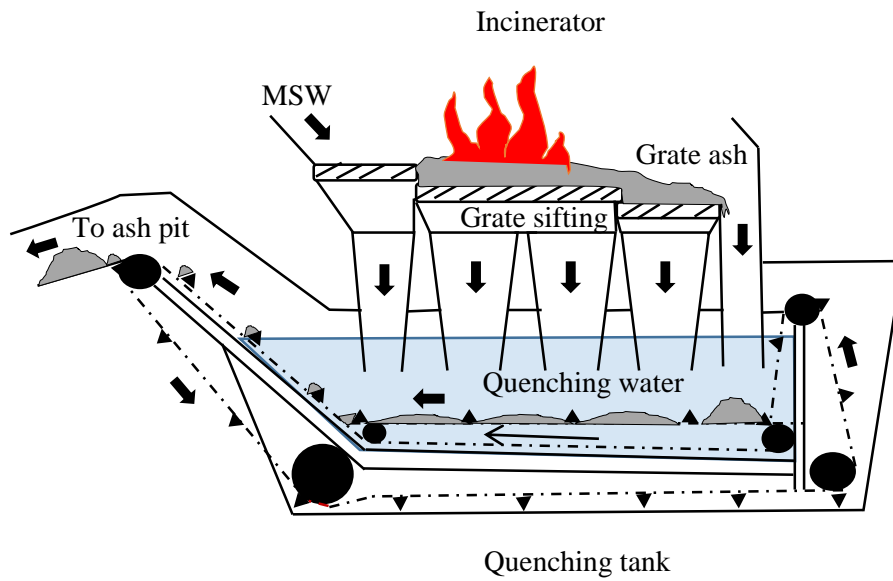


Figure 1.6 Schematic of quenching tank equipped with a drag-chain conveyer discharger (wet system, adopted from [Chandler et al., 1997](#)).

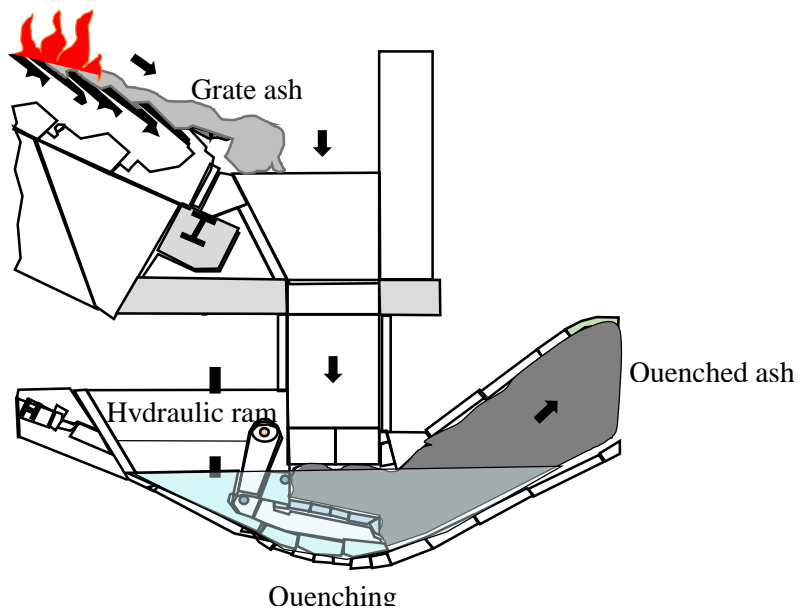


Figure 1.7 Schematic of hydraulic ram (Martin) wet discharger (adopted from [Bourtsalas, 2013](#)).

The types of the discharge system can influence the moisture of the outcome bottom ash. The moisture content of the bottom ash discharged from the drag-chain conveyor could remain up to 50 %, while it is about 20-25 % in case of the hydraulic ram type. Besides, the discharger which is a part of operation can also influence the residual carbon content and loss on ignition (LOI) of bottom ash (Bourtsalas, 2013; Chandler et al., 1997; Lam et al., 2010). However, details of the impact of discharge technology on MSWI bottom ash characteristics retain less information and call for further investigation.

1.1.5 BOTTOM ASH CHARACTERIZATION IN ENVIRONMENTAL ENGINEERING FIELD

In the environmental engineering field, bottom ash characterization is very crucial in the view of hazardous control and utilization. Since, the bottom ash is the active material with heterogeneity (details will be later discussed in following section), the characterization data may be used to evaluate the potential applications and its environmental hazards, and to evaluate the possibilities of recycling its main components (Chimenos et al., 1999). By knowing the characteristics or the properties of ashes, we can ensure selection the most suitable way for dispose or utilization. For example, data of the minerals present in the ash, and their chemical composition is necessary in order to be able to assess quantitatively the correlation between microstructure and leaching behavior of the leachable substances. This could help to predict the potential alteration behavior of the bottom ash under the implicational condition/the disposal condition in either short or long term situation.

1.1.5.1 BOTTOM ASH CHARACTERIZATION

Bottom ash could be characterized by identifying the main constituent materials. Generally, the properties of ashes can be separated broadly into two parts; 1) physical properties, and 2) chemical properties (Table 1.3). Physical properties commonly refer to those parameters that could be observed or measured without changing the composition of materials, such as particle size distribution, moisture content, bulk density, compress strength, permeability, and porosity. Chemical properties of the bottom ash are characteristic

Table 1.3 Examples of characterization method of bottom ash.

Characterization	Example of test method
Physical properties	
• Particle size distribution	ASTM D-422-63
• Moisture content	ASTM D-2216-10
• Bulk density	ASTM C29
• Compressive strength	ASTM C109, D1633
• Permeability	ASTM D3588, D2434
• Porosity	ASTM D5856-15
Chemical properties	
• Chemical composition	XRF, Acid digestion
• Loss on ignition	ASTM D7348-13
• Heavy metals and leachability	JLT13
• Organic constituents	ASTM D 2974-07a
• Chloride content	ASTM D512-12
• Mineral composition	XRD

that is observed during a reaction in which the chemical composition of the bottom ash is changed. The chemical properties of bottom ash include chemical composition, loss on ignition, heavy metal and leachability, organic constituents, chloride content, and mineral composition.

However, characterization of bottom ash could be done in various aspects depending upon the purpose of study. For example, [Kirby and Rimstidt \(1993\)](#) studied mineralogy and surface properties of bottom ash. [Eighmy et al. \(1994\)](#) studied in the view of particle petrogenesis and speciation of elements. [Zevenbergen et al. \(1994\)](#) observed morphological and chemical properties of bottom ash with respect to the glassy constituent. [Pfrang-Stotz and Schneider \(1995\)](#) conducted the comparative studies from various grate and firing systems with respect to the mineralogical and geochemical method. [Chimenos et al. \(1999\)](#) characterized the bottom ash in the aspect of main constituent materials. [Speiser et al. \(2000\)](#) studied morphological and chemical characterization of Calcium-hydrate phases formed in alteration processes of deposited bottom ash. [Piantone et al. \(2004\)](#) studied the weathered

bottom ash in the aspect of mineralogy of secondary mineral phases. [Eggenberger et al. \(2004\)](#) studied the chemistry and mineralogy of bottom ash. [Bayuseno and Schmahl \(2010\)](#) focus on the chemical and mineralogical properties of the inorganic portion of the bottom ash. [Wei et al. \(2011\)](#) characterized bottom ash by focusing metal-bearing phases. From these examples, it could be implied that since 1990s until to date the characterization of bottom ash has been studied continuously with different perspective.

1.1.5.2 FACTOR CONTROLLING THE CHARACTERISTIC OF BOTTOM ASH

Generally, the chemical and physical characterization of ash will depend on several factors, namely the raw waste composition, the operational conditions, the type of incinerator, the type of ash discharger and the air pollution control design ([Chang and Wey, 2006](#)). The compositions of the raw MSW usually vary over times and from country to country due to the differences in lifestyle and waste recycling processes ([Lam et al., 2010](#)). MSW generally included plastics, kitchen waste, and glasses; therefore, it has a great influence on Cl and S content as well as on the Ca/Si ratio ([Rendek et al., 2007](#)). Likewise, the operational conditions and the type of incinerator also have an excessive influence on bottom ash quality. It is perceived that in normal operation, the incineration does not achieve a complete mineralization of organic constituents of MSW, which reflect by the value of carbon content and LOI in bottom ash ([Brunner et al., 1987](#); [Ferrari et al., 2002](#); [Rocca et al., 2013](#)). [Rendek et al. \(2007\)](#) also supported that the combustion parameter had an influence on the quantity and mobility of the residual organic matter. However, the operation condition could be controlled to enhance the burning completion, thus, it is also reported that the waste is burned has a limited influenced on the final bottom ash leaching behavior, but large different in bottom ash quality and leaching behavior caused by the different of process operation. Even the same waste was fed, the different in characteristic is attributed to different process condition ([Marchese and Genon, 2011](#)). Besides, the type of ash discharger reflects the quenching/non-quenching condition of the bottom ash. The influence of quenching process on the MSWI bottom ash is quite less in details. However, it is reported that a different degree of washing caused by quenching led to a different residual alkalinity in the bottom ash ([Marchese and Genon, 2011](#)). For the factor of the air pollution control design, generally it reflects the characteristic of the APC residues. The design of air pollution control system is not much effect to bottom ash unless the APC

residues is also collected to the ash discharger and is mixed to the bottom ash which could be found in some facilities.

1.1.5.3 BOTTOM ASH COMPOSITION AND CLASSIFICATION

As a heterogeneous material, bottom ash composed at least six groups of components (Müller and Rübner, 2006); 1) crystalline silicate in glass matrix, 2) oxides, sometimes in siliceous glass matrix, 3) bottle glass which composed of Na_2O , CaO and SiO_2 , 4) Metal such as aluminium, brass, steel, copper, size, 5) ceramic fragments, and 6) organic component such as bone fragment, charcoal, plant fibres, etc. Many other materials in addition to those listed above could be detected, but only occasionally, and in very low amounts. Iron oxides were usually embedded in a siliceous glass matrix but in particular, magnetite could also appear together with hedenbergite or ferrohedenbergite. In general, bottom ash residues comprise mainly ceramic materials, silicates, phosphates, sulfates or carbonates, which easily broken down by the mechanical system of transport within the furnace or by the effect of the thermal shock. It is possible to find some particles over 25 mm massed together whose matrix, mainly silicates, melted at the combustion temperature inside the furnace (Chimenos et al., 1999).

The unweathered bottom ash or the unquenched bottom ash exhibit fragments corresponding to two typologies; 1) refractory, and 2) melt. Refractory materials mainly correspond to fragments of rocks, ceramic, metals and bone remains. Melt materials consist chiefly of sub-rounded and irregular dark glass fragments (Vegas et al., 2008).

The quenched bottom ash contains 19 wt% CaO that is 1/5 of the bulk composition in silicates, glasses, oxides, hydroxides, and sulfates. Thus there is a high potential for the formation of Ca-hydrate phases. Immediately after the quenching process, the formation of single isolated Ca-hydrate crystals could be observed on the surface of the bottom ash particles. Gradually, the hydrate phases are arranged in clusters. With increased alteration, particles are covered with a reaction shell (<1 mm) composed of Ca-hydrate phases and, partly, carbonated Ca-hydrate phases (Speiser et al., 2000). The encountered dissolution-precipitation process is capable of cementing bottom ash particles. Bottom ash particles are completely coated with a cementation cover and the whole aggregate is hardened gradually. Besides, the crystallization processes of the Ca-hydrate phases, are exothermic.

The enthalpies of this type of reactions range between -40 and -140 kJ/mol (e.g. C-S-H phase) (Speiser et al., 2000).

The characteristic of the bottom ash that contains precipitated layer bounded to the particles was mentioned by some researchers. Speiser et al. (2001, 2000) characterized the weather bottom ash by scanning electron microscope and found that morphological surface of the bottom ash precipitated by Calcium-hydrate phases formed during the alteration process in the deposited site. The term “quench phase” was also mentioned in their study but referred the high-temperature phase. Piantone et al. (2004) reported the photo of weathered bottom ash that contained “slag”, “melt”, and “carb” by slag and melt corresponded to the slag and melt fractions of bottom ash, and carb corresponded to precipitated calcite. Wei (2011) and Saffarzadeh et al. (2011) seemed to be the first groups whose proposed that the fresh quenched bottom ash contained “fragile phases” as the fine ash particle that adhere to the melt phase during quenching, and “quenching product” which formed by reaction with water and air during cooling process. In this thesis work, the term “quench product” will be further used to define the adhered product on the melt particles. It should be noted here that the term “quench product” used in this study refers to all precipitates that attach to the core ash particle caused by quenching, thus this term may differ from the term “quench product” used in geological science.

By their external characteristics, bottom ashes can be subdivided into three main categories (Pfrang-Stotz and Schneider, 1995);

- 1) Vitreous type of bottom ash; these bottom ashes are partly black, with a bright metal surface and a very dense structure. They exhibit conchoidal fracture patterns reminiscent of obsidian (volcanic glass).
- 2) Porous type of bottom ash; these bottom ashes are light/dark brown, gray and reddish brown in color; dark brown/black shades are less frequent. Large and small degassing voids are very frequent, and there may be a minor melting process in some places, given rise to vitreous structure.
- 3) Microcrystalline type of bottom ash; these bottom ashes are very dense in structure and contain only a few degassing voids. Their color shades range between light/medium gray to reddish brown and black.

Considering only glassy particle, bottom ash can be subdivided into three groups (Zevenbergen et al., 1994);

- 1) Rounded or angular amorphous glassy particles consisting predominantly of silica or aluminosilicate with variable calcium content and low iron concentration. This type may contain inclusions of crystalline phases or other glassy phases, and makes up most of the bottom ash sample.
- 2) Rounded or angular amorphous glassy particles with a high iron content. Iron can be present as discrete iron oxide particulates engulfed by molten silicates, in form of dendritic iron oxide growths, or it can be dissolved in the glassy matrix.
- 3) Rounded vesicular glassy particles. Vesicular particles are quite common in the larger sizes (>200 micron) and consist predominantly of calcium aluminosilicates.

1.1.5.4 BOTTOM ASH CHEMICAL CHARACTERISTIC

The chemical characteristics of ashes and residues are the main reason for the concern regarding their classification as hazardous or non-hazardous waste and their ultimate management requirements (Wiles, 1996). There is a large data exist on the chemical characteristic of bottom ash. The chemical analysis of bottom ash from many facilities in the world indicates that the major components are Si, Ca, Al, Fe, Na, Mg, and K (Bayuseno and Schmahl, 2010; Chandler et al., 1997; Eggenberger et al., 2004; Sabbas et al., 2003; Tang et al., 2015; Zevenbergen et al., 1994). The ranges of total content of elements in bottom ash comparing to other residues are given in Table 1.4.

Although the chemical composition of bottom ash depends on the MSW characteristics, it is also found that several plants generated the fairly similar major composition which influenced by the combustion system, (Izquierdo et al., 2002; Marchese and Genon, 2011). Besides, the content of elements on bottom ash is the particle size/grain-size dependent. For example, Ca, P, Mg and Ti decrease with increasing grain-size while Fe, Al increase when particle size decreases (Speiser et al., 2000). The distribution of element which regards to particle size is owing to their thermodynamic characteristic (Yao et al., 2013).

One of the challenges and concern in bottom ash chemical characterization is the emission of heavy metals. Heavy metal may be harmful to the environment and humans when exposed to concentration above what can be found in the natural environment. The heavy metal in bottom ash compares to fly ash or APC residues is relatively low due to evaporation/volatilization. However, it is slightly high when compare to other solid fuels

Table 1.4 Ranges of total content of elements in MSWI residues (adopted from [Sabbas et al., 2003](#); [Wiles, 1996](#)).

Elements	Concentrations (mg/kg)			
	Bottom ash	Fly ash	Dry APC residues	Wet APC residues
Si	91,000-308,000	95,000-210,000	36,000-120,000	78,000
Ca	37,000-123,000	74,000-130,000	110,000-350,000	87,000-200,000
Al	22,000-73,000	49,000-90,000	12,000-83,000	21,000-39,000
Fe	4,100-150,000	12,000-44,000	2,600-71,000	20,000-97,000
Na	2,800-42,000	15,000-57,000	7,600-29,000	720-3,400
Mg	400-26,000	11,000-19,000	5,100-14,000	19,000-170,000
K	750-16,000	22,000-62,000	5,900-40,000	810-8,600
Pb	100-13,700	5,300-26,000	2,500-10,000	3,300-22,000
P	1,400-6,400	4,800-9,600	1,700-4,600	-
S	1,000-5,000	11,000-45,000	1,400-25,000	2,700-6,000
Cu	190-8,200	600-3,200	16-1,700	440-2,400
Zn	610-7,800	9,000-70,000	7,000-20,000	8,100-53,000
Cl	800-4,200	29,000-210,000	62,000-380,000	17,000-51,000
Ni	7-4,200	60-260	19-710	20-310
Cr	23-3,200	140-1,100	73-570	80-560
Ba	400-3,000	330-3,100	51-14,000	55-1,600
Mn	80-2,400	800-1,900	200-900	5,000-12,000
Sb	10-430	260-1,100	300-1,100	80-200
Mo	2-280	15-150	9-29	2-44
As	0.1-190	37-320	18-530	41-210
V	20-120	29-150	8-62	25-86
Cd	0.3-70	50-450	140-300	150-1400
Hg	0.02-8	0.7-30	0.1-51	2.2-2,300

such as coal and biomass. The variation of heavy metal concentrations in bottom ash depending on particle size distribution. [Chimenos et al. \(2003\)](#) found that heavy metals are concentrated in the bottom ash particle less than 4mm. The heavy metals that generally concerned and contained in the bottom ash are Zn, Pb, Ni, Hg, Cu, Cr, Cd, and As. [Sørum et al. \(2003\)](#) stated that under the reduction and oxidation condition on the grate, Cd, Hg, and Pb are fully volatilized while Cr stabled in solid phases. Besides, As, Cu, Ni, Zn are strong influenced by one or more of the parameters, including temperature, waste feed, air supply, chlorine/metal ratios. However, the chemical composition of bottom ash is similar to basaltic and other geological materials ([Chimenos et al., 2000](#); [Wiles, 1996](#)), except the concentration of heavy metals which slightly higher. Therefore, in order to dispose or utilize safely, the concentration of heavy metal needs to be controlled under regulation. It is always found that leaching of heavy metals /soluble salts from bottom ash exceeds some of the limit values for recycling the material as granular construction application. In particular, leaching of Cu, Zn and Pb often exceed the limit value, with Cu being the most critical ([Arickx et al., 2006](#)). In order to recycle bottom ash, treatment is therefore required.

1.1.5.5 BOTTOM ASH MINERAL CHARACTERISTIC

Bottom ash is a material where the crystalline and the amorphous phase is observed. The mineralogy of bottom ash is important to understanding the leaching behavior of bottom ash. It is also plays a vital role in the compatibility and strength development of bottom ash as it ages with time ([Chandler et al., 1997](#)). The mineralogy of bottom ash described by previous authors ([Eusden et al., 1999](#); [Kirby and Rimstidt, 1993](#); [Meima and Comans, 1997](#)) is very complex with a significant glassy content. It has been reported that minerals such as corundum, melilite, magnetite and quartz are generally present in the bottom ash and are very easily identified by traditional XRD search match procedures with high confidence. However, many mineral phases could not be identified reliably with conventional methods due to the large number of overlapping peaks and due to shift of peak position as a result of solid solution members which are not contained in the referent powder diffraction file ([Bayuseno and Schmahl, 2010](#)). Generally, the mineral that percent composition lower than 5 % is hardly to be detected by XRD.

1.1.5.6 CHLORIDE AND FRIEDEL'S SALT IN BOTTOM ASH

Over two decades, a lot of effort has been made to reuse bottom ash as a raw material for cement production, but in practical only a few could be used due to the hinder by chloride content (Ito et al., 2008). Chlorine in the bottom ash is mainly originated from plastic and organic waste. During the incineration, most of the chlorine is vaporized as HCl and mixed with fly ash, however, the significant amount may have remained up to 3.5 % by weight (Yang et al., 2014). The remain chlorine in bottom ash is divided into two groups of salt; soluble and insoluble. The soluble salt could be easily removed by dissolved into water, so a water washing has been introduced to reduce chlorine content in the bottom ash. Conversely, the main problem regard to chlorine is the insoluble salt which could not be easily removed by simple washing, but in acidic condition (Ito et al., 2008). When the bottom ash is aged via carbonation, its pH condition is reduced, so chloride in the insoluble salt is released (Abbas et al., 2003; Ahn et al., 2006). In construction and cement production, it is concerned with the factor that caused corrosion in reinforcement concrete. Therefore, the raw materials for cement production should fall below the regulation limit. For example, there is a limit on chloride (Cl) content on cements, e.g. 350 ppm in Japan and less than 1,000 ppm in Europe (Ito et al., 2008). Water washing is generally known to be the most economical and simple method. However, it is difficult to lower the Cl content to less than the regulation limit because of insoluble chloride as above mention.

The insoluble salt in bottom ash that is known to be easily detected by XRD is Friedel's or hydrocalumite. Friedel's salt was firstly synthesized and identified by Georges Friedel in 1897. It is the polymer derivative of hydrocalumite (Vieille et al., 2003), so their XRD diffractogram is significantly similar. The formation of Friedel's salts is known to be due to the direct reaction between CaCl_2 and tricalcium aluminate ($3\text{CaO}\cdot\text{Al}_2\text{O}_3$) (Birnin-Yauri and Glasser, 1998; Suryavanshi et al., 1996; Takemoto et al., 2008). According to Suryavanshi et al. (1996), Friedel's salt is formed by two separated mechanism; 1) an adsorption mechanism, and 2) an anion-exchange mechanism. In the adsorption mechanism, Friedel's salt form due to the adsorption of the bulk Cl^- ions into the interlayers hydrate to balance the charge. In ion-exchange mechanism, a fraction of free Cl^- bind with the OH^- ion presented on the inter layer of hydrate phase, as a result of Friedel's salt formation the Na^+ ions are released in equivalent with Cl^- ions.

1.1.6 ALTERATION OF BOTTOM ASH UNDER WEATHERING AND ITS ENVIRONMENTAL CONCERNS

The intrinsic reactivity of fresh bottom ash is well established. Bottom ash, as well as other MSWI residues, is produced by high-temperature processes. Due to differences in local composition, in the grain size of material, and in other physical and chemical parameters, no complete thermodynamic equilibrium is usually reached during incineration (Speiser et al., 2000). Besides, it is cooled fairly rapidly by quenching process downstream of the combustion unit, therefore, its thermodynamically unstable under ambient conditions (Meima and Comans, 1997a, 1997b). The bottom ash is considered as highly reactive, and it can change their mineralogical and physio-chemical characteristics until the thermodynamic equilibrium conditions with the surrounding environment are attained (Sabbas et al., 2003). The mineralogical and physio-chemical alteration influence the leaching behavior of ions or substances from the bottom ash, especially under wet/alkaline conditions (Polettoni and Pomi, 2004). The alteration process starts immediately after quenching of the hot bottom ash (Speiser et al., 2000), and continues at the deposit site until the equilibrium with the environment is attained. Generally, the instability of bottom ash at the landfill site could prolong to 10 years or over.

The major alteration reaction in the bottom ash is included dissolution/precipitation of salts, glass corrosion, hydration and oxidation reaction of metal or metal oxides, slaking of lime, and hardening reaction (cementation and carbonation). During weathering, some of the chemical and mineralogical characteristics of the material undergo significant changes, including; oxidation of some metals (e.g. aluminum, iron, copper), dissolution and precipitation of the hydroxides and salts of the main cations, carbonation, neutralization of pH and neoformation of clay-like minerals from glass (Meima and Comans, 1997a, 1997b; Wiles, 1996). The reported alteration products are anhydrite, ettringite, calcite, iron oxides and hydroxide as well as gibbsite to name a few of the resulting weathering phases. Usually, the formation of these phases is interpreted in terms of chemical and mineralogical concepts of aging process (Meima and Comans, 1997b; Speiser et al., 2000).

According to several reactions under weathering, it has long been recognized as having a significant effect on the leaching of trace heavy metals from the bottom ash. Generally, less heavy metal is released from bottom ash than from fly ash; therefore,

bottom ash has been used as one of the ingredients of concrete and admixtures used in the construction of roads and bridges. However, the re-use of admixtures may be hazardous since leachate from the bottom ash cannot be predicted or controlled in practice (Bruder-Hubscher et al., 2001; Shim et al., 2003). Hence, the release of heavy metal (mainly Pb and Zn) is one of the main limitations to the reuse of MSW bottom ash as a secondary building material as stated in most of the environmental regulations.

Although heavy metals are concentrated in the small particle size fractions (< 4 mm), however, for all size fractions studied, a period of natural weathering less than 50 days is enough to diminish the release of most of the heavy metals below the maximum required limits. This means that the smallest fractions can also be reused as a secondary building material, in accordance with local regulation (Chimenos et al., 2003). Therefore, in the management of bottom ash, natural weathering is the most cost-effective method of treatment, since it results in the chemical stability of the bottom ash. One-to-three-month exposure to natural weathering is enough to reduce the release of heavy metals from residues (Chimenos et al., 2003, 2000; Wiles, 1996)

1.1.7 BOTTOM ASH DISPOSAL STRATEGY

The management of residues from incineration plants is an integral part of waste management system. The primary goal of managing incineration residues is to prevent any impact on human or environment caused by unacceptable particulate, gaseous and/or solute emissions (Sabbas et al., 2003). Since bottom ash contains heavy metal and soluble salts, it should be managing as a hazardous material to prevent the contamination of soil and ground water, especially in long term disposal (Wiles, 1996). In Japan, handling of MSWI residues is directly to controlled landfill. However, recently constructing the landfill is difficult, in particular for industrialized countries according to land limit and the Not-In-My Backyard (NIMBY) syndrome. Therefore, the great challenge is due to how to convert the bottom ash into a new resource practically. There are at least seven options of bottom ash utilization, namely, cement and concrete production, road pavement, glasses and ceramics, agriculture, stabilizing agent, adsorbents, and zeolite production (Lam et al., 2010). For bottom ash to be recycled, the material must comply with strict regulations, including civil-technical and environmental requirements. Therefore, the appropriate management

of bottom ash can lead to advanced means of obtaining chemical stabilization to maintain the contaminant release rates over time at the environmentally limited level (Um et al., 2013).

1.2 RESEARCH OBJECTIVES

In the attempt to manage bottom ash effectively, many researchers investigated the characteristics of bottom ash in various aspects. Broadly, bottom ash could be considered as a hazardous material that possible to put a treat to human/environment, or a synthetic material that could be used as a resource for several purposes, particular in construction or cement production. As the heterogeneity active material, bottom ash commonly alters under an exposure condition under weathering process. Although characterization of the bottom ash investigated by numbers of researchers, there is no study particularly focus on the influence of quenching process, and the formation of the quench product on bottom ash. Besides, alteration of bottom ash could occur immediately after contacting to water, quenching process in the discharger should cause a great impact on the ash as the initial stage of weathering. Therefore, the main objective of this study is to obtain the fundamental data regarding to the changing pattern resulted from quenching process and the detail of quench product formation. The specific objectives are as following:

- 1) To get a basic understanding concerning the characteristic of material mixed to be the quenched bottom ash which included grate sifting, unquenched bottom ash, and the quenched bottom ash itself.
- 2) To evaluate the influence of quenching process on the unquenched bottom ash characterization.
- 3) To investigate the characterization of the quench product.
- 4) To disclose the phenomena during quenching and to investigate the formation of the quench layer.

1.3 SIGNIFICANCE OF THIS STUDY

The outcome of this research is expected to be a clear understanding of the distinguish between the characteristic of the unquenched bottom ash and the freshly quenched bottom ash, and a proposed mechanical model of the formation of the quench layer. The information obtained from this research would benefit as precursory information for estimating possible

alteration trends if bottom ash were discharged by the wet or dry system, which is essential for technology selection and proper management of the bottom ash.

1.4 RESEARCH FLOW AND THESIS STRUCTURE

To achieve the expected outcome and to meet objectives of this study, a large effort has been made through comprehensive research works. There are two main assumptions that guided in the development of research methodology in this study. The first assumption is that the thoroughly investigation of the materials involved in quenching system would provide a fundamental information about characterization of bottom ash as well as the influence of quenching process on the bottom ash. The second assumption is that the lab-scale artificial quenching may result in the characteristic of the bottom ash as same as the commercial-scale discharge quenching, the lab-scale quenching would provide the chance for observing the phenomena during quenching which is difficult in the real-operation. Regardless of this chapter (Chapter 1) which provides the background of this research and literature review of current situation and fundamental knowledge involved in the area of study, the achievements from investigation and lab-scale quenching simulation are presented and discussed in four chapters from Chapter 2 to Chapter 5. The last chapter (Chapter 6) is the conclusion of the whole research work. The flow structure of this dissertation is presented in [Figure 1.8](#). This thesis is divided into six chapters; each chapter is given to provide a brief outline as following:

Chapter 1 the background of this research as well as objectives and research flow were introduced with the review of literature regarding to MSW generation and treatment strategy in Japan, incineration technology, ash discharge technology/quenching system, MSWI residue generations, bottom ash characterization, and its disposal strategy.

Chapter 2 the detail of physical and chemical characterization of materials that was mixed to be bottom ash is investigated using representative sample obtained from the incineration facility.

Chapter 3 the influence of quenching process on the bottom ash characterization was evaluated by comparing the characteristic of the unquenched bottom ash and the quenched bottom ash that obtained from the incineration plant. The details of differentiation in parameters namely, physical morphology, particle size distribution, chemical composition, pH, mineral composition and Cl distribution are presented.

Chapter 4 the quenching experiments were conducted. The details of the characteristic of the quench product from the experiment, and the reference sample were compared.

Chapter 5 the phenomena during quenching and the detail of the formation of the quench product from the experiment were described in this chapter. The model of the formation mechanism of the quench product is also presented.

Chapter 6 the key results of this research were concluded, and the recommendations for application and further research were given.

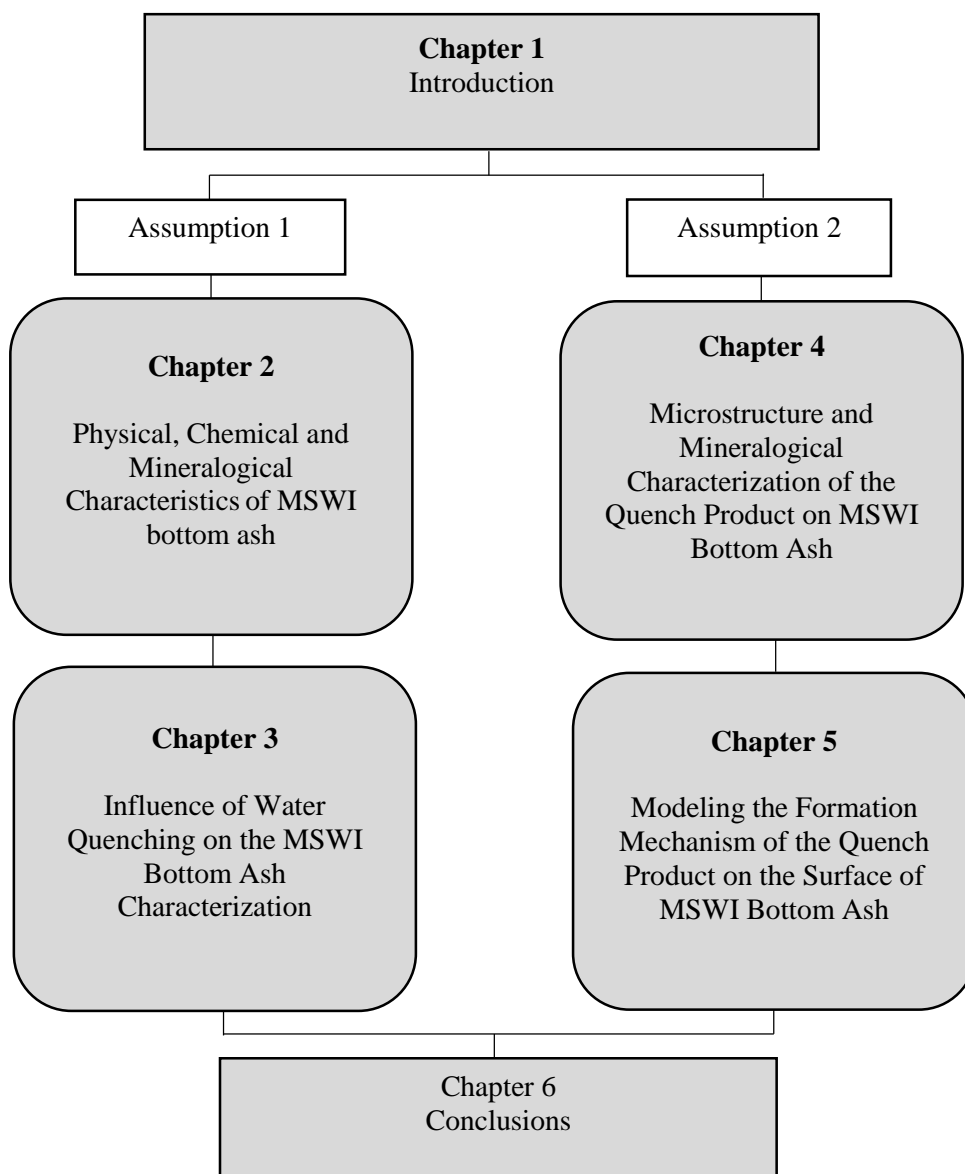


Figure 1.8 The dissertation structure.

REFERENCES

- Abbas, Z., Moghaddam, A.P., Steenari, B.-M., 2003. Release of Salts from Municipal Solid Waste Combustion Residues. *Waste Manag.* 23, 291–305. doi:10.1016/S0956-053X(02)00154-X
- Ahn, J.-W., Um, N.-I., Han, G.-C., You, K.-S., Cho, H.-C., 2006. Effect of Carbonation in Removal of Chloride from Municipal Solid Waste Incineration Bottom Ash. *Geosystem Eng.* 9, 87–90. doi:10.1080/12269328.2006.10541260
- Bayuseno, A.P., Schmahl, W.W., 2010. Understanding the Chemical and Mineralogical Properties of the Inorganic portion of MSWI Bottom Ash. *Waste Manag.* 30, 1509–1520. doi:10.1016/j.wasman.2010.03.010
- Birnin-Yauri, U.A., Glasser, F.P., 1998. Friedel's Salt, $\text{Ca}_2\text{Al}(\text{OH})_6(\text{Cl},\text{OH})\cdot 2\text{H}_2\text{O}$: Its Solid Solutions and Their Role in Chloride Binding. *Cem. Concr. Res.* 28, 1713–1723. doi:10.1016/S0008-8846(98)00162-8
- Bourtsalas, A., 2013. Review of WTE Ash Utilization Processes Under Development in North West Europe. URL <http://www.seas.columbia.edu/earth/wtert/sofos/WTEBA.pdf> (accessed 8.17.15).
- Bruder-Hubscher, V., Lagarde, F., Leroy, M.J., Coughanowr, C., Enguehard, F., 2001. Utilisation of Bottom Ash in Road Construction: Evaluation of the Environmental Impact. *Waste Manag. Res. J. Int. Solid Wastes Public Clean. Assoc. ISWA* 19, 545–556.
- Brunner, P.H., Müller, M.D., McDow, S.R., Moench, H., 1987. Total Organic Carbon Emissions from Municipal Incinerators. *Waste Manag. Res.* 5, 355–365. doi:10.1177/0734242X8700500146
- Chandler, A.J., Eighmy, T.T., Hjelmar, O., Kosson, D.S., Sawell, S.E., Vehlow, J., Sloat, H.A. van der, Hartlén, J., 1997. *Municipal Solid Waste Incinerator Residues*. Elsevier.
- Chang, F.-Y., Wey, M.-Y., 2006. Comparison of the Characteristics of Bottom and Fly Ashes Generated from Various Incineration Processes. *J. Hazard. Mater.* 138, 594–603. doi:10.1016/j.jhazmat.2006.05.099
- Chimenos, J.M., Fernández, A.I., Miralles, L., Segarra, M., Espiell, F., 2003. Short-Term Natural Weathering of MSWI Bottom Ash as a Function of Particle Size. *Waste Manag.* 23, 887–895. doi:10.1016/S0956-053X(03)00074-6
- Chimenos, J.M., Fernández, A.I., Nadal, R., Espiell, F., 2000. Short-Term Natural Weathering of MSWI Bottom Ash. *J. Hazard. Mater.* 79, 287–299. doi:10.1016/S0304-3894(00)00270-3
- Chimenos, J.M., Segarra, M., Fernández, M.A., Espiell, F., 1999. Characterization of the Bottom Ash in Municipal Solid Waste Incinerator. *J. Hazard. Mater.* 64, 211–222. doi:10.1016/S0304-3894(98)00246-5
- Diaz, L.F., Savage, G.M., Eggerth, L.L., Rosenberg, L., Diaz, L.F., UNEP International Environmental Technology Centre, CalRecovery, I., 2005. *Solid Waste Management*. United Nations Environment Programme, Paris.

- Eggenberger, U., Schenk, K., Mäder, U., 2004. Chemistry and Mineralogy of Municipal Solid Waste Incinerator Bottom Ash. *Geol. Soc. Lond. Spec. Publ.* 236, 411–422. doi:10.1144/GSL.SP.2004.236.01.23
- Eighmy, T.T., Eusden Jr., J.D., Marsella, K., Hogan, J., Domingo, D., Krzanowski, J.E., Stämpfli, D., 1994. Particle Petrogenesis and Speciation of Elements in MSW incineration Bottom Ashes, in: J.J.J.M. Goumans, H.A. van der S. and T.G.A. (Ed.), *Studies in Environmental Science, Environmental Aspects of Construction with Waste Materials Proceeding of the International Conference on Environmental Implications of Construction Materials and Technology Developments*. Elsevier, pp. 111–136.
- Ferrari, S., Belevi, H., Baccini, P., 2002. Chemical Speciation of Carbon in Municipal Solid Waste Incinerator Residues. *Waste Manag.* 22, 303–314. doi:10.1016/S0956-053X(01)00049-6
- Hoorweg, D., Bhada-Tata, P., 2012. *What a Waste - A Global Review of Solid Waste Management*, Urban Development Series Knowledge Papers. World Bank.
- Ito, R., Dodbiba, G., Fujita, T., Ahn, J.W., 2008. Removal of Insoluble Chloride from Bottom Ash for Recycling. *Waste Manag.* 28, 1317–1323. doi:10.1016/j.wasman.2007.05.015
- Izquierdo, M., López-Soler, Á., Vazquez Ramonich, E., Barra, M., Querol, X., 2002. Characterisation of Bottom Ash from Municipal Solid Waste Incineration in Catalonia. *J. Chem. Technol. Biotechnol.* 77, 576–583. doi:10.1002/jctb.605
- Kirby, C.S., Rimstidt, J.D., 1993. Mineralogy and Surface Properties of Municipal Solid Waste Ash. *Environ. Sci. Technol.* 27, 652–660. doi:10.1021/es00041a008
- Lam, C.H.K., Ip, A.W.M., Barford, J.P., McKay, G., 2010. Use of Incineration MSW Ash: A Review. *Sustainability* 2, 1943–1968. doi:10.3390/su2071943
- Mahajan, N., 2015. *A Comparative Study of Municipal Solid Waste Management in India and Japan*.
- Marchese, F., Genon, G., 2011. Effect of Leaching Behavior by Quenching of bottom ash from MSW Incineration. *Waste Manag. Res. J. Int. Solid Wastes Public Clean. Assoc. ISWA* 29, 39–47. doi:10.1177/0734242X10387848
- Meima, J.A., Comans, R.N.J., 1997a. Geochemical Modeling of Weathering Reactions in Municipal Solid Waste Incinerator Bottom Ash. *Environ. Sci. Technol.* 31, 1269–1276. doi:10.1021/es9603158
- Meima, J.A., Comans, R.N.J., 1997b. Overview of Geochemical Processes Controlling Leaching Characteristics of MSWI Bottom Ash, in: J.J.J.M. Goumans, G.J.S. and H.A. van der S. (Ed.), *Studies in Environmental Science, Waste Materials in Construction Putting Theory into Practice Proceedings of the International Conference on the Environment and Technical Implications of Construction with Alternative Materials*. Elsevier, pp. 447–457.
- Ministry of the Environment, 2015. *Municipal Solid Waste Emissions and Disposal in FY2013*. URL <https://www.env.go.jp/en/headline/2137.html> (accessed 11.12.15).

- Ministry of the Environment, 2014. History and Current State of Waste Management in Japan.
- Ministry of the Environment, 2013. Waste Treatment in Japan. URL http://www.env.go.jp/recycle/waste_tech/ippan/h25/data/disposal.pdf (accessed 10.5.15).
- Ministry of the Environment, 2012. Solid Waste Management and Recycling Technology of Japan-Toward a Sustainable Society.
- Pfrang-Stotz, G., Schneider, J., 1995. Comparative Studies of Waste Incineration Bottom Ashes From Various Grate and Firing Systems, Conducted With Respect To Mineralogical and Geochemical Methods of Examination. *Waste Manag. Res.* 13, 273–292. doi:10.1177/0734242X9501300307
- Piantone, P., Bodéan, F., Chatelet-Snidaro, L., 2004. Mineralogical Study of Secondary Mineral Phases from Weathered MSWI Bottom Ash: Implications for the Modelling and Trapping of Heavy Metals. *Appl. Geochem.* 19, 1891–1904. doi: 10.1016/j.apgeochem.2004.05.006
- Polettini, A., Pomi, R., 2004. The Leaching Behavior of Incinerator Bottom Ash as Affected by Accelerated Ageing. *J. Hazard. Mater.* 113, 209–215. doi:10.1016/j.jhazmat.2004.06.009
- Rendek, E., Ducom, G., Germain, P., 2007. Influence of Waste Input and Combustion Technology on MSWI Bottom Ash Quality. *Waste Manag., Wascon 2006 6th International Conference: Developments in the re-use of mineral waste* 27, 1403–1407. doi:10.1016/j.wasman.2007.03.016
- Rocca, S., Zomeren, A. van, Costa, G., Dijkstra, J.J., Comans, R.N.J., Lombardi, F., 2013. Mechanisms Contributing to the Thermal Analysis of Waste Incineration Bottom Ash and Quantification of Different Carbon Species. *Waste Manag.* 33, 373–381. doi:10.1016/j.wasman.2012.11.004
- Sabbas, T., Polettini, A., Pomi, R., Astrup, T., Hjelm, O., Mostbauer, P., Cappai, G., Magel, G., Salhofer, S., Speiser, C., Heuss-Assbichler, S., Klein, R., Lechner, P., 2003. Management of Municipal Solid Waste Incineration Residues. *Waste Manag.* 23, 61–88. doi:10.1016/S0956-053X(02)00161-7
- Saffarzadeh, A., Shimaoka, T., Wei, Y., Gardner, K.H., Musselman, C.N., 2011. Impacts of Natural Weathering on the Transformation/Neoformation Processes in Landfilled MSWI Bottom Ash: A Geoenvironmental Perspective. *Waste Manag.* 31, 2440–2454. doi:10.1016/j.wasman.2011.07.017
- Sakai, S., 1996. Municipal Solid Waste Management in Japan. *Waste Manag., Cycle and Stabilization Technologies of MSW Incineration Residue* 16, 395–405. doi:10.1016/S0956-053X(96)00107-9
- Sawell, S., Chandler, A., Eighmy, T., Hartlén, J., Hjelm, O., Kosson, D., Van Der Sloot, H., Vehlow, J., 1995. An International Perspective on the Characterisation and Management of Residues from MSW Incinerators. *Biomass Bioenergy, International Energy Agency Bioenergy Agreement Progress and Achievements 1992/94* 9, 377–386. doi:10.1016/0961-9534(95)00105-0

- Shim, Y.-S., Kim, Y.-K., Kong, S.-H., Rhee, S.-W., Lee, W.-K., 2003. The Adsorption Characteristics of Heavy Metals by Various Particle Sizes of MSWI Bottom Ash. *Waste Manag.* 23, 851–857. doi:10.1016/S0956-053X(02)00163-0
- Sørum, L., Frandsen, F.J., Hustad, J.E., 2003. On the Fate of Heavy Metals in Municipal Solid Waste Combustion Part I: Devolatilisation of Heavy Metals on the Grate. *Fuel* 82, 2273–2283. doi:10.1016/S0016-2361(03)00178-9
- Speiser, C., Baumann, T., Niessner, R., 2001. Characterization of Municipal Solid Waste Incineration (MSWI) Bottom Ash by Scanning Electron Microscopy and Quantitative Energy Dispersive X-ray Microanalysis (SEM/EDX). *Fresenius J. Anal. Chem.* 370, 752–759. doi:10.1007/s002160000659
- Speiser, C., Baumann, T., Niessner, R., 2000. Morphological and Chemical Characterization of Calcium-Hydrate Phases Formed in Alteration Processes of Deposited Municipal Solid Waste Incinerator Bottom Ash. *Environ. Sci. Technol.* 34, 5030–5037. doi:10.1021/es990739c
- Suryavanshi, A.K., Scantlebury, J.D., Lyon, S.B., 1996. Mechanism of Friedel's Salt Formation in Cements Rich in Tri-calcium aluminate. *Cem. Concr. Res.* 26, 717–727. doi:10.1016/S0008-8846(96)85009-5
- Takemoto, T., Etoh, J., Naruoka, T., Shimaoka, T., 2008. Mechanism of Formation and Decomposition of Insoluble Chlorine Compounds in Municipal Solid Waste Bottom Ash. *J. Jpn. Soc. Waste Manag. Experts* 19, 293–302. doi:10.3985/jswme.19.293
- Tanaka, N., Tojo, Y., Matsuto, T., 2005. Past, Present, and Future of MSW Landfills in Japan. *J. Mater. Cycles Waste Manag.* 7, 104–111. doi:10.1007/s10163-005-0133-6
- Tang, P., Florea, M.V.A., Spiesz, P., Brouwers, H.J.H., 2015. Characteristics and Application Potential of Municipal Solid Waste Incineration (MSWI) Bottom Ashes from Two Waste-to-Energy Plants. *Constr. Build. Mater.* 83, 77–94. doi:10.1016/j.conbuildmat.2015.02.033
- Um, N., Nam, S.-Y., Ahn, J.-W., 2013. Effect of Accelerated Carbonation on the Leaching Behavior of Cr in Municipal Solid Waste Incinerator Bottom Ash and the Carbonation Kinetics. *Mater. Trans.* 54, 1510–1516. doi:10.2320/matertrans.M-M2013809
- US EPA, 2013. Municipal Solid Waste. URL <http://www3.epa.gov/epawaste/nonhaz/municipal/> (accessed 11.16.15).
- Vieille, L., Rousselot, I., Leroux, F., Besse, J.-P., Taviot-Guého, C., 2003. Hydrocalumite and Its Polymer Derivatives. 1. Reversible Thermal Behavior of Friedel's Salt: A Direct Observation by Means of High-Temperature in Situ Powder X-ray Diffraction. *Chem. Mater.* 15, 4361–4368. doi:10.1021/cm031069j
- Wei, Y., 2011. Geoenvironmental Study of MSWI Bottom Ash with Emphasis on Secondary Mineralization and Behavior of Heavy Metals. Kyushu University, Fukuoka, Japan.
- Wei, Y., Shimaoka, T., Saffarzadeh, A., Takahashi, F., 2011. Mineralogical Characterization of Municipal Solid Waste Incineration Bottom Ash With an Emphasis on Heavy Metal-Bearing Phases. *J. Hazard. Mater.* 187, 534–543. doi:10.1016/j.jhazmat.2011.01.070

- Wiles, C.C., 1996. Municipal Solid Waste Combustion Ash: State-of-the-Knowledge. *J. Hazard. Mater.* 47, 325–344. doi:10.1016/0304-3894(95)00120-4
- Yang, S., Saffarzadeh, A., Shimaoka, T., Kawano, T., 2014. Existence of Cl in Municipal Solid Waste Incineration Bottom Ash and Dechlorination Effect of Thermal Treatment. *J. Hazard. Mater.* 267, 214–220. doi:10.1016/j.jhazmat.2013.12.045
- Yao, J., Kong, Q., Zhu, H., Long, Y., Shen, D., 2013. Content and Fractionation of Cu, Zn and Cd in Size Fractionated Municipal Solid Waste Incineration Bottom Ash. *Ecotoxicol. Environ. Saf.* 94, 131–137. doi:10.1016/j.ecoenv.2013.05.014
- Zevenbergen, C., Wood, T.V., Bradley, J. p., Van Der Broeck, P. f. c. w., Orbons, A. j., Van Reeuwijk, L. p., 1994. Morphological and Chemical Properties of MSWI Bottom Ash with Respect to the Glassy Constituents. *Hazard. Waste Hazard. Mater.* 11, 371–383. doi:10.1089/hwm.1994.11.371

CHAPTER 2

PHYSICAL, CHEMICAL AND MINERALOGICAL CHARACTERISTICS OF MSWI BOTTOM ASH

CHAPTER 2

PHYSICAL, CHEMICAL AND MINERALOGICAL CHARACTERISTICS OF MSWI BOTTOM ASH

2.1 ABSTRACT

In current operation, most of the incineration transferred the grate sifting and the grate ash simultaneously into the discharger. These two ashes become the mixture of bottom ash. In order to get better understanding in the characteristic of the bottom ash that was quenched, it is necessary to characterize the original materials that involve in the system. In this chapter, the grate sifting, and the grate ash, from here on referred to unquenched bottom ash, and the bottom ash which referred to the quenched bottom ash were investigated on their physical chemical and mineralogical characteristics. The methodologies used to characterize samples were included visual observation, analysis of particle size distribution, particle thin section analysis, measurement of pH, moisture content, and loss on ignition, bulk chemical analysis, and mineral composition analysis.

2.2 INTRODUCTION

Mass-burn moving grate incineration is one of the most common thermal treatment technologies used for handling waste in Japan. This technology can handle waste that is heterogeneous, both in terms of material size and in terms of energy content. It can reduce waste volume by up to 90 %, and the heat produced during combustion can be recovered to generate electricity. Recently, over 300 incineration facilities have been installed to generate electricity from waste. Of these, 197 facilities make use of moving grate incineration ([Themelis and Mussche, 2013](#)).

Although incineration enables reduction in waste volume, substantial amounts of residues are remained. After combustion, the unquenched bottom ash that remained on the post combustion grate inside the incinerator will be transferred to the quenching tank. This process is purposed mainly to cool down the ash and to control dust. In the same time, the ash that drops into the gap between the grate called “grate sifting” is also transferred to the quenching tank. Therefore, the quenched bottom ash is commonly known as the mixture

between unquenched bottom ash and grate sifting. The quenched bottom ash, or general term bottom ash, is the most significant by-product from waste-to-energy incineration plants. It accounts for 85-95 % of solid products resulting from the combustion process (Abdulahi, 2009). In some plants, the air pollution control residues and the boiler ash are also directed into the quenching tank; however, these types of ash are excluded in this research. Since the incineration process is not the final waste treatment stage, solid residues generated during/after incineration still requires further treatment for safe disposal/utilization.

In Japan, most bottom ash is landfilled (Ministry of the Environment, 2014). Numerous studies have proposed several methods for recycling bottom ash, for example, by using it as an aggregate, as a construction material, and/or in cement production (Abbà et al., 2014; del Valle-Zermeño et al., 2014; Lam et al., 2011, 2010; Saikia et al., 2015; Thomas et al., 2012; Wegen et al., 2013). However, only a portion of the bottom ash can be used in the manufacturing process (Ito et al., 2008). The main factor that prevents use of bottom ash is the heterogeneous nature of heavy metals and its Cl content. In aggregated quantities, leaching of heavy metal from bottom ash may harm human and environment health. In cement production, Cl leads to corrosion of metal in reinforced concrete, rendering bottom ash unsuitable for cement production. In order to utilize bottom ash effectively, it is necessary to treat it prior to use. Details of such treatments have been reported elsewhere (Ito et al., 2008; Lam et al., 2010; Sabbas et al., 2003).

Several previous studies have focused on the bottom ash characterization, which is a key to proper handling of bottom ash. However, most studies focus on metal distribution, heavy metal leaching, geoenvironmental weathering, road and construction applications, and treatment options of bottom ash generated from the end line of different incinerator types (Bayuseno and Schmahl, 2010; Chang and Wey, 2006; Eusden et al., 1999; Forteza et al., 2004; Kirby and Rimstidt, 1993; Speiser et al., 2001; van der Sloot et al., 2001). Only few papers have discussed about the unquenched bottom ash and the grate sifting (Wiles, 1996; Yamamoto et al., 2007), while, these ash types are source of the quenched bottom ash. The characterization of these ash types is used in this chapter as approach to get better understanding of the effect of water quenching on bottom ash characteristics as well as nature of the bottom ash.

2.3 MATERIALS AND METHODS

2.3.1 PLANT DESCRIPTION

The sample used in this study came from a waste-to-energy incineration plant in Japan. The plant has two parallel incineration lines, with total process capacity of 300 tons of “as received” municipal solid waste per day. Both incineration lines make use a three-step movable grate system (Figure 2.1). The temperature in the combustion chamber is controlled at 850-1,100 °C. The incinerator is a closed system connected to a quenching tank. Bottom ash, a product of quenching hot ash, and grate sifting deposition ash are transported outwards through a linear conveyor belt. Emission gas is transferred to the gas treatment system, while heat is recovered to generate electricity.

2.3.2 SAMPLING

Three types of materials were sampled from four sampling points (Figure 2.1), including; 1) the grate sifting deposition ash collected from the shoot under the combustion grate, 2) the grate sifting deposition ash collected from the chute under the post-combustion grate, 3) the unquenched bottom ash sampled from the end of the combustion chamber, and 4) the quenched bottom ash collected at the outlet of the quenching tank.

In this study, all samples were taken on a typical routine maintenance day in January 2013. Samples of grate siftings under the combustion grate, grate siftings under the post-combustion grate, and unquenched bottom ash were of approximately 30 kg. In the case of the quenched bottom ash, a sample of 60 kg was collected; this was then air dried for three days, and later freeze dried for 12 h prior to being used in the subsequent analyses.

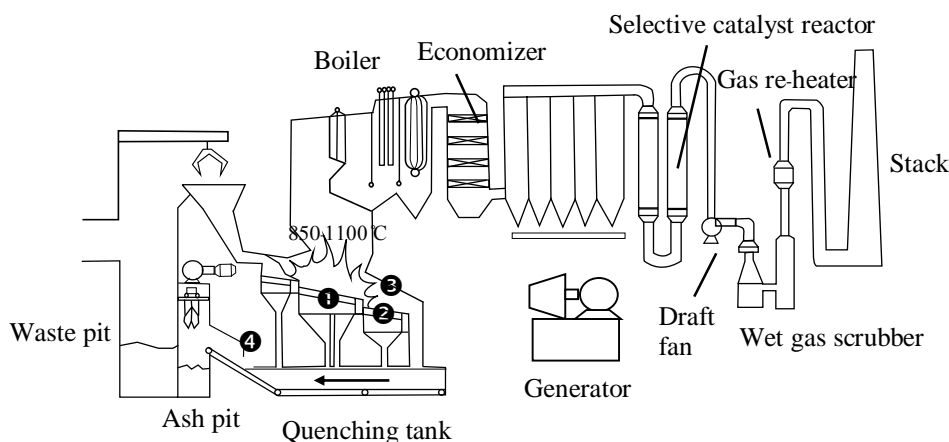


Figure 2.1 A schematic overview of a typical mass burn waste-to-energy plant, showing the four material sampling locations: 1) the grate siftings under the combustion grate; 2) the grate siftings under the post-combustion grate; 3) the unquenched bottom ash; and 4) the quenched bottom ash.

2.3.3 ANALYSIS

Pre-treatment: To obtain representative samples, large unburned material was removed. All samples were initially homogenized by being passed through a 2 cm mesh. A coning and quartering method was applied to each sample. One part of the subsample was used, with other parts kept as stock for further research. About 1 kg of the used subsample was ground and later used in subsequent investigation.

Particle size distribution: After quartering, one part of the subsample was used to determine particle size distribution in five categories; <0.425 mm, 0.425-1.00 mm, 1.00-2.00 mm, 2.00-4.75 mm, and >4.75 mm.

pH, moisture content and loss on ignition (LOI): Samples were saturated with water in a solid: liquid ratio of 1:10 and pH was measured using a pH meter. All samples were dried in a drying oven at 105 °C for 24 h for subsequent water content measurement. Loss on ignition (LOI) was measured using a muffle furnace to heat the dried sample (at 105 °C for 24 h) to 440 °C for 2 h. This method was developed and used in our laboratory to avoid decomposition of hydrate and carbonate in bottom ash (Yang et al., 2012).

Thin section analysis: Several particles were carefully picked out of the middle-sized fractions (1.00-2.00 mm) using a stereo microscope. The representative specimens were then resin-impregnated, lapped and polished to prepare a standard thin section. Thin section observations were completed using a BX51-33 MB Olympus petrographic polarized microscope.

Bulk chemical analysis: Bulk chemicals of major elements, and heavy metals were determined using wavelength dispersive X-ray fluorescence (XRF, Rigaku RIX3100). For this examination, 8 g of each sample was mixed thoroughly with acetone binder in an agate mortar. The powder was put into a sample O-ring and pressed at 20 kg/cm² for 1 minute. Finally, the sample pellets were analyzed using XRF. The analytical result was calculated automatically by setting measurement parameters concerning standard samples.

Mineral analysis: Each sample was ground into powder using an agate pestle and mortar and then manually pressed into the sample ring for analysis through X-ray Diffraction (XRD). Specimens were subsequently analyzed using XRD with scan parameters set to 2-75°, 2 θ ; 0.020 steps, and 15/step. Data were recorded digitally. Peak positions and intensities were identified using the PC-based peak finder software namely PDXL (Rigaku Integrated X-ray Powder Diffraction Software). The positions and peak heights were checked against the entry database of the International Center for Diffraction Data (ICDD) and the Japan Information Center of Science and Technology (JICST).

2.4 RESULTS AND DISCUSSION

2.4.1 GRATE SIFTINGS

Grate siftings are those materials falling from the furnace grate. Those are usually collected in hoppers beneath the grate and added to the grate ash to produce the bottom ash process stream. The characteristic of grate siftings under the different stage of combustion grates showed the distinct characteristics regarding to the degree of combustion. Further details are discussed in following section.

2.4.1.1 PHYSICAL CHARACTERISTICS

Figure 2.2 shows the physical appearance of grate siftings from two sampling points. Figure 2.2a) is the sample obtained from the chute under the combustion grate, and Figure 2.2b) is the sample obtained from the chute under the post-combustion grate. As it can

be seen, the grate siftings may be described as the dusty sand-like materials. Generally, it appearance slightly similar to the unquenched bottom ash and the quenched bottom ash (please refer to section 2.3.2.1 and section 2.3.3.1, respectively), however, their color is different. The grates siftings under the combustion grate is dominant by the uncomplete-burnt materials indicated by a dark-gray color. In contrast, the color of the grate siftings under the post-combustion grate is white-gray showing that it reaches the complete burning.

Considering to particle sized distribution, the grate siftings can vary given the spacing between the grate bars inside the furnace. Molten aluminum, zinc, copper and lead can drip down to the hoppers. It is found that grate siftings mainly composed of particles smaller than 1 mm with the cumulative percent passing through the sieve is up to about 70 % (Figure 2.3). Although the main distribution of grate siftings' particle is smaller than 1 mm, however, particle larger than 4.75 mm is also able to find (Figure 2.4). Those large particles are classified to be a slag and a refractory of glass, ceramic, bottle cap and metal from stationary/kitchen tools. Occasionally, the piece of melt aluminum is found in the grate sifting under the combustion grate.

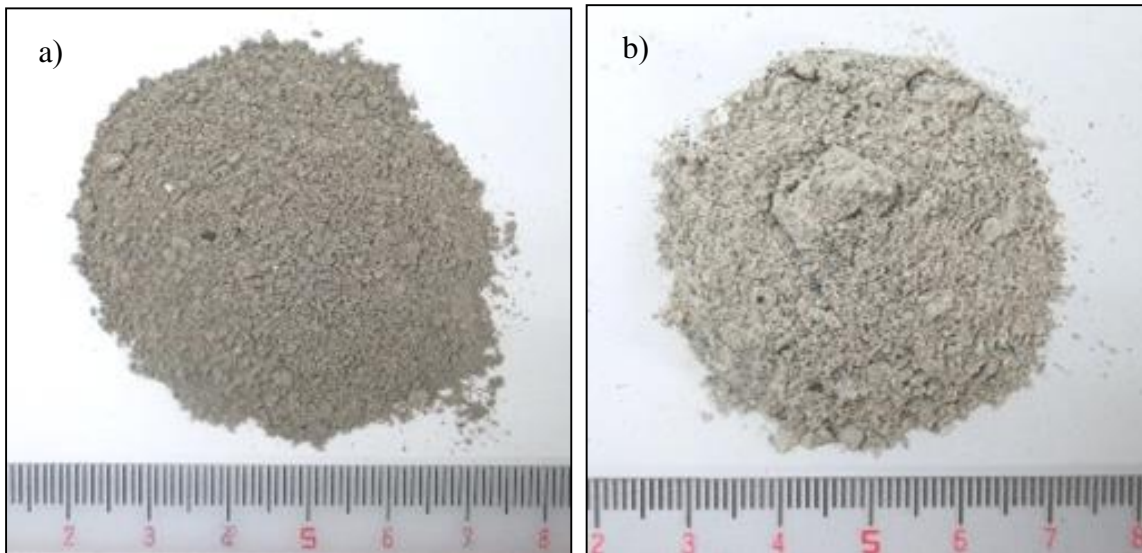


Figure 2.2 Physical appearance of grate siftings; a) the grate siftings under the combustion grate, and b) the grate siftings under the post-combustion grate.

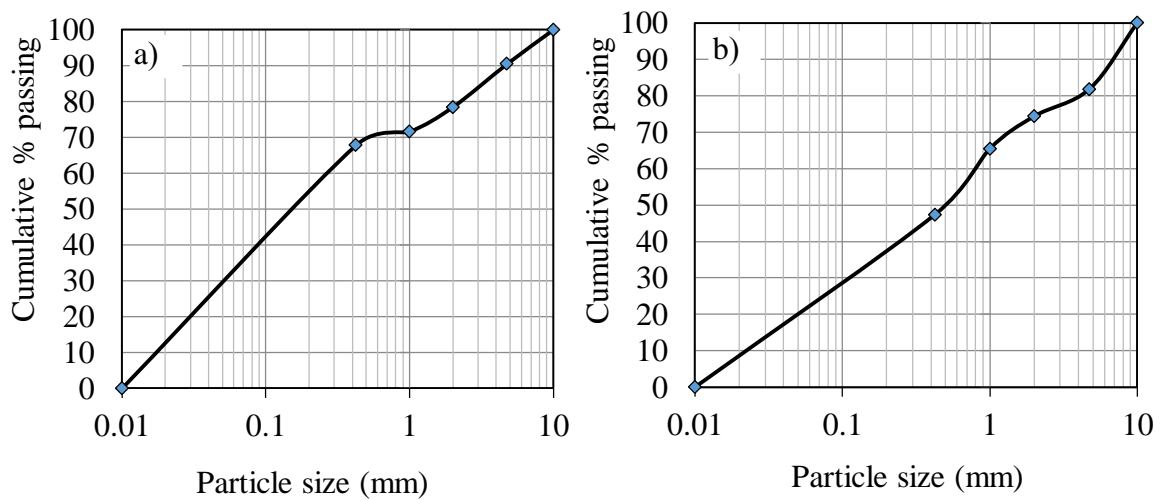


Figure 2.3 Particle size distributions of grate siftings; a) the grate siftings under the combustion grate, and b) the grate siftings under post-combustion grate.



Figure 2.4 Grate siftings with particles larger than 4.75 mm obtained after sieving by mesh.

In addition, the slag particles separated from the bulk grate siftings showed similarity of their morphology that could be determined as a porous aggregate in light/dark brown, grey/reddish-brown color as described by [Pfrang-Stotz and Schneider \(1995\)](#). The representative slag particles of grate siftings were picked up to prepare thin-section and were observed under a petrographic microscope. The observation showed that the structure of the slag in grate sifting from two different stage of combustion were dominant with the melt glass. The particles partly melted in some places giving rise to vitreous structures. Voids or vesicles are

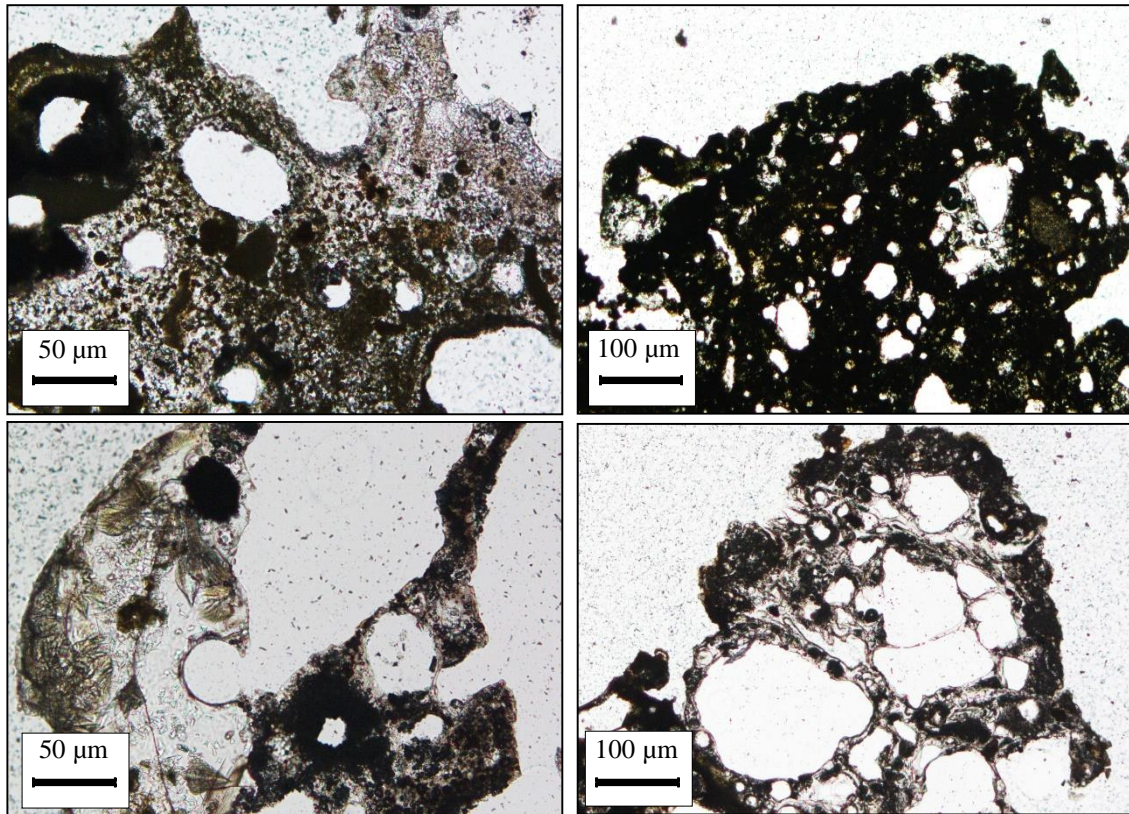


Figure 2.5 Morphological characteristic of the grate siftings' thin sections under plane polarized light mode of petrographic light microscope.

commonly found in the melt product. It is formed during boiling/degassing of the melt product (Eighmy et al., 1994). Large and small voids are very frequent showing that the particles were degassed under the temperature lower than 800 °C (Pfrang-Stotz and Schneider, 1995). However, there is no obvious outer layer at the external surface of the material.

2.4.1.2 CHEMICAL CHARACTERISTICS

The results of bulk analysis of major chemical composition by XRF are given in Table 2.1, as well as loss on ignition (LOI), moisture content and pH value. The composition of elements is reported in the form of oxides (excepted Cl and S) due to the analysis was done in the presence of air at high temperature in a platinum crucible with lithium borates. It was found that approximately 80-86 % of samples consist of CaO, SiO₂, Al₂O₃, and Fe₂O₃. All samples also contained TiO₂, MnO, P₂O₅, MgO, Na₂O K₂O, Cl, and S, however, in proportions of each lower than 5 % by dry weight. Unsurprisingly, the LOI of grate sifting under the different combustion stage was different. It is found that although all samples had the same moisture content (0.3 %), but the grate siftings under

the combustion grate had higher LOI than the grate siftings under the post-combustion grate. The results of LOI 4.1 % in the former and 0.4 % in the later indicated the containment degree of volatile substances. The major volatile that caused the high LOI in this case is presumed to be the uncompleted burnt organic carbon due to it is found that the grate sifting under the combustion grate has the darker color comparing to the sample under the post-combustion grate. This presumption is confirmed by the pH level of the samples which are 12.3 in the former and 12.8 in the later, respectively.

Table 2.1 Chemical compositions, LOI, moisture contents and pH of grate siftings.

Element	Units	Grate sifting under combustion grate	Grate sifting under post-combustion grate
CaO	%wt	42.03	43.86
SiO ₂	%wt	18.40	24.53
Al ₂ O ₃	%wt	9.90	10.62
Fe ₂ O ₃	%wt	9.33	6.65
P ₂ O ₅	%wt	4.06	2.86
MgO	%wt	3.71	4.67
Cl	%wt	2.60	1.51
Na ₂ O	%wt	2.48	2.33
TiO ₂	%wt	1.65	1.66
K ₂ O	%wt	0.77	0.52
MnO	%wt	0.43	0.11
S	%wt	0.48	0.25
LOI (440 °C)	%	4.1	0.4
Moisture content	%	0.3	0.3
pH (1:10)		12.3	12.8

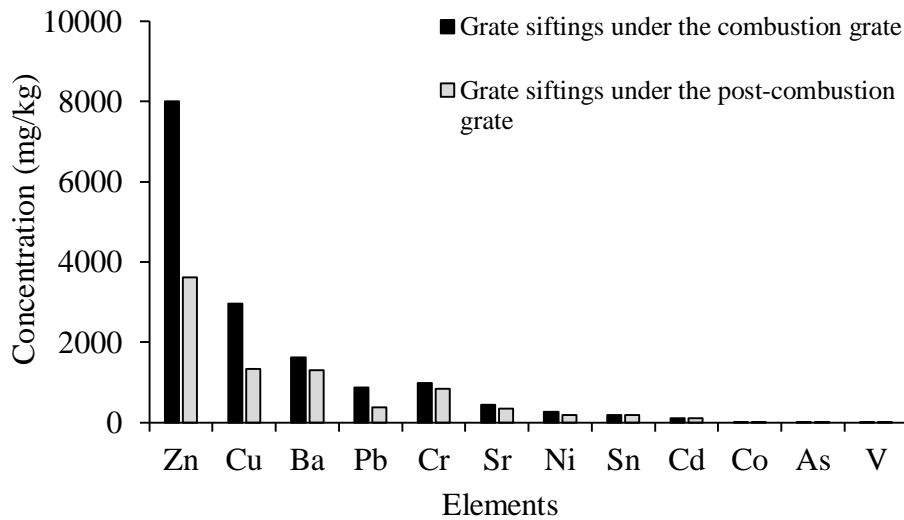


Figure 2.6 Total heavy metals concentrations in grate siftings.

Figure 2.6 shows the total concentration of heavy metals in the grate siftings. It is found that grate siftings deposited under the combustion grate and the post-combustion grate might be the potential source of Zn, Cu, Ba, Pb, and Cr in the bottom ash with the total concentration in excess of 500 mg/kg. Ni, Sn, Sr, and Cd were found in ranges between 100-400 mg/kg, while As, V and Co were found at concentrations below 10 mg/kg. The result obtained from this study was slightly lower than that reported by Wiles (1996). In addition, it should be noted here that the concentration of heavy metals in the grate siftings under the combustion grate was usually found to be higher than the grate siftings under the post-combustion grate, particularly the concentration of Zn and Cu. This probably due to the volatilization of these elements during combustion.

2.4.1.3 MINERALOGICAL CHARACTERISTICS

Figure 2.7 shows the X-ray diffraction data of grate siftings. It was found that the minerals that could identify by traditional search-match utilizing the XRD data included calcite, quartz, gehlenite, lime, halite, tricalcium aluminate, hematite, plagioclase feldspar, and mayenite. Among identified mineral, calcite was the most dominant phase. The mineral patterns of two grate sifting samples were quite similar; however, the height of peak of each identified mineral was different. Besides, lime was also found in two grate sifting samples.

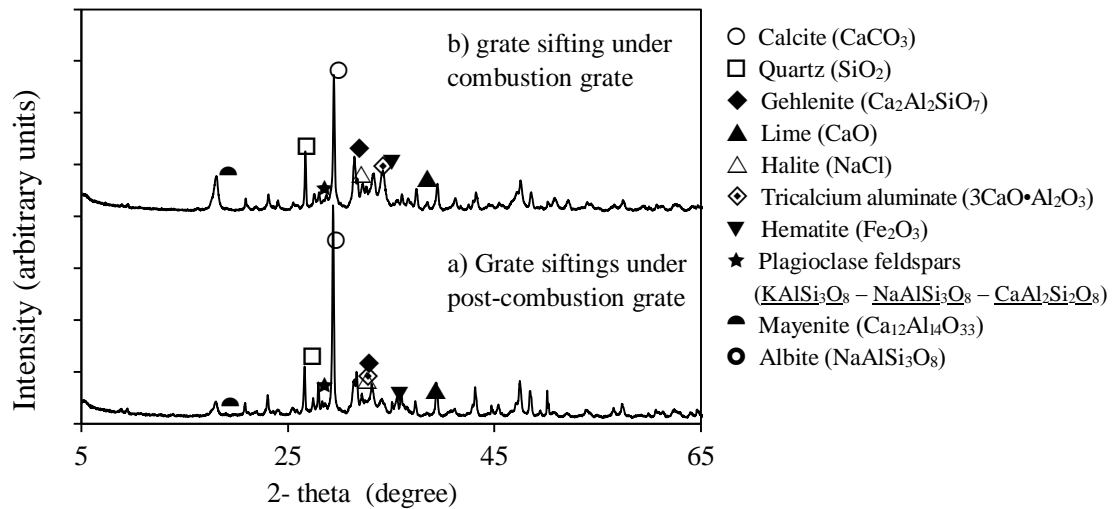


Figure 2.7 X-ray diffraction data of grate siftings.

2.4.2 UNQUENCHED BOTTOM ASH

Regardless to the incineration plant with dry ash discharger, generally all ashes on the post-combustion grate will be transferred to the quenching tank simultaneously. The grate ash which is referred here as the unquenched bottom ash should have the same characteristic as the bottom ash that discharged from the dry ash discharger in terms of no reaction with water. The results of physical, chemical, and mineralogical characteristic investigation are discussed in following section.

2.4.2.1 PHYSICAL CHARACTERISTIC

The unquenched bottom ash is a heterogeneous mixture of slag, ferrous and non-ferrous metals, ceramics, glass, other non-combustible, and uncomplete-burnt organics. The physical appearance of the unquenched bottom ash looked coarser than the grate siftings and its color is white/brown-gray in the shade between the grate siftings under the combustion grate and the grate siftings under the post-combustion grate (Figure 2.8).



Figure 2.8 Physical appearance of unquenched bottom ash.

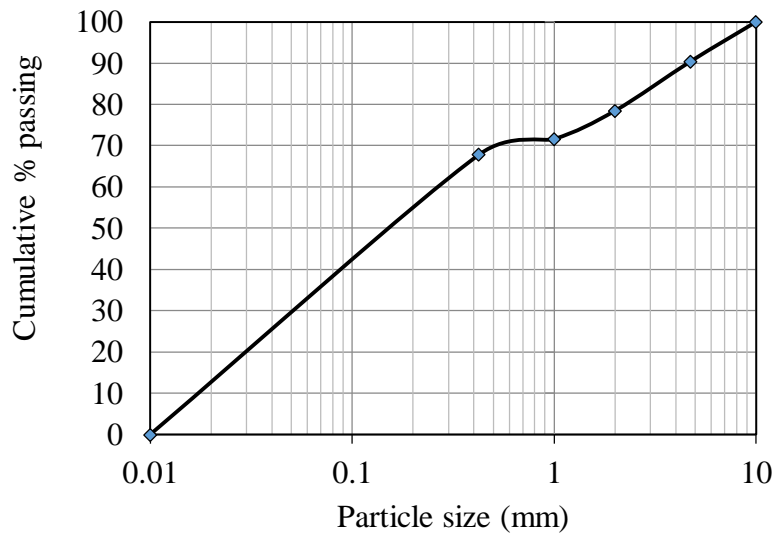


Figure 2.9 Particle size distribution of the unquenched bottom ash.

The analyses (Figure 2.9) indicated that up to 70 % of the unquenched bottom ash has a particle smaller than 1 mm, consisting mainly a powder-like ash and fine grain slag particle with partly ferrous and non-ferrous metal. The particle larger than 4.75 mm is accounted for 10 %. The thin section morphology of the unquenched bottom ash slag with particle size between 1.00-4.75 mm is resembled to the slag of grate siftings (Figure 2.10). From Figure 2.10, the particles are mainly composed of the melt products with porous microstructure. The melt product consists principally of vitreous phases in which an embedded crystalline fraction. Likewise, there is no obvious layer on the melt product external surface.

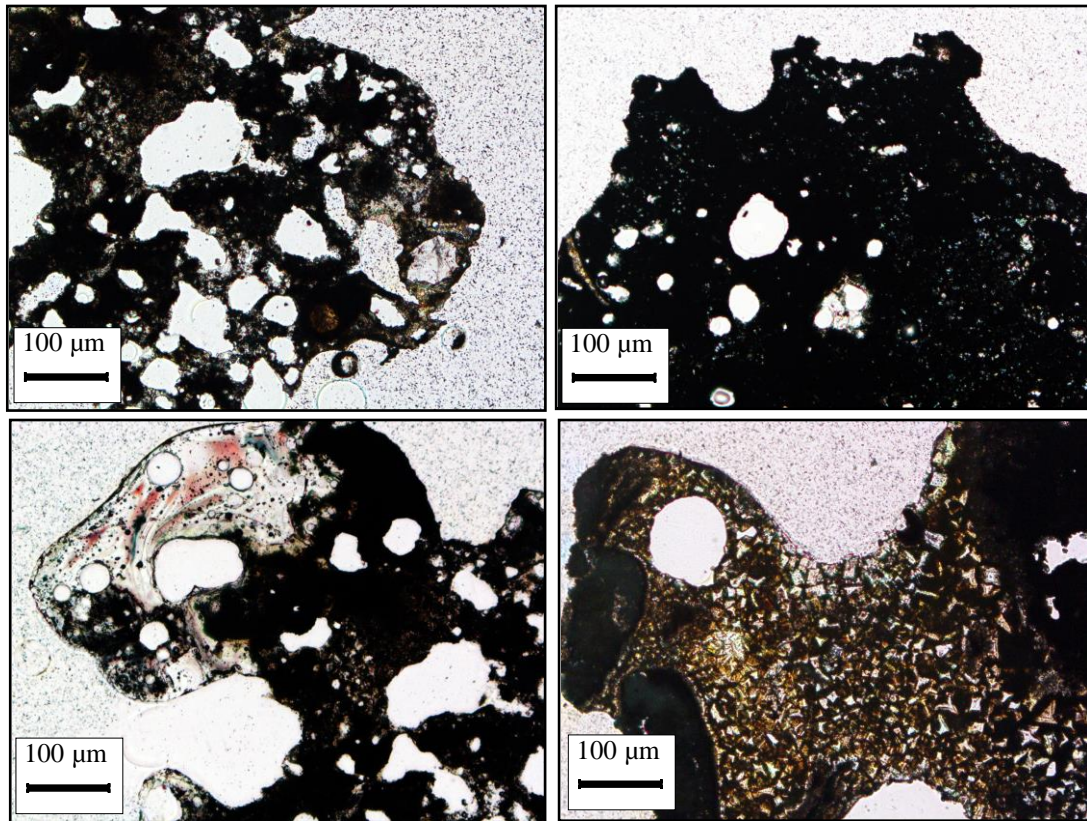


Figure 2.10 The thin section of unquenched bottom ash particles under plane polarized light mode of petrographic microscope.

Based on the thin section observation, the author quite agrees with [Pfrang-Stotz and Schneider \(1995\)](#) that the melt products in the bottom ash may be classified into three types; 1) vitreous type which consists of the partly black and dense structure with conchoidal fracture patterns reminiscent of obsidian volcanic glass, 2) porous type which large and small degassing voids are very frequent, 3) microcrystalline type which their structure contains only few degassing voids but dominated with secondary microcrystalline.

2.4.2.2 CHEMICAL CHARACTERISTIC

The results of XRF analysis showed that the chemical characteristic of the unquenched bottom ash was similar to the grate siftings, particularly to that deposited under the combustion grate. [Table 2.2](#) shows chemical composition, LOI, moisture contents and pH of unquenched bottom ash. Apparently, about 83 % by weight of the unquenched bottom ash composed of CaO, SiO₂, Al₂O₃ and Fe₂O₃. The minor compositions of the ash comprised of P₂O₅, MgO, Na₂O, TiO₂, Cl, K₂O, S and MnO in total amount of

about 13 %. The volatile substance contents, the moisture content and the pH value in the unquenched bottom ash were 4.1 %, 0.3 % and 12.2, respectively.

Considering heavy metals concentration ash as shown in [Figure 2.11](#), Zn is the most significant heavy metal contained in the unquenched bottom with the total concentration over 5,000 mg/kg. Additionally, Cu, Ba, Pb and Cr are also founded in the unquenched bottom ash by their concentration are in range between 500-1,700 mg/kg. Moreover, the unquenched bottom ash also contains Ni, Sn, Cd, Co, As and V but in trace concentration

Table 2.2 Chemical compositions, LOI, moisture contents and pH of unquenched bottom ash.

Compositions	Units	Unquenched bottom ash
CaO	%wt	44.21
SiO ₂	%wt	17.97
Al ₂ O ₃	%wt	12.34
Fe ₂ O ₃	%wt	8.70
P ₂ O ₅	%wt	3.18
MgO	%wt	2.88
Na ₂ O	%wt	1.98
TiO ₂	%wt	1.81
Cl	%wt	1.72
K ₂ O	%wt	0.45
S	%wt	0.45
MnO	%wt	0.22
LOI (440 °C)	%	4.1
Moisture content	%	0.3
pH (1:10)		12.2

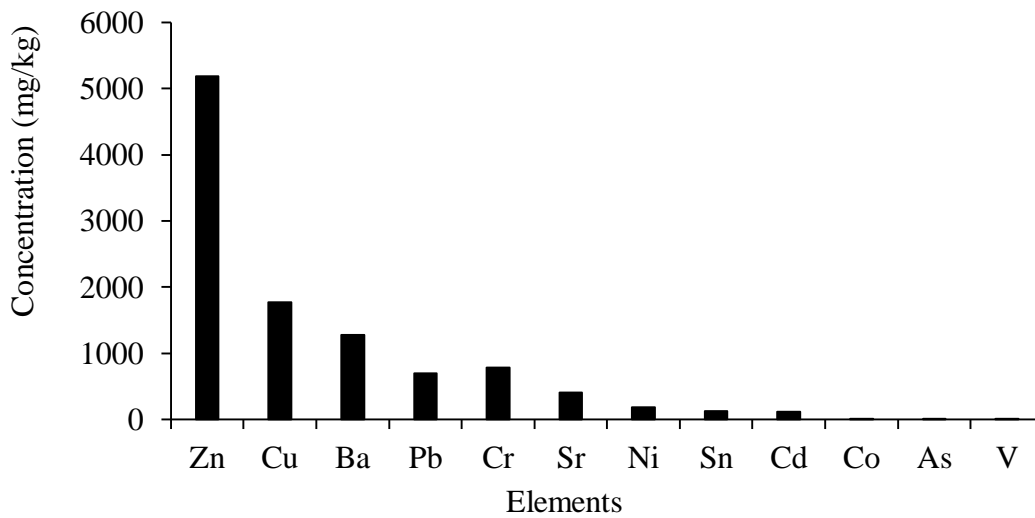


Figure 2.11 Heavy metals concentration in the unquenched bottom ash.

2.4.2.3 MINERALOGICAL CHARACTERISTIC

Figure 2.12 presents the result of XRD analysis of the unquenched bottom ash. The analytical result was fairly similar to the grate siftings. The unquenched bottom ash was dominant, mainly by calcite, gehlenite, halite, lime, quartz and tricalcium aluminate. Another mineral that possibly identified by XRD were hematite, plagioclase feldspars and mayenite. Clearly, lime intensity in the unquenched bottom is higher than grate siftings. This probably due to the burning condition inside furnace is between 850-1,100 °C which appropriate for the conversion of Ca into the oxide form.

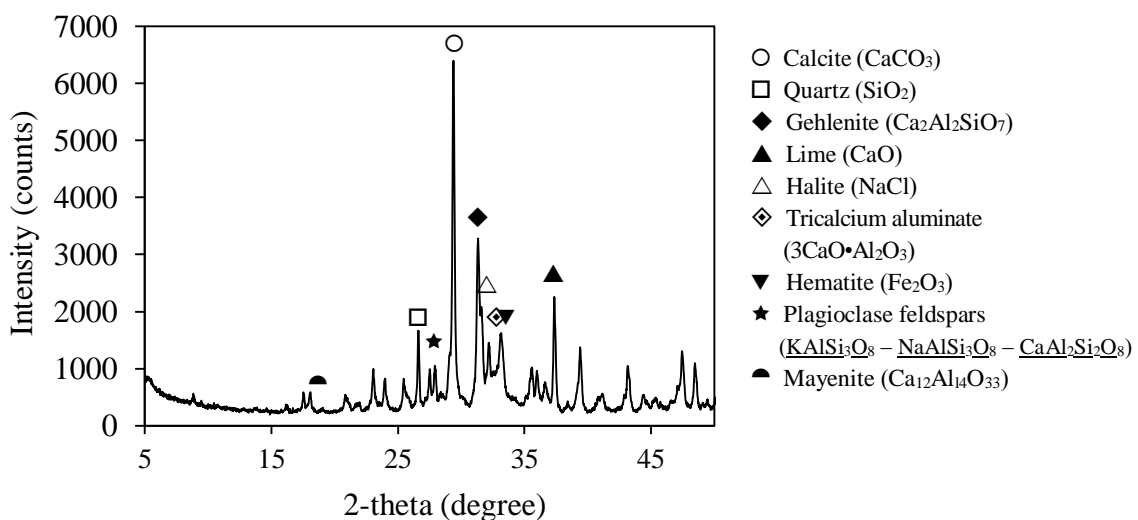


Figure 2.12 X-ray diffraction data of unquenched bottom ash.

2.4.3 QUENCHED BOTTOM ASH

The quenched bottom ash is obtained from the discharge end of the quenching tank. This ash is unique in term of exposing to water when compare to other residues generated from incineration.

2.4.3.1 PHYSICAL CHARACTERISTIC

The physical appearance of the dried quenched bottom ash ([Figure 2.3](#)) is quite similar to the unquenched bottom ash and grate siftings when it is piled, however, the quenched bottom ash has a whiter color comparatively. Besides, the individual particle is found to be agglomerated by the finer fraction. This agglomeration is different from the agglomeration caused by static force that found in the grate siftings and the unquenched bottom ash. By sieving, the finer fraction in the grate sifting and the unquenched bottom ash were separated easily, the slag particle that acts as the core clearly isolated. In case of the quenched bottom ash, even some fine particles were removed but most of the agglomerated particles still remained. Moreover, the sieve analyses provided the information that about 40 % of the quenched bottom ash particle less than 1 mm ([Figure 2.14](#)) in turn, about 60 % of the particle distributed mainly in the particles larger than 1 mm. This finding is different to the grate sifting and the unquenched bottom ash; thus, agglomeration of the quenched bottom ash seemingly caused by the quenching process. As the quenched bottom ash is coated by finer particles, it is hardly to classify the type of particle unless washing out by water. Unsurprisingly, the quenched bottom ash is the mixture of those that found in the grate sifting and the unquenched bottom ash such as slag, glass, ceramics, metals and other those remains after combustion. However, due to ferrous metals are vulnerable to be oxidized when exposed to water, they usually appear with rust in the quenched bottom ash.



Figure 2.13 Physical appearance of the quenched bottom ash.

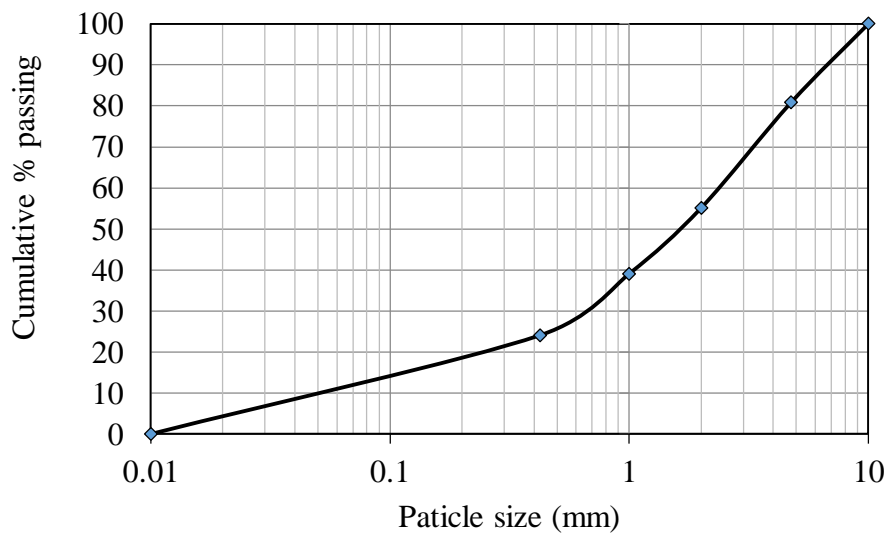


Figure 2.14 Particle size distribution of the quenched bottom ash.

The thin section analyses provided evidence that the quenched bottom ash contained the distinct layer outer the melt product. [Figure 2.15](#) reveals the internal microstructure of selective quenched bottom ash particles with diameter size range between 1.00-4.75 mm. The investigation indicated that over 90 % of the representative samples from this study accommodated by this kind of additional product. From the particle distribution analyses, it is assumed that this product originated from the fine fraction of the grate siftings and the unquenched bottom ash, however, the assumption need for further investigation.

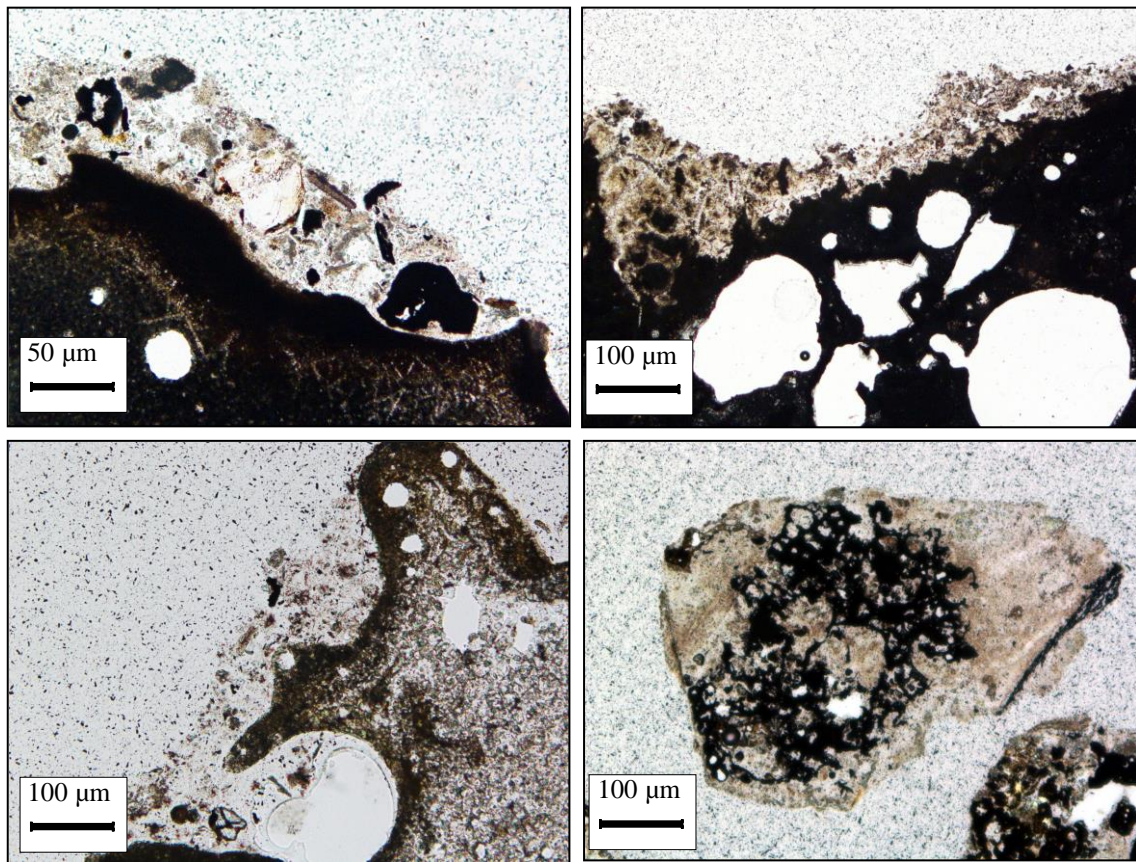


Figure 2.15 The thin section of quenched bottom ash particles under plane polarized light mode of petrographic microscope.

The adhered product on the quenched bottom ash was defined as “the quench product”, due to it was found after the bottom ash was quenched. The author quite agrees with [Wei \(2011\)](#) and [Saffarzadeh et al. \(2011\)](#) that this product was the fine ash particles that adhere to the melt phases during the water quenching process. However, details about its microstructure, composition and the formation mechanism remain less information. Basically, the quench product has a fragile characteristic with transparency under the plane polarized light of the petrographic microscope. The color of this product is found to be vary from the brow-yellow to slightly pale-clear yellow or color less. The texture of the quench product is heterogeneous contains microcrystalline, tiny pieces of the melt product, glass, ceramics, metal, organic matter and other unidentified substance ([Saffarzadeh et al., 2011](#)).

2.4.3.2 CHEMICAL CHARACTERISTIC

The results obtained from the bulk chemical analysis by XRF (Table 2.3) indicates that CaO, SiO₂, Al₂O₃, and Fe₂O₃ are main composition of the quenched bottom ash in which accounted for about 85 % by weight. The minor elements are included P₂O₅, MgO, TiO₂, Na₂O, MnO, K₂O, Cl and S with the concentration of each lesser than 3 % by weight. The composition of the quenched products is somewhat different from the grate sifting and the unquenched bottom ash, particularly CaO, Na₂O and Cl which lower in comparison. This probably due to dissolution of these substances into quenching water. Moreover, it is found that in the quenched bottom ash, LOI is 5.3 %, pH value is lower than 12, but moisture content is fairly high up to 45 %.

Table 2.3 Chemical compositions, LOI, moisture contents and pH of quenched bottom ash.

Compositions	Units	Quenched bottom ash
CaO	%wt	37.03
SiO ₂	%wt	18.14
Al ₂ O ₃	%wt	16.44
Fe ₂ O ₃	%wt	13.33
P ₂ O ₅	%wt	2.86
MgO	%wt	2.22
TiO ₂	%wt	1.66
Na ₂ O	%wt	1.45
MnO	%wt	0.16
K ₂ O	%wt	0.31
Cl	%wt	0.68
S	%wt	0.40
LOI (440 °C)	%	5.3
Moisture content	%	45.3
pH (1:10)		11.7

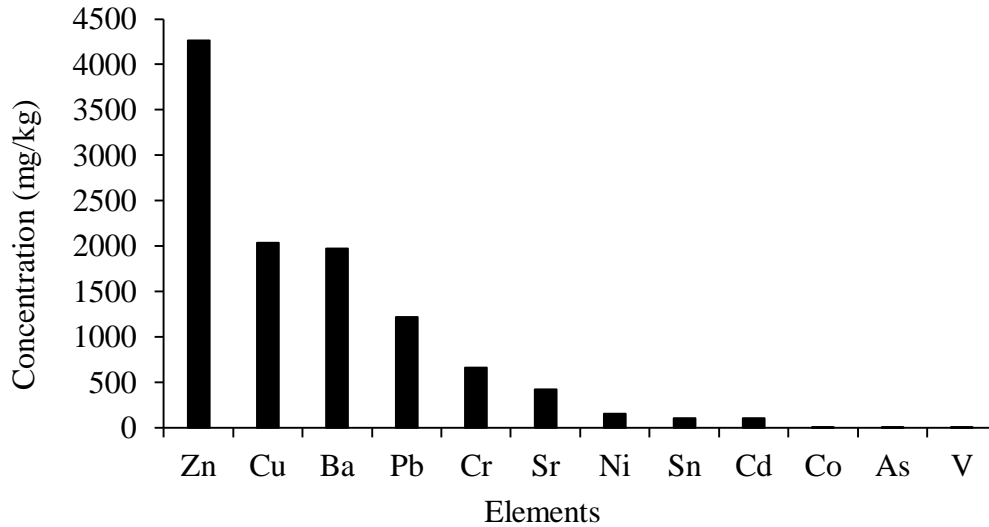


Figure 2.16 Heavy metals content in the bottom ash.

Figure 2.16 shows heavy metals content in the quenched bottom ash. In consistent with above statement, quenching process seem to influence to the concentration of some heavy metals in the bottom ash. Apparently, the concentration of Zn is lower two folds comparing to the grate sifting under the combustion grate, and lower about 1,000 mg/kg when compare to the unquenched bottom ash. This indicates that partly of Zn is removed out by quenching water. Among other heavy metals, Cu, Ba and Pb concentrations seem to increase in comparative to unquenched bottom ash. This is probably due to the quenched bottom ash receives these metal from grate siftings, so the concentrations in the quenched bottom ash is found to be higher than the unquenched bottom ash. Although Cu, Cr are also lithophillic metal, only Zn is affected by quenching evidently.

2.4.3.3 MINERAL CHARACTERISTIC

Due to the quenched bottom ash is produced under the high temperature and subsequently quenched into quenching water, the mineral characteristic of the quenched bottom ash is expected to be different from the unquenched bottom ash. Figure 2.17 shows mineral patterns of the quenched bottom ash. Clearly, the quenched bottom ash consists calcite, quartz, and gehlenite as basic mineral that could readily have identified as reported by other researchers (Eighmy et al., 1994; Eusden et al., 1999; Pfrang-Stotz and Schneider, 1995; Piantone et al., 2004; Saffarzadeh et al., 2011; Speiser et al., 2000; Wei et al., 2011).

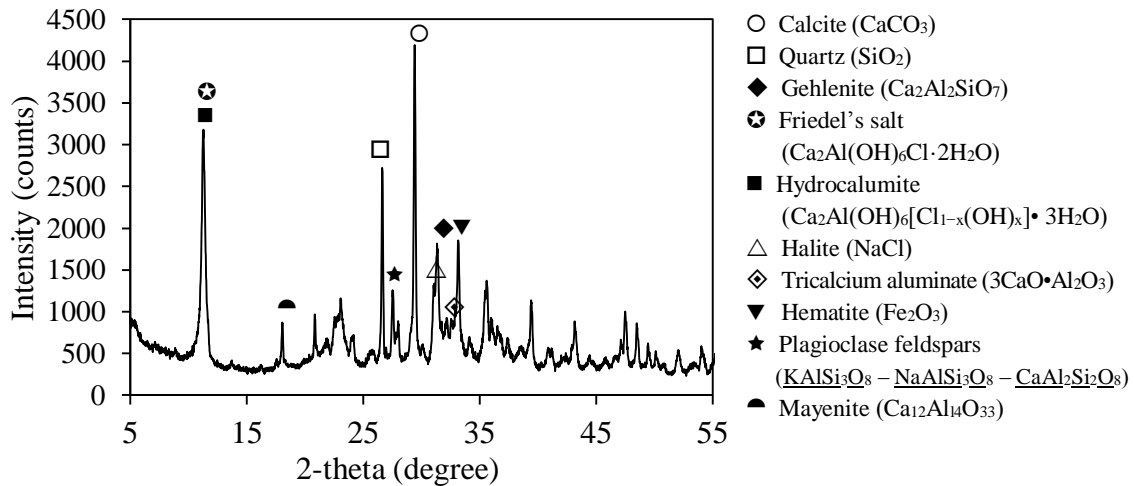


Figure 2.17 X-ray diffraction data of quenched bottom ash.

The other minerals that could be identified by XRD in this study are also included hydrocalumite/Friedel's salt, hematite, halite, plagioclase feldspars, mayenite and tricalcium aluminate. Obviously, hydrocalumite/Friedel's salt is only the mineral that could be found in the quenched bottom ash. This finding is consistent with [Yang et al. \(2014\)](#).

2.5 FINDING SYNTHESIS AND DISCUSSION

Based on results, grate siftings, unquenched bottom ash and quenched bottom ash were made up of different proportions of slag particles, relic metal, glass, ceramics, and unburned organic matter. These constituents are reported world-wide as the basic component of bottom ash ([Chandler et al., 1997](#); [Lam et al., 2010](#); [Li et al., 2004](#); [Wiles, 1996](#)). Commonly, the component of MSWI residues could be easily classified in a particle larger than 4.75 mm. However, it is impractical to classify particles smaller than 4.75 mm by visual observation and the percentage of these constituents is not included in this thesis.

The result of particle size distribution analysis indicated some impact of water quenching on quenched bottom ash particle size distribution/transformation. During quenching, fine particles from grate siftings and unquenched bottom ash may accumulate in larger particles by attaching to its surface and transforming into a quenched bottom ash. [Saffarzadeh et al. \(2011\)](#) reported that quenched bottom ash fragments were made up of a rigid core wrapped in a coating of poorly-bound and ultra-fine particles. This explains why

60 % by weight of quenched bottom ash particles were made up of particles larger than 1 mm. However, literature on the transformation of bottom ash during water quenching is very limited. The mechanisms of bottom ash transformation during the quenching process still remain challenging to investigate.

As it is already mentioned, incineration bottom ash (including grate sifting deposition ash) is generated through partial melting of the inorganic constituents of the waste stream. A complex of ash particles normally includes the amorphous melt glass phase, the mineral crystalline phase, and the refractory product (Saffarzadeh et al., 2011; Wei et al., 2011). A fragile phase, or quench product, is also found in fresh-quenched bottom ash in this study. Although it was reported that this layer seemed to provide effective porosity to fresh bottom ash particles (Saffarzadeh et al., 2011), there have been very limited study of it. Further research concerning its characterization, formation mechanisms, and particular functions, may therefore be required to enhance understanding of bottom ash transformation characteristics, in turn providing useful insights for subsequent management and utilization. Results showed that pH values of all samples are alkaline, in the range of 11.7-12.8., but the quenched bottom ash has the lowest pH of the samples. This indicates that water quenching influenced the pH of bottom ash by reducing its alkalinity. As unquenched products (grate siftings and unquenched bottom ash) have pH over 12, with moisture content less than 1 % by weight, interaction of these materials with water during quenching leads to absorption of water into ash particles. At the same time, soluble salt dissolves into the quenching water, leading to lower pH in quenched bottom ash. Through adsorption and micro-capillary forces, some water is absorbed by the ash particle surface, and some water fills in particle pores, resulting in high moisture content of up to 45 % in the quenched bottom ash.

Loss on ignition (LOI) is normally a measurement of the amount of volatile solids and/or unburned carbon in incineration residues. LOI can be used to determine the efficiency to the combustion process. The grate sifting under post-combustion grate was found to have LOI value of less than 1 % by dried mass while the grate sifting under combustion grate and the unquenched bottom ash have LOI of about 4 %. In the case of quenched bottom ash, LOI was about 5 % by dried mass. Given that the unquenched bottom ash was produced from high temperature (850-1,100 °C) treatment during incineration and the ignition temperature of LOI in this study was only 440 °C, the higher LOI percentage

of quenched bottom ash compared with other samples indicated content of decomposable salts that may precipitate during the quenching process, or incomplete burnt materials from the grate sifting under the combustion grate.

When comparing samples, it was found that the concentrations of CaO, Al₂O₃, and Fe₂O₃ in the quenched bottom ash were higher than in the grate siftings, and the unquenched bottom ash, while the concentrations of other compounds in the quenched bottom ash were lower than in the unquenched bottom ash. Since the quenched bottom ash was transformed as a result of quenching of hot grate siftings, and unquenched bottom ash in the quenching tank, elements contained in those hot ashes may undergo thermodynamic reactions to reach equilibrium (Speiser et al., 2000). There are several reactions that may occur during water quenching, including dissolution/precipitation of salt, oxidation, hydration, and carbonation (Chimenos et al., 2000). Although these reactions were studied from the point of view of alteration/aging of weathered bottom ash (Wei et al., 2011), these reactions require further investigation in terms of their role in quenching of bottom ash. Taking the example of Cl as one element that needs to be considered in terms of criteria for ash recycling, the result shows that grate siftings and unquenched bottom ash had a higher Cl content than the quenched bottom ash (by approximately 2-4 times). This indicates that substantial portions of Cl from unquenched bottom ash and grate siftings were dissolved in quenching water. Only limited quantities of Cl were precipitated in quenched bottom ash, in the form of decomposable salt (halite) and insoluble salts (Friedel's salt/ hydrocalumite).

Friedel's salt is a well-known insoluble chloride that cannot be easily removed from bottom ash. It poses an obstacle to the utilization of bottom ash in cement production. Some studies (Ito et al., 2008; Yang et al., 2014) have explored the removal of Friedel's salt from bottom ash for recycling purposes. However, the most effective method is washing with sulfuric acid, a solution that is rarely applied in reality. Understanding the formation and behavior of Friedel's salt in quenched bottom ash still requires further investigation.

2.5 CONCLUSIONS

The physical, chemical, and mineral characteristics of grate siftings, unquenched bottom ash, and quenched bottom ash were investigated in this study by using visual observation, analysis of particle size distribution, thin sections, bulk chemicals and mineral composition, and measurement of pH, moisture content, and LOI. It was found that the characteristics of grate siftings unquenched bottom ash and quenched bottom ash were heterogeneous. Characteristic of the origin ashes (grate siftings and unquenched bottom ash) and water quenching influenced to quenched bottom ash characteristic. The grate sifting deposition ash and the unquenched bottom ash were dominated by particles smaller than 1 mm. These two types of ash had lower moisture content, higher pH (over 12), and higher concentrations of CaO, P₂O₅, MgO, Na₂O, K₂O, and Cl, when compared to the quenched bottom ash. On the other hand, the latter was dominated by particles larger than 1 mm, with pH lower than 12, higher moisture content, higher LOI, and higher concentrations of Al₂O₃, Fe₂O₃, Ba, and Pb than grate siftings and unquenched bottom ash. The presence of the quench product in the quenched bottom ash and of Friedel's salt, the decline in pH, and the distinct elemental concentration of the quenched bottom ash all indicate the influence of water quenching on characteristics of the latter. Further research is required in details to explain the detail influence of water quenching, the formation mechanisms and functions of the quench product, the phenomena that undergoes during the quenching process; this would allow a better understanding of bottom ash characteristics, in turn enabling appropriate utilization or disposal.

REFERENCES

- Abbà, A., Collivignarelli, M.C., Sorlini, S., Bruggi, M., 2014. On the Reliability of Reusing Bottom Ash from Municipal Solid Waste Incineration as Aggregate in Concrete. *Compos. Part B Eng.* 58, 502–509. doi:10.1016/j.compositesb.2013.11.008
- Abdulahi, M.M., 2009. Municipal Solid Waste Incineration Bottom Ash as Road Construction Material. *AU.J.T.* 13, 121–128.
- Bayuseno, A.P., Schmahl, W.W., 2010. Understanding the Chemical and Mineralogical Properties of the Inorganic Portion of MSWI Bottom Ash. *Waste Manag.* 30, 1509–1520. doi:10.1016/j.wasman.2010.03.010
- Chandler, A.J., Eighmy, T.T., Hjelmar, O., Kosson, D.S., Sawell, S.E., Vehlow, J., Sloot, H.A. van der, Hartlén, J., 1997. *Municipal Solid Waste Incinerator Residues*. Elsevier.
- Chang, F.-Y., Wey, M.-Y., 2006. Comparison of the Characteristics of Bottom and Fly Ashes Generated from Various Incineration Processes. *J. Hazard. Mater.* 138, 594–603. doi:10.1016/j.jhazmat.2006.05.099
- Chimenos, J.M., Fernández, A.I., Nadal, R., Espiell, F., 2000. Short-term Natural Weathering of MSWI Bottom Ash. *J. Hazard. Mater.* 79, 287–299. doi:10.1016/S0304-3894(00)00270-3
- del Valle-Zermeño, R., Chimenos, J.M., Giró-Paloma, J., Formosa, J., 2014. Use of Weathered and Fresh Bottom Ash Mix Layers as a Subbase in Road Constructions: Environmental Behavior Enhancement by Means of a Retaining Barrier. *Chemosphere* 117, 402–409. doi:10.1016/j.chemosphere.2014.07.095
- Eighmy, T.T., Eusden Jr., J.D., Marsella, K., Hogan, J., Domingo, D., Krzanowski, J.E., Stämpfli, D., 1994. Particle Petrogenesis and Speciation of Elements in MSW Incineration Bottom Ashes, in: J.J.J.M. Goumans, H.A. van der S. and T.G.A. (Ed.), *Studies in Environmental Science, Environmental Aspects of Construction with Waste Materials Proceeding of the International Conference on Environmental Implications of Construction Materials and Technology Developments*. Elsevier, pp. 111–136.
- Eusden, J.D., Eighmy, T.T., Hockert, K., Holland, E., Marsella, K., 1999. Petrogenesis of Municipal Solid Waste Combustion Bottom Ash. *Appl. Geochem.* 14, 1073–1091. doi:10.1016/S0883-2927(99)00005-0
- Forteza, R., Far, M., Seguí, C., Cerdá, V., 2004. Characterization of Bottom Ash in Municipal Solid Waste Incinerators for Its Use in Road Base. *Waste Manag.* 24, 899–909. doi:10.1016/j.wasman.2004.07.004
- Ito, R., Dodbiba, G., Fujita, T., Ahn, J.W., 2008. Removal of Insoluble Chloride From Bottom Ash for Recycling. *Waste Manag.* 28, 1317–1323. doi:10.1016/j.wasman.2007.05.015
- Kirby, C.S., Rimstidt, J.D., 1993. Mineralogy and Surface Properties of Municipal Solid Waste Ash. *Environ. Sci. Technol.* 27, 652–660. doi:10.1021/es00041a008

- Lam, C.H.K., Barford, J.P., McKay, G., 2011. Utilization of Municipal Solid Waste Incineration Ash in Portland Cement Clinker. *Clean Technol. Environ. Policy* 13, 607–615. doi: 10.1007/s10098-011-0367-z
- Lam, C.H.K., Ip, A.W.M., Barford, J.P., McKay, G., 2010. Use of Incineration MSW Ash: A Review. *Sustainability* 2, 1943–1968. doi:10.3390/su2071943
- Li, M., Xiang, J., Hu, S., Sun, L.-S., Su, S., Li, P.-S., Sun, X.-X., 2004. Characterization of Solid Residues From Municipal Solid Waste Incinerator. *Fuel* 83, 1397–1405. doi:10.1016/j.fuel.2004.01.005
- Ministry of the Environment, 2014. History and Current State of Waste Management in Japan.
- Mohamed, B.M., Sharp, J.H., 2002. Kinetics and Mechanism of Formation of Tricalcium Aluminate, $\text{Ca}_3\text{Al}_2\text{O}_6$. *Thermochim. Acta* 388, 105–114. doi:10.1016/S0040-6031(02)00035-7
- Pfrang-Stotz, G., Schneider, J., 1995. Comparative Studies of Waste Incineration Bottom Ashes From Various Grate and Firing Systems, Conducted With Respect To Mineralogical and Geochemical Methods of Examination. *Waste Manag. Res.* 13, 273–292. doi:10.1177/0734242X9501300307
- Piantone, P., Bodéan, F., Chatelet-Snidaro, L., 2004. Mineralogical Study of Secondary Mineral Phases from Weathered MSWI Bottom Ash: implications for the modelling and trapping of heavy metals. *Appl. Geochem.* 19, 1891–1904. doi:10.1016/j.apgeochem.2004.05.006
- Sabbas, T., Poletini, A., Pomi, R., Astrup, T., Hjelmar, O., Mostbauer, P., Cappai, G., Magel, G., Salhofer, S., Speiser, C., Heuss-Assbichler, S., Klein, R., Lechner, P., 2003. Management of Municipal Solid Waste Incineration Residues. *Waste Manag.* 23, 61–88. doi:10.1016/S0956-053X(02)00161-7
- Saffarzadeh, A., Shimaoka, T., Wei, Y., Gardner, K.H., Musselman, C.N., 2011. Impacts of Natural Weathering on the Transformation/Neoformation Processes in Landfilled MSWI Bottom Ash: A geoenvironmental perspective. *Waste Manag.* 31, 2440–2454. doi:10.1016/j.wasman.2011.07.017
- Saikia, N., Mertens, G., Van Balen, K., Elsen, J., Van Gerven, T., Vandecasteele, C., 2015. Pre-treatment of Municipal Solid Waste Incineration (MSWI) Bottom Ash for Utilisation in Cement Mortar. *Constr. Build. Mater.* 96, 76–85. doi:10.1016/j.conbuildmat.2015.07.185
- Speiser, C., Baumann, T., Niessner, R., 2001. Characterization of Municipal Solid Waste Incineration (MSWI) Bottom Ash by Scanning Electron Microscopy and Quantitative Energy Dispersive X-ray Microanalysis (SEM/EDX). *Fresenius J. Anal. Chem.* 370, 752–759. doi:10.1007/s002160000659
- Speiser, C., Baumann, T., Niessner, R., 2000. Morphological and Chemical Characterization of Calcium-Hydrate Phases Formed in Alteration Processes of Deposited Municipal Solid Waste Incinerator Bottom Ash. *Environ. Sci. Technol.* 34, 5030–5037. doi:10.1021/es990739c

- Suryavanshi, A.K., Scantlebury, J.D., Lyon, S.B., 1996. Mechanism of Friedel's salt formation in cements rich in tri-calcium aluminate. *Cem. Concr. Res.* 26, 717–727. doi:10.1016/S0008-8846(96)85009-5
- Themelis, N.J., Mussche, C., 2013. Municipal Solid Waste Management and Waste-to-Energy in the United States, China and Japan. Presented at the 2nd International Academic Symposium on Enhanced Landfill Mining, Houthalen-Helchteren, pp. 1–19.
- Thomas, B.S., Anoop, S., Kumar, V.S., 2012. Utilization of Solid Waste Particles as Aggregates in Concrete. *Procedia Eng.*, International Conference on Modelling Optimization and Computing 38, 3789–3796. doi:10.1016/j.proeng.2012.06.434
- van der Sloot, H.A., Kosson, D.S., Hjelm, O., 2001. Characteristics, treatment and utilization of residues from municipal waste incineration. *Waste Manag.* 21, 753–765. doi:10.1016/S0956-053X(01)00009-5
- Wegen, G. van der, Hofstra, U., Speerstra, J., 2013. Upgraded MSWI Bottom Ash as Aggregate in Concrete. *Waste Biomass Valorization* 4, 737–743. doi:10.1007/s12649-013-9255-6
- Wei, Y., 2011. Geoenvironmental Study of MSWI Bottom Ash with Emphasis on Secondary Mineralization and Behavior of Heavy Metals. Kyushu University, Fukuoka, Japan.
- Wei, Y., Shimaoka, T., Saffarzadeh, A., Takahashi, F., 2011. Mineralogical Characterization of Municipal Solid Waste Incineration Bottom Ash with an Emphasis on Heavy metal-bearing phases. *J. Hazard. Mater.* 187, 534–543. doi:10.1016/j.jhazmat.2011.01.070
- Wiles, C.C., 1996. Municipal Solid Waste Combustion Ash: State-of-the-Knowledge. *J. Hazard. Mater.* 47, 325–344. doi:10.1016/0304-3894(95)00120-4
- Yamamoto, H., Yokoyama, T., Oshita, K., Takaoka, M., Takeda, N., 2007. The Study of Shifting of Valuable Metals to Riddling Ash in Municipal Solid Waste Incineration Process. *J. Jpn. Soc. Waste Manag. Experts* 18, 314–324. doi:10.3985/jswme.18.314
- Yang, S., Saffarzadeh, A., Shimaoka, T., 2012. Influence of Ignition process on the Weight Loss and Mineral Phase Change in MSWI Ash: LOI of Incineration ash, in: EAEP2012 The 6th International Symposium on the East Asian Environmental Problems. Presented at the EAEP2012 The 6th International Symposium on the East Asian Environmental Problems, Research Institute for East Asia Environments, Inamoricenter, Kyushu University, Japan, pp. 42–46.
- Yang, S., Saffarzadeh, A., Shimaoka, T., Kawano, T., 2014. Existence of Cl in Municipal Solid Waste Incineration Bottom Ash and Dechlorination Effect of Thermal Treatment. *J. Hazard. Mater.* 267, 214–220. doi:10.1016/j.jhazmat.2013.12.045

CHAPTER 3

INFLUENCE OF WATER QUENCHING ON THE MSWI BOTTOM ASH CHARACTERIZATION

CHAPTER 3

INFLUENCE OF WATER QUENCHING ON THE MSWI BOTTOM ASH CHARACTERIZATION

3.1 ABSTRACT

Water quenching is a fundamental process of the wet discharge system widely used in MSWI plant. In this chapter, representative samples from two incineration plants (Kamitsu and Nishiyodo) with the different quenching system; drag chain conveyer tank and hydraulic ram discharger were investigated. Unquenched and freshly quenched bottom ashes were sampled from the same combustion line of each incineration. The particle size distribution analysis, thin section analysis, intact particle analysis, specific surface area analysis, pH and bulk chemical composition analysis, and mineralogical analysis were conducted to evaluate the impacts of water quenching on the characterization of bottom ash products. The result showed that water quenching was considerable influence on the bottom ash characterization by changing particle size, increasing specific surface area, changing its morphology by forming the quench product, reducing pH, altering the chemical composition, and enhancing portlandite, hydrocalumite and Friedel's salt formation.

3.2 INTRODUCTION

Water quenching is a process to cool down hot bottom ash that applied at the end of the combustion furnace of municipal solid waste incineration plant before discharging to the ash storage pit. Since the combusted ash may still contain carbon that would continue to smolder after leaving the grate, the water serves to extinguish any remaining combustibles and cool the ash. Besides, it also helps to reduce the size of the large clinker and helps to prevent dust pollution inside the plant (Chandler et al., 1997). Therefore, Water quenching is a fundamental process adapted to the wet discharge system widely used in the incineration plant.

There are several types of quenching system such as drag chain conveyers, plate conveyers, and hydraulically ram type systems (Chandler et al., 1997). However, the drag chain conveyer with the water tank and the hydraulic ram discharger are the most common in Japan. Due to bottom ash is formed at high temperature and subsequently quenched, the alteration is immediately started (Chimenos et al., 2005). As the initial stage of weathering, reactions in quenching tank may involve a complex series of hydrolysis of the oxides of Ca, Al, Na, and K, the dissolution/precipitation of hydroxides and salts, and carbonation (Meima and Comans, 1997a). It is recognized that water quenching lead to remarkably change of bottom ash characteristics (Chandler et al., 1997).

Until recently, most researches have focused on the alteration of bottom ash as reactive materials, particularly under the landfill condition or road construction application (Chimenos et al., 2005; Marchese and Genon, 2011; Meima and Comans, 1999; Saffarzadeh et al., 2011; Zevenbergen et al., 1998). Although bottom ash becomes more and more interesting in point of view of material recycling and environmentally disposal, only a few reports are available for the influence of quenching on bottom ash characteristic (Marchese and Genon, 2011; Speiser et al., 2000). Meima and Comans (1997a) identified the geochemical processes that control leaching characteristics of bottom ash and defined that early stage of weathering in bottom ash took place in the quenching tank. Marchese and Genon, (2011) studied the effect of leaching behavior by quenching of bottom ash and found that the formation and dissolution of soluble alkalis depend on the washing ratio and on the residence time. A distinctive washing degree leads to a different residual alkalinity in the bottom ash, and consequently, to a variable value of leachate pH and metal release. Some previous studies noticed the existence of the fragile zone (or so-called the quench phase/product) after quenching (Inkaew et al., 2014; Saffarzadeh et al., 2011; Wei et al., 2011; Yang et al., 2014). However, details of this product and the influence on bottom ash characterization remain a challenge to investigate.

In order to uncover the influence of water quenching on bottom ash thoroughly with respecting to system design, unquenched and freshly quenched bottom ashes were

characterized. The influence of water quenching was particularly focused on particle size distribution, particle morphology, specific surface area, mineral composition, pH value and Cl distribution. The novel of research will allow more understanding the complexity of water quenching and the nature of quenched bottom ash product that may guide to modify the constituency for subsequent reuse or disposal.

3.3 MATERIALS AND METHODS

3.3.1 PLANT DESCRIPTION

Samples of unquenched and freshly quenched bottom ash were obtained from two mass-burn incineration plants (Kamitsu and Nishiyodo). Both plants are three stages combustion grate designed for thermal treatment of household waste. Nishiyodo incineration plant (Plant N) has total capacity of 600 tons per day. Following combustion, bottom ash is water-quenched in the tank filled with water and then is carried out by a drag chain conveyer with moisture contents about 45 wt%. Kamitsu incineration plant (Plant K) has total capacity of 300 tons per day. The water quenching system is hydraulic ram discharger (Martin designed). In addition, the moisture content of freshly quenched bottom ash of this plant is about 24 wt%.

3.3.2 SAMPLING

The unquenched bottom ash was sampled from the top of the burnout grate during the routine maintenance, and the freshly quenched bottom ash was sampled at the discharge exit of the quenching tank before transferring to the ash storage pit. The freshly quenched bottom ash was air dried to remove the moisture, followed by freeze drying for 24 h. After that, the large particles that are initially composed of refractory ceramic, glass and metal were removed by a 9.5 mm sieve. Then they were split into sub-sample using cone and quartering technique. A 10 kg sub-sample was kept in air-tight container and used for further analyses. The supply water for quenching (5 l) and quenching water (20 l) were also sampled and kept in air tight plastic bottles in a cool environment (4 °C) for further analyses.

3.3.3 ANALYTICAL METHOD

To investigate the impacts of water quenching process, bottom ash samples were subjected to following analyses: The particle size distribution analysis was done by the conventional sieving method and classifying the samples into particle size classes of diameter (d) < 0.075mm, 0.075-0.125 mm, 0.125-0.250 mm, 0.250-0.425 mm, 0.425-1.00 mm, 1.00-2.00 mm, 2.00-4.75 mm, and > 4.75 mm, respectively. Several particles were carefully picked out from middle size range fraction (1.00-2.00 mm) by the binocular stereo microscope in order to prepare standard petrographic thin sections. Thin section observation was completed by Olympus BX51 petrographic polarized microscope. Scanning electron microscope in combination with Energy-dispersive X-ray spectroscopy (SEM/EDX) was applied to polished thin sections and intact particle observation. The specific surface area was measured by automatic adsorption apparatus (BELSORP-mini) using Brunauer, Emmett and Teller (BET) method. The total chemical composition of bulk sample was analyzed by means of X-ray fluorescence spectrometry (XRF, Rigaku RIX3100). The pH of bottom ash was measured by pH meter (Horiba F-55) under liquid/solid ratio 1:2.5. In addition, the mineral composition was investigated by X-ray diffraction spectrometry (XRD, Rigaku Multiflex). Diffraction patterns were analyzed by using search-match software (PDXL2.0 and JADE 6.5) utilizing the international center for diffraction data (ICDD) and the Japanese Information Center of Science and Technology (JICST) database. For liquid sample, the pH was measured by pH meter (Horiba F-55). The ionic compositions in the samples were analyzed by Ion Chromatography (DIONEX 120).

3.4 RESULTS

3.4.1 CHARACTERIZATION OF SAMPLES

3.4.1.1 MSWI BOTTOM ASH

The major and minor constituents in bulk samples are presented in [Table 3.1](#). Both unquenched and freshly quenched bottom ashes are Ca-based materials with Si, Al and Fe as the predominant materials. Other materials, including P, Mg, Na, Ti and Cl exist as minor constituents.

Table 3.1 The major and minor constituents in bulk samples measured by XRF.

Elements (wt%)	Plant N		Plant K	
	Unquenched	Quenched	Unquenched	Quenched
CaO	43.73	36.60	44.63	38.28
SiO ₂	17.76	17.93	22.46	23.90
Al ₂ O ₃	12.21	16.25	12.21	14.67
Fe ₂ O ₃	8.60	13.17	4.47	5.85
P ₂ O ₅	3.15	2.83	3.70	3.33
MgO	2.86	2.20	3.10	2.27
Na ₂ O	1.96	1.44	2.09	2.07
TiO ₂	1.79	1.65	2.71	1.55
Cl	1.70	0.67	2.32	1.90
LOI	4.05	5.28	0.45	4.03
Others	2.19	1.98	1.86	2.15

The results from two sampling sites display similar heterogeneity between the components of unquenched and freshly quenched bottom ashes in spite of their temporal and spatial difference. However, regardless of the waste feed and combustion condition, this heterogeneity may reflect the chemical variations which involve dissolution and precipitation of metastable phases as well as hydration and oxidation of different phases that take place during quenching (Chimenos et al., 2005; Speiser et al., 2000). It is found that several components, including CaO, P₂O₅, MgO, Na₂O, TiO₂ and Cl decreased after quenching due to their dissolvability. Besides, it should be noted that some metal oxides, including SiO₂, Al₂O₃, and Fe₂O₃ increase after quenching. This might be the result from the accumulation of grate sifting ashes in quenching tank (Inkaew et al., 2014).

3.4.1.2 QUENCHING WATER

The results from ions analyses as shown in Table 3.2 confirmed the dissolution phenomenon during quenching. The dominant ions dissolved in quenching water were Cl⁻, SO₄⁻², Na⁺, K⁺ and Ca⁺. The quenching water from plant K where the hydraulic ram discharger used has significant higher concentration of ions than plant N where the drag chain conveyer used. In addition, the pH value of quenching water was obvious increased by the dissolution phenomenon. This suggests that the system design of quenching has a

Table 3.2 The concentration of cation and anion in liquid samples.

Ions	Plant N		Plant K	
	Supply water	Quenching water	Supply water	Quenching water
F ⁻	0.23 ± 0.01	8.13 ± 0.76	0.49 ± 0.00	79.45 ± 1.36
Cl ⁻	15.24 ± 0.03	1,312.15 ± 4.60	462.53 ± 0.68	26,097.50 ± 37.99
Br ⁻	n.d.	7.38 ± 0.46	1.02 ± 0.01	62.24 ± 0.19
NO ₃ ⁻²	1.19 ± 0.39	2.34 ± 0.63	0.22 ± 0.01	4.16 ± 0.80
PO ₄ ⁻³	0.12 ± 0.00	n.d.	16.01 ± 0.39	5.11 ± 1.81
SO ₄ ⁻²	23.76 ± 0.07	65.22 ± 2.16	27.99 ± 0.04	33,932.26 ± 87.34
Li ⁺	0.02 ± 0.01	0.12 ± 0.07	n.d.	1.10 ± 0.01
Na ⁺	1.43 ± 0.01	71.98 ± 0.20	217.60 ± 0.90	1,229.37 ± 5.57
K ⁺	0.31 ± 0.15	33.28 ± 0.24	52.87 ± 0.23	736.67 ± 7.71
Mg ²⁺	0.16 ± 0.00	0.03 ± 0.02	5.92 ± 0.02	0.18 ± 0.00
Ca ²⁺	1.29 ± 0.01	64.71 ± 0.58	23.42 ± 0.05	225.94 ± 0.61
pH	7.30	12.53	6.80	13.23

Remark: The results are reported as mean ± standard deviation (S.D.), unit: mg/L, n.d.= not detected.

significant role on quenching water quality with identical characteristic at different facilities. Specifically, hydraulic ram quenching tank has a high saturation condition than drag chain conveyer tank. This probably caused by the water ratio in quenching tank, which is much lower in hydraulic ram discharger (Chandler et al., 1997). Since the supply water used in two plants was recycled water, the slightly high concentration of Cl⁻ and Na⁺ of supply water in plant K indicated an additional source of Cl⁻ and Na⁺ in the quenching system.

3.4.2 IMPACT OF WATER QUENCHING PROCESS ON MSWI BOTTOM ASH

3.4.2.1 PARTICLE SIZE DISTRIBUTION

Generally, particle size distribution of bottom ash depends on various factors, including waste composition, temperature and residence time in the combustion chamber, wear status of the grates, efficiency in the flue gas aspiration, and mechanical grinding in the solid transport system inside the furnace (Chandler et al., 1997; Chimenos et al., 1999; Marchese and Genon, 2011). However, we found that quenching process also contributed to particle size distribution of quenched bottom ash. Figure 3.1 shows cumulative particle size distribution of quenched bottom ash.

It is found that about 59-70 wt% of unquenched samples distributed in particles smaller than 1.00 mm, while about 40-55 wt% of quenched sample distributed in this fraction. This indicates that after quenching the particle size distribution of MSWI bottom ash samples changed. The comparison between the unquenched samples and the quenched samples from two sites showed that the cumulative percent passing through the sieve of quenched samples were always lower than the unquenched samples in particles larger than 0.425 mm. This could be inferred that after quenching the particles larger than 0.425 mm becomes bigger by adhering of finer residues. [Chimenos et al \(2005\)](#) stated that the fine particles that adhered to the coarse ones had a high content of calcium and reactive silica, which enable the formation of secondary phases in bottom ash. Therefore, quenched bottom ash was predominant by hydrate phases at its surface. However, another finding is that the amount of particles smaller than 0.250 mm increased after quenching in Plant K. This might be due to the mechanical breakdown of bottom ash particles by hydraulic ram discharger.

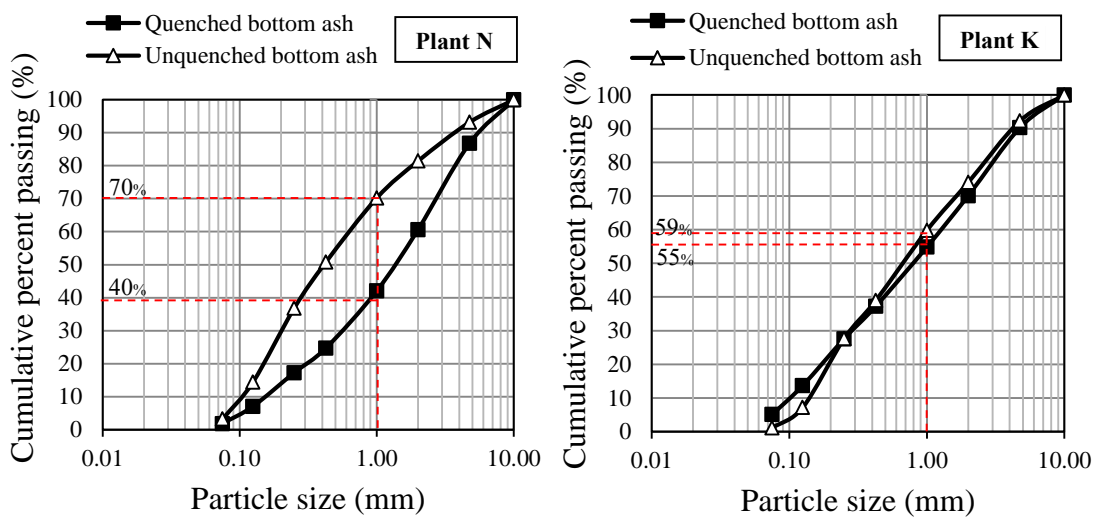


Figure 3.1 The cumulative particle size distribution of samples.

3.4.2.2 BOTTOM ASH SURFACE MORPHOLOGY

Optical and microscopic observations reveal the adhering of fine particles to the coarse rigid core as a result of quenching (Figure 3.2). In general, both unquenched and quenched bottom ash particles have irregular, angular and rough-texture nature. However, it is clear that unquenched bottom ash is generally free of a clump of fine ash particles that attached to its surface (Figure 3.2 a). The exception is of micro particles, which loosely attached (can be removed easily by washing) as can be seen under scanning electron microscope (Figure 3.2 b). Furthermore, unquenched bottom ash exhibits merely the melt product, which is glassy, rough and slag-like material (Figure 3.2 c).

In contrast, the quenched bottom ash particles are usually found to be coated by other smaller particles (Figure 3.2 d). Previous studies described in the same way that the intact particles of quenched bottom ashes are made up of a rigid inner core that are wrapped by the poorly bound and ultra-fine particles (Chimenos et al., 2005; Saffarzadeh et al., 2011; Yang et al., 2014). By this, quenched bottom ash particle can be divided into two zones with obvious boundary in between (Figure 3.2 e) and 3-2 f); the melt product/phase as a core, and the quench product/phase bound into the melt surface (Yang et al., 2014). However, the clot of the quench product without any core also presented during investigations.

It is known that the melt product is the direct output from incineration, which resembles to the intact particle of unquenched bottom ash. Its major constituent is amorphous glass with some crystalline and/or refractory components. Due to the escaping/entrapping of air during agglomeration, the melt product is highly porous and vesicular (Figure 2.2 c) and 2.2 f). Details of its characteristic and morphology were well described elsewhere (Saffarzadeh et al., 2011; Wei et al., 2011). It is suggested that the quench product is a mixture of ash particles smaller than 0.425 mm, which includes tiny pieces of metal, glassy melt particles, fragment of mineral, organic matter and those remain after combustion as refractory. Therefore, the physical of surface of quenched bottom ash dominates by numerous materials. The predominant microcrystals/hydrate phases that usually observed in

the quench product are illustrated in [Figure 3.3](#). Their morphology appears to be rod/needle-like, fibrous, or ribbon-like in the form of clump or nests ([Speiser et al., 2000](#)).

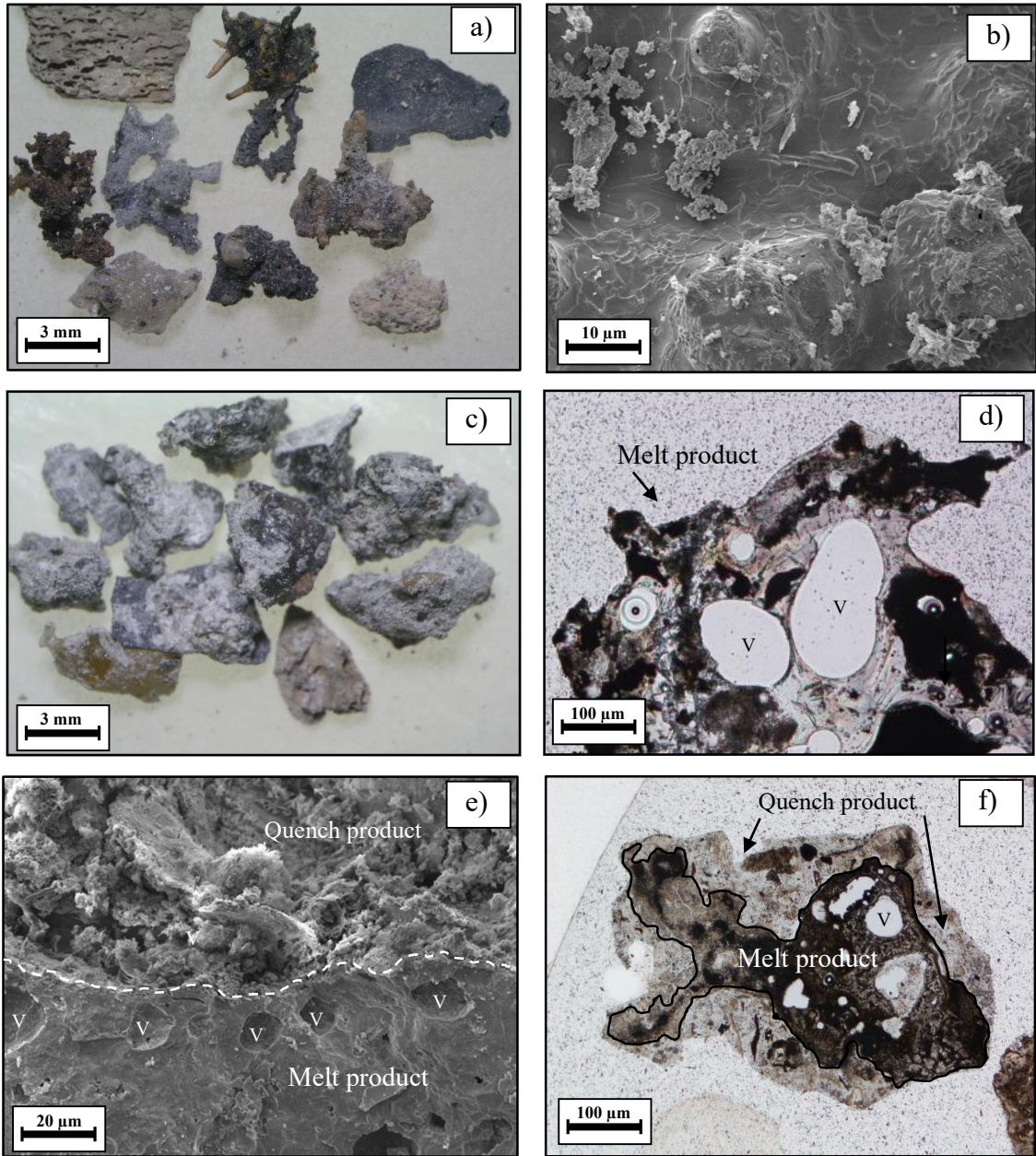


Figure 3.2 Unquenched bottom ash (top row) and quenched bottom ash (bottom row) morphology under different microscopic observation; a) and d) binocular stereo microscope, b) and e) scanning electron microscope; c) and f) petrographic polarized microscope. V is a vesicle.

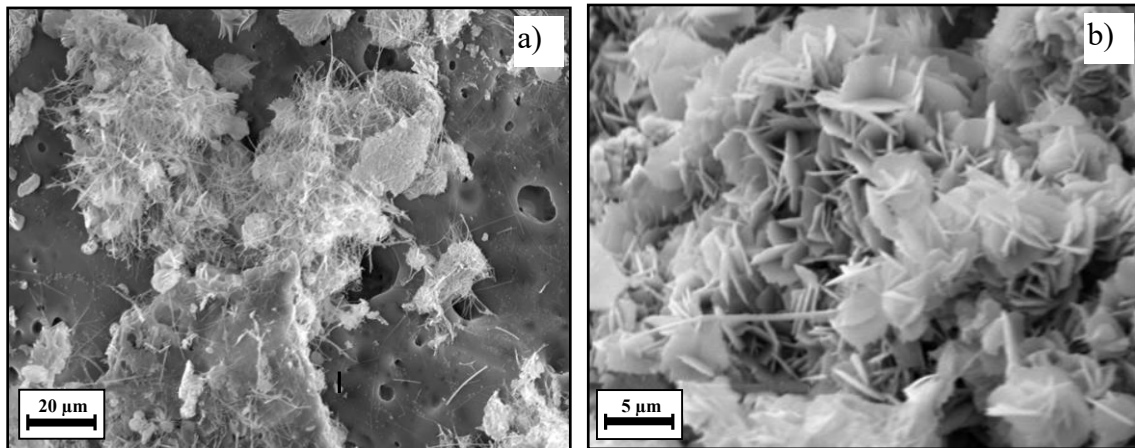


Figure 3.3 Hydrate phase microcrystals at the surface of quenched bottom ash which represent the alteration of bottom ash as a function of water-quenching: a) nests of rod-like/fibrous microcrystals, and b) cluster of platy microcrystals.

3.4.2.3 SPECIFIC SURFACE AREA

Since the water-quenching causes adhering of fine particles ($d < 0.425$ mm) to coarser particles, its influence on specific surface area of MSWI bottom ash particle range between 1.00-2.00 mm has been investigated. The value obtained by N_2 gas adsorption/desorption measurements using BET methods are presented in [Table 3.3](#). As expected, it is evident that by quenching the specific surface area of samples increased 4-7 times and the pore size of sample increased 5-7 times. Considering to the result from [section 3.2.2](#), the surface of quenched bottom ash usually covered by the quench product. This fairly loose formation provides intensive active porosity ([Saffarzadeh et al., 2011](#)). Moreover, the melt product is predominantly composed of a glassy constituent ([Zevenbergen et al., 1998](#)), thermal shock during quenching may transform the inactive pore inside it to be active via cracking paths. Such cracking paths in the bottom ash particles were identified by microscopic observation. Therefore, these should be accounted for the increasing of specific surface area and pore size in the quenched bottom ash.

Table 3.3 Specific surface area and pore size of representative samples.

Parameter	Plant N		Plant K	
	Unquenched	Quenched	Unquenched	Quenched
Surface area (m ² g ⁻¹)	0.98	4.53	0.46	3.05
Pore size (cm ³ g ⁻¹)	0.22	1.04	0.11	0.7

3.4.2.4 MINERALOGICAL COMPOSITION

In order to ascertain which species were formed during the quenching process, the mineral compositions of unquenched and quenched bottom ash were determined by X-ray diffraction (Figure 3.4). The result showed that although the operation system of two sites was different, the mineral diffractogram of samples were relatively similar in the same type of samples. Nonetheless, there was distinct difference between unquenched and quenched samples. Calcite (CaCO₃), quartz (SiO₂) and gehlenite (Ca₂Al₂SiO₇) were the main crystalline phases present in both unquenched and quenched bottom ash. The minerals that merely existed in unquenched bottom ash are lime (CaO). On the other hand, the minerals that only existed in quenched bottom ash were Friedel's salt (Ca₂Al(OH)₆Cl·2H₂O), Hydrocalumite (Ca₂Al(OH)₆[Cl_{1-x}(OH)_x]·3H₂O) and portlandite (Ca(OH)₂). The presences of calcite, quartz and gehlenite were commonly reported as the main minerals that were found in bottom ash (Chandler et al., 1997). Quartz and feldspar group of mineral such as anorthite and albite are reported to be refractory waste product minerals (Eusden et al., 1999; Meima and Comans, 1997a). Gehlenite, hematite, spinel and partially lime are the minerals that formed during combustion. Generally, at about 800-1,100°C, most calcite is decomposed into lime and carbon dioxide (equation 3-1). Lime is then hydrated into portlandite during quenching at the furnace exit (equation 3-2).



Since calcite was found dominantly in both unquenched and quenched bottom ashes, this might be because of either large pieces of waste calcite waste were not totally

decomposed, or the carbonation of lime occurred in the bottom ashes during/after quenching. In addition, Friedel's salt and hydrocalumite are hydrate phases formed during quenching. With only the presence of $\text{Ca}(\text{OH})_2$ and $\text{Al}(\text{OH})_3$, Friedel's salt could be synthesized in the ash by hydration (Ito et al., 2008). According to Ito et al. (Ito et al., 2008), since Ca, Al, Cl exist in the quenching tank, the basic mechanism of Friedel's salt formation via hydration of tricalcium aluminate ($3\text{CaO}\cdot\text{Al}_2\text{O}_3$) with calcium chloride (CaCl_2) is also theoretically feasible. Friedel's salt or hydrocalumite can be synthesized when the temperature is at about 65°C and the pH is over 11.5 (Um et al., 2014). The formation of Friedel's salt in the quenching tank may be described as equation 3-3.

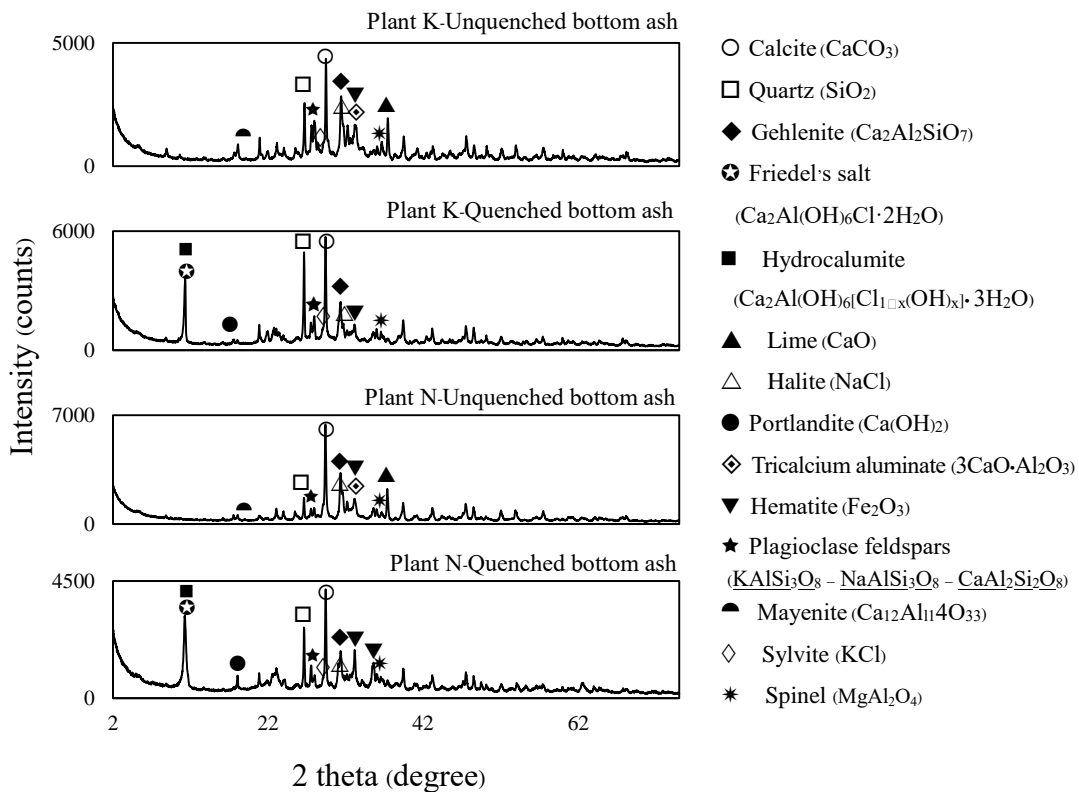


Figure 3.4 X-ray diffractogram of bulk samples.

3.4.2.5 BOTTOM ASH pH

Generally, bottom ash is alkaline. The initial pH value of bottom ash usually ranges from 10.5 to about 12.2 (Chandler et al., 1997). The pH value of samples in this study is presented in Figure 3.5. As it can be seen, pH of unquenched bottom ash ranged from 12.3 to 13.9, while pH of quenched bottom ash ranged from 11.1 to 12.7. The results were consistent between two incineration plants that indicate the influence of quenching on the pH of bottom ash by decreasing the pH value.

During and after quenching, there are a number of alterations that initiate by exposing to water including dissolution/precipitation of major cations, hydrolysis, hydration and oxidation of different phases as well as carbonation. These reactions contribute to the acid neutralization capacity and govern the development of pH (Bendz et al., 2007; Meima and Comans, 1997a). As pH of bottom ash under alkaline and neutral conditions is mainly dependent upon the relatively fast dissolution of Ca and Mg minerals (Bendz et al., 2007), depletion of those minerals out of the bottom ash system results in lower pH level. The pH over 12 are reported to be controlled by the equilibrium solubility of portlandite ($\text{Ca}(\text{OH})_2$) (Johnson et al., 1995; Meima and Comans, 1997a). When pH decreases close to 11, its value is controlled by the formation of aluminium sulphates (Meima and Comans, 1997a) and aluminium hydroxide (del Valle-Zermeño et al., 2014).

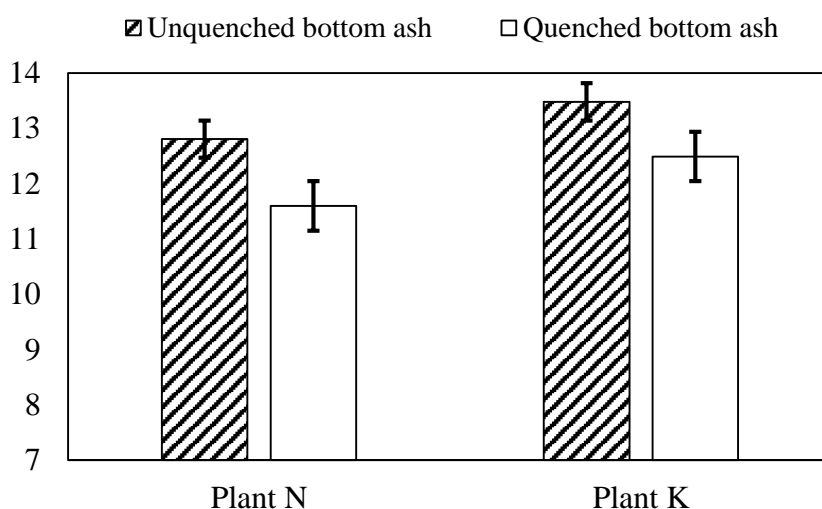
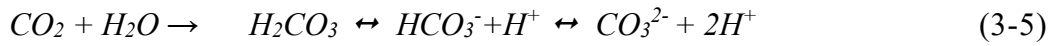


Figure 3.5 The pH value of unquenched bottom ash and water quenched bottom ash.

In addition, the other factor that may influence the pH of quenched bottom ash is carbonation (Meima et al., 2002; Meima and Comans, 1997b). This reaction involves the uptake of atmospheric carbon dioxide (CO₂) and precipitation of carbonate phases, such as calcite (CaCO₃). It is known that this reaction can cause the decrease of pH value in bottom ash. During and after quenching, many hydroxide phases can be converted to carbonate phases; the most remarkable is the conversion of portlandite to calcite by the following equation.



When bottom ash submerges into water, portlandite dissolves and generates calcium ion and hydroxide ion (equation 3-4). With the existence of hydroxide ion, carbon dioxide is captured and transformed to carbonic acid, bicarbonate, carbonate and hydrogen ions (equation 3-5). In the same time, water molecules are also generated by reaction between hydroxide and hydrogen ion (equation 3-6). Then calcium ion in the system is consumed to form calcite (equation 3-7). The uptake of carbon dioxide by portlandite and the formation of calcite may be simplified as equation 3-8. In the quenching tank or high moisture condition, these reactions are considerably fast, however, the rate of reactions may be reduced as a result of a very thin absorbed water film that remains on bottom ash particles after quenching (Sun et al., 2008). The pH of bottom ash can further decrease to calcite equilibrium value of 8-8.5 in aging condition (Meima and Comans, 1997b).

3.4.2.6 CHLORINE DISTRIBUTION

It was found that Cl in the unquenched bottom ash is higher than the quenched bottom ash (Table 3.1). This indicates that the major portion of Cl dissolved in the quenching water. However, the significant amounts of Cl still remained in the quenched

bottom ash. Based on SEM/EDX analyses, the remained Cl is dominantly distributed at the surface, particularly on various hydrate phases in the quench product. Figure 6 presents the SEM photomicrograph of a quenched bottom ash particle and some hydrate microcrystals that contain a significant amount of Cl. The chemical composition of the points marked on [Figure 3.6](#) is shown in [Table 3.4](#).

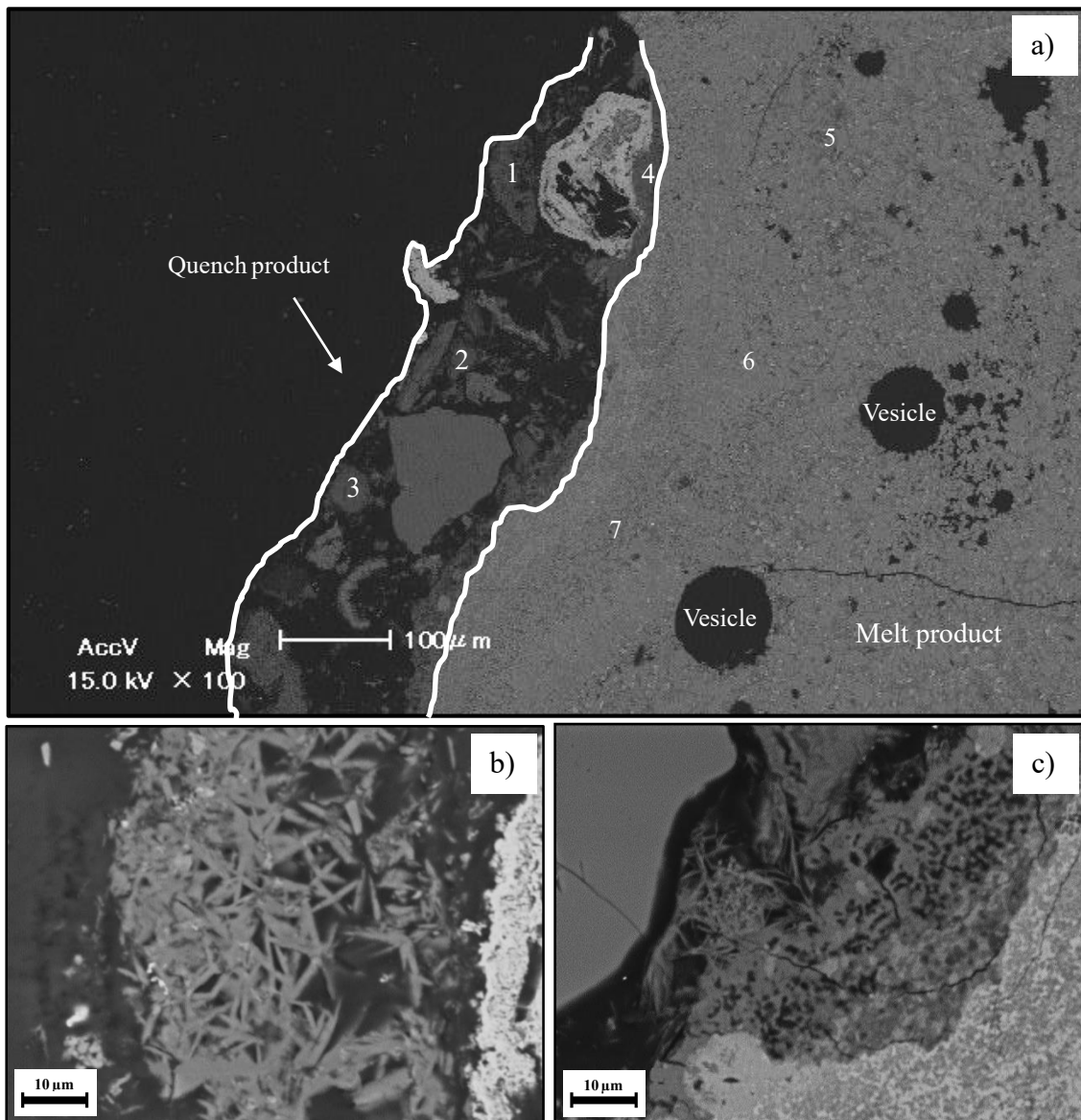


Figure 3.6 Photomicrograph of a bottom ash particle showing the designated points of EDX analyses and the distribution of hydrate microcrystals on the quenched product; b) and c) show the enlarged image of spot 1 and 2 of the panel a), respectively.

Table 3.4 Chemical compositions of the designated in [Figure 3.6](#) measured by SEM/EDX.

Elements (%)	Points of analysis						
	1	2	3	4	5	6	7
O	48.66	47.37	43.08	45.96	35.51	33.56	33.16
Ca	28.16	27.73	35.55	28.78	28.99	31.90	23.19
Al	10.22	9.68	6.18	13.23	7.93	10.97	14.30
Si	2.23	5.40	7.77	2.72	12.60	12.33	7.29
Cl	2.60	1.70	1.45	2.49	-	-	0.17
Fe	2.09	1.57	0.81	2.54	7.69	5.54	7.59
Mg	1.86	1.22	0.42	0.66	1.86	1.43	1.80
Na	1.18	1.65	0.66	1.03	1.70	1.16	8.18
S	0.96	1.16	1.40	0.59	0.22	0.12	0.24
P	0.64	0.42	0.48	0.26	0.37	0.43	0.30
Ni	0.55	0.64	0.87	0.28	0.31	0.75	0.74
F	0.24	0.25	0.14	0.39	1.74	1.00	1.45
K	0.22	0.48	0.32	0.24	0.09	0.00	0.25
Mn	0.20	0.34	0.35	0.44	0.00	0.00	0.15
Ti	0.18	0.41	0.52	0.38	0.98	0.81	1.18

From [Table 3.4](#), it is found that the concentration of Cl in the melt product (point 5-7) is very low due to partially encapsulation of Cl in the glass phase. In contrast, the accumulations of Cl in the hydrate phase (point 1-4) were in range between 1.45-2.6 wt%. These results are consistent with Yang et al ([Yang et al., 2014](#)). The quenched products are composed of fine particles, and it is assumed that the precipitation of Cl during quenching essentially occurs in the quenched product. The mechanism of Cl precipitation may be explained by the replacement of OH-groups in the structure of hydrate phases and the precipitation of hydrocalumite or Friedel's salt. Ito et al. [Ito et al. \(2008\)](#) mentioned that insoluble chlorides in bottom ash were formed by the wet hydration reaction of secondary phases with Cl⁻ in the quenched water after incineration.

3.5 GENERAL DISCUSSION

The methods used to identify the influence of quenching process on bottom ash characterization provided satisfactory results because they showed the difference between unquenched and freshly quenched bottom ash clearly. The results from particle analyses and microscopic analyses showed the relationship between fine particle of bottom ash,

and the existence of the quench product after quenching. The chemical analyses, mineral analyses and SEM/EDX provided an in-depth characterization of the quench product and its corresponding phenomena during quenching. Although there are several factors limit this study, the overall results were quite similar between two sites in terms of the impact of water quenching.

As expected, it is evident that water quenching has a great influence on bottom ash characterization resulting in the difference between unquenched and freshly quenched bottom ash. Based on the results, the main reasons that cause the difference between unquenched and quenched bottom ash are the chemical alterations and the formation of quench product after quenching. It is evident that fine particle of bottom ash plays a crucial role on the formation of quench product as already discussed in 3.2.1 and 3.2.2 sections. Generally, major alteration reactions in weathered bottom ash, which start immediately after quenching, included dissolution/precipitation of salts, glass corrosion, hydration and oxidation reaction of metal or metal oxides, slaking of lime, carbonation and hardening/cementation reaction (Speiser et al., 2000). For the formation of quench product, its mechanism may be divided into two stages; 1) changing of bottom ash characteristics via these reactions, and 2) attaching/coating of finer particles to coarser melt product. The first stage initially starts during quenching and continues gradually after quenching. This stage involves all the above-mentioned reactions, except hardening/cementation. The second stage likely takes place after quenching when bottom ash is conveyed inside the quenching tank, and moisture content is removed. At the second stage, all particles are mixed and fine particles adhere to the rough surface of the melt product. In the course of drying, precipitations of newly-formed products bind fine particles to coarse particles strongly. This mechanism may be explained as cementation/ hardening of quenched bottom ash (Tojo et al., 2012). The bond between the fine particle and the coarse particle is notably time dependent and gradually becomes stronger in aged bottom ash or in the landfill site.

3.6 CONCLUSIONS

This study investigated the impact of water quenching on bottom ash characterization by evaluating the unquenched and the freshly quenched samples from two types of quenching system. The thorough investigation on particle size distribution, morphological observations, specific surface area analyses, pH analyses, mineral and chemical composition analyses lead to the fact that water quenching obviously impacts on the bottom ash product. The results showed that after quenching the particle size distribution of the bottom ash changed, and the size of particles with a diameter larger than 0.425 mm became bigger by coating of finer particles. As a consequence, specific surface area of bottom ash product increased up to 7 times. During quenching several chemical reactions occurred and led to changing of bottom ash pH, chemical and mineral composition. The predominant reactions were dissolution and precipitation of various phases that led to decreasing of pH value and the formation of hydrate phases. It is found that water quenching process enhances the formation of portlandite, Friedel's salt and hydrocalumite. These hydrate phases distributed mainly on the quench product at the surface of quenched bottom ash particle. The quench product was identified as the mixture of fine ash particle, tiny pieces of metal and glassy melt particles, fragment or cluster of minerals, organic matter and those remain after combustion. The most dominant hydrate microcrystals in the quench product are needle-like or platy microcrystals that usually form nests rather than individual distribution in the mixture. However, it is considerable that the existence of quench product highly correlates to the presence of insoluble chlorides (Friedel's salt/hydrocalumite) in the quenched bottom ash. Since the quench product originates from fine ash residues, removing these fractions prior to quenching may help to reduce insoluble salt formation and Cl content in bottom ash. The appropriate method that is possible to adopt is to separate the fine ash particles by vibrating screen. By removing of fine particles from large ones, the formation of quench product and Friedel's salt would be prevented. This would benefit the reduction of Cl contents in bottom ash for recycling purpose.

REFERENCES

- Bendz, D., Tüchsen, P.L., Christensen, T.H., 2007. The Dissolution Kinetics of Major Elements in Municipal Solid Waste Incineration Bottom Ash Particles. *J. Contam. Hydrol.* 94, 178–194. doi:10.1016/j.jconhyd.2007.05.010
- Chandler, A.J., Eighmy, T.T., Hjelmar, O., Kosson, D.S., Sawell, S.E., Vehlow, J., Sloop, H.A. van der, Hartlén, J., 1997. *Municipal Solid Waste Incinerator Residues*. Elsevier.
- Chimenos, J.M., Fernández, A.I., Miralles, L., Rosell, J.R., Ezquerro, A.N., 2005. Change of Mechanical Properties during Short-Term Natural Weathering of MSWI Bottom Ash. *Environ. Sci. Technol.* 39, 7725–7730. doi:10.1021/es050420u
- Chimenos, J.M., Segarra, M., Fernández, M.A., Espiell, F., 1999. Characterization of the Bottom ash in Municipal Solid Waste Incinerator. *J. Hazard. Mater.* 64, 211–222. doi:10.1016/S0304-3894(98)00246-5
- del Valle-Zermeño, R., Chimenos, J.M., Giró-Paloma, J., Formosa, J., 2014. Use of Weathered and Fresh Bottom Ash Mix Layers as a Subbase in Road Constructions: Environmental Behavior Enhancement by Means of a Retaining Barrier. *Chemosphere* 117, 402–409. doi:10.1016/j.chemosphere.2014.07.095
- Eusden, J.D., Eighmy, T.T., Hockert, K., Holland, E., Marsella, K., 1999. Petrogenesis of Municipal Solid Waste Combustion Bottom Ash. *Appl. Geochem.* 14, 1073–1091. doi:10.1016/S0883-2927(99)00005-0
- Inkaew, K., Saffarzadeh, A., Shimaoka, T., 2014. Characterization of Grate Sifting Deposition Ash, Unquenched Bottom Ash and Water-Quenched Bottom Ash from Mass-Burn Moving Grate Waste to Energy Plant. *J. Jpn. Soc. Civ. Eng. Ser G Environ. Res.* 70, III_469–III_475. doi:10.2208/jscej.70.III_469
- Ito, R., Dodbiba, G., Fujita, T., Ahn, J.W., 2008. Removal of Insoluble Chloride from Bottom Ash for Recycling. *Waste Manag.* 28, 1317–1323. doi:10.1016/j.wasman.2007.05.015
- Johnson, C.A., Brandenberger, S., Baccini, P., 1995. Acid Neutralizing Capacity of Municipal Waste Incinerator Bottom Ash. *Environ. Sci. Technol.* 29, 142–147. doi:10.1021/es00001a018
- Marchese, F., Genon, G., 2011. Effect of Leaching Behaviour by Quenching of Bottom Ash from MSW Incineration. *Waste Manag. Res. J. Int. Solid Wastes Public Clean. Assoc. ISWA* 29, 39–47. doi:10.1177/0734242X10387848
- Meima, J.A., Comans, R.N.J., 1999. The Leaching of Trace Elements from Municipal Solid Waste Incinerator Bottom Ash at Different Stages of Weathering. *Appl. Geochem.* 14, 159–171. doi:10.1016/S0883-2927(98)00047-X

- Meima, J.A., Comans, R.N.J., 1997a. Overview of Geochemical Processes Controlling Leaching Characteristics of MSWI Bottom Ash, in: J.J.J.M. Goumans, G.J.S. and H.A. van der S. (Ed.), *Studies in Environmental Science, Waste Materials in Construction Putting Theory into Practice Proceedings of the International Conference on the Environment and Technical Implications of Construction with Alternative Materials*. Elsevier, pp. 447–457.
- Meima, J.A., Comans, R.N.J., 1997b. Geochemical Modeling of Weathering Reaction in Municipal Solid Waste Incinerator Bottom Ash. *Environ. Sci. Technol.* 31, 1269–1276.
- Meima, J.A., van der Weijden, R.D., Eighmy, T.T., Comans, R.N.J., 2002. Carbonation Processes in Municipal Solid Waste Incinerator Bottom Ash and Their Effect on the Leaching of Copper and Molybdenum. *Appl. Geochem.* 17, 1503–1513. doi:10.1016/S0883-2927(02)00015-X
- Saffarzadeh, A., Shimaoka, T., Wei, Y., Gardner, K.H., Musselman, C.N., 2011. Impacts of Natural Weathering on the Transformation/Neoformation Processes in Landfilled MSWI Bottom Ash: A Geoenvironmental Perspective. *Waste Manag.* 31, 2440–2454. doi:10.1016/j.wasman.2011.07.017
- Speiser, C., Baumann, T., Niessner, R., 2000. Morphological and Chemical Characterization of Calcium-Hydrate Phases Formed in Alteration Processes of Deposited Municipal Solid Waste Incinerator Bottom Ash. *Environ. Sci. Technol.* 34, 5030–5037. doi:10.1021/es990739c
- Sun, J., Bertos, M.F., Simons, S.J.R., 2008. Kinetic Study of Accelerated Carbonation of Municipal Solid Waste Incinerator Air Pollution Control Residues for Sequestration of Flue Gas CO₂. *Energy Environ. Sci.* 1, 370–377. doi:10.1039/B804165M
- Tojo, Y., Ishii, M., Matsuo, T., Matsuto, T., 2012. Study on the Influence of Hardening of MSWI Bottom Ash on the Emission of Easily Mobile Salts. *Proc. Annu. Conf. Jpn. Soc. Mater. Cycles Waste Manag.* 23, 527.
- Um, N., Nam, S.-Y., Thiriveni, T., Ahn, J.-W., 2014. Effect of Accelerated Carbonation on the Mineral Phase of Alkaline Inorganic Waste. *Resour. Process.* 61, 39–48. doi:10.4144/rpsj.61.39
- Wei, Y., Shimaoka, T., Saffarzadeh, A., Takahashi, F., 2011. Mineralogical Characterization of Municipal Solid Waste Incineration Bottom ash with an Emphasis on Heavy Metal-Bearing Phases. *J. Hazard. Mater.* 187, 534–543. doi:10.1016/j.jhazmat.2011.01.070
- Yang, S., Saffarzadeh, A., Shimaoka, T., Kawano, T., 2014. Existence of Cl in Municipal Solid Waste Incineration Bottom Ash and Dechlorination Effect of Thermal Treatment. *J. Hazard. Mater.* 267, 214–220. doi:10.1016/j.jhazmat.2013.12.045
- Zevenbergen, C., Van Reeuwijk, L.P., Bradley, J.P., Comans, R.N.J., Schuiling, R.D., 1998. Weathering of MSWI Bottom Ash with Emphasis on the Glassy constituents. *J. Geochem. Explor.* 62, 293–298. doi:10.1016/S0375-6742(97)00033-2

CHAPTER 4

MICROSTRUCTURE AND MINERALOGICAL CHARACTERIZATION OF THE QUENCH PRODUCTS ON MSWI BOTTOM ASH

CHAPTER 4

MICROSTRUCTURE AND MINERALOGICAL CHARACTERIZATION OF THE QUENCH PRODUCTS ON MSWI BOTTOM ASH

4.1 ABSTRACT

The characterization of the quench product on the bottom ash was performed with the aim of describing this material in terms of microstructure and mineralogy. A variety of microscopic and spectroscopic analyses were carried out in both intact particles, thin section, and bulk particles. In addition, the relationship between the existence of Friedel's salt and the quench product was evaluated. Microstructure characterization revealed that the quench product commonly distributed on the surface of the melt products. The thickness was variable from 10 μm to 1 mm. The quench product mainly exhibited by amorphous and microcrystalline of hydrate phases. Mineral such as quartz, iron-oxide, feldspar was embedding in the matrix of amorphous hydrate as well as refractory glass, relics, metal, and organic matter.

4.2 INTRODUCTION

The bottom ash represents approximately 80 % of remained residues from incineration (Chandler et al., 1997). It is produced under high temperature and subsequently cool-down by quenching process, thus remains active and readily to alter under air or water exposure. Recently, considerable progress has been made in understanding the characteristic of bottom ash with the attempt to handling or recycling effectively.

A number of researchers have utilized a variety of microscopic techniques to characterize the speciation and microstructure of the bottom ash. For example, Kirby and Rimstidt (1993) used X-ray powder diffraction (XRD) and scanning electron microscope with X-ray microanalysis (SEM/EDS) to study mineralogy and surface properties of municipal solid waste ash and found gypsum, hematite, quartz, halite, calcite, a variety of

spenels, and small amounts of mullite, sylvite, anhydrite, and wustite. [Zevenbergen et al. \(1994\)](#) used XRD and electron microscopy to analyze fresh and aged bottom ashes. They found interparticle heterogeneity in ash composition with evidence of weathering reactions forming clay-like rinds on exterior particle surfaces. Besides, they also found that over 50 % of the surface area of the ash particle belong to silicon rich, calcium-silicon rich, and aluminum-silicon rich particle types. [Pfrang-Stotz and Schneider \(1995\)](#) used petrography and SEM/EDS to characterize the melt structures in a variety of bottom ash slags. They found amorphous glasses, magnetite, quartz, gehlenite, and many additional phases. [Krzanowski et al. \(1998\)](#) used an analytical electron microscopy investigated bottom ash and found a variety of microstructure in the bottom ash included submicron size crystalline precipitates in a glassy matrix, twinned structures, including compound twins, dendritic structures, and fine-grain poly crystalline structures of hydrate. [Speiser et al. \(2001\)](#) characterized fresh and altered bottom ash by SEM/EDX to evaluate chemical alteration process in the bottom ash. They found that the newly-formed alteration phases are usually micro-fine hydroxide phase in thin layers on the surface of the bottom ash particles.

While much of work reviewed here gives information on speciation in both fresh and aged bottom ash, the quench product microstructure and mineralogy has not been closely examined. Those studies mainly focus on the melts product or in the form of the bulk particle or the aged/ weathered ash. Only a few research available for the mineralogy of the quench product in the freshly quenched bottom ash ([Saffarzadeh et al., 2011](#); [Wei, 2011](#)), while the mineralogy of the quench product may link to the characteristic of the weathered one. The knowledge of this study would enable for better understanding of alteration in the bottom ash, particularly the initial stage of weathering that would be available for further waste handling, particular to predict the leaching behavior in the subsequent environmental exposure.

Therefore, to gain a proper appreciation role of the quench product on the bottom ash, it is essential to understand the relationships between their microstructure and mineral composition. Novel findings from this work are discussed based on the experiment utilizing a variety of microscopic observations with the combination of EDX and XRD.

4.3 MATERIALS AND METHODS

4.3.1 SAMPLING

Samples were obtained from two separate facilities (Kamitsu, Kurume city) and Nishiyodo, Osaka city) in Japan. Both facilities are mass burn moving grate combusting municipal solid waste. Kamitsu facility (Plant K) has total capacity of 300 tons per day using wet hydraulic ram discharger to discharge the bottom ash after combustion. Nishiyodo facility (Plant N) has total capacity of 600 tons per day and use the quenching tank combined dragging chain linear conveyor for bottom ash discharging.

About 60 kg of samples were collected from each source of ashes, including unquenched bottom ash, grate siftings, and freshly quenched bottom ash. The unquenched bottom ash and the grate siftings were collected after the waste was completely incinerated and cooled down during routine maintenance. All samples were screened at 9.5 mm to remove refractory glass, ceramic and metal. The unquenched bottom ash and the grate siftings were dried at 65 °C for 24 h to remove moisture. In parallel, the freshly quenched bottom ash was freeze-dried for 24 h after sampling. All dried samples were kept in the air-tight container for further analysis. Besides, quenching water was also sampled from the quenching tank and was kept in the air-tight container for further investigation.

4.3.2 INVESTIGATION AND ANALYTICAL METHODS

The quantitative mineral composition was determined by X-ray diffraction (XRD, Multiflex, Rigaku) using CuK α radiation at 30 kV and 40 mA. The mineral patterns were manually identified using PDXL software.

To investigate the mineral distribution with regard to the ash particle size distribution, samples were separated to different size fractions. The standard sieve class 0.075, 0.125, 0.250, 0.425, 1.00, 2.00 and 4.75 mm were used to classify fractions. After that the samples were pulverized (into powder), and the mineral composition were determined.

The suspended solids in quenching water were obtained by using vacuum filtration. Solids were freeze-dried, and then analyzed for mineral composition and morphological characteristic.

The intact particles were picked and used for micro-analysis. Some of the particles were directly analyzed by SEM/EDX for the surface study. Some particles in the diameter larger than 1 mm were made into polished thin sections. The polished thin sections were primarily subjected to optical microscopy observation, and then the chemical composition of each phase was determined by SEM/EDX with an acceleration voltage of 5-20 kV. Thin section analyses were completed using petrographic polarized light microscope and SEM/EDX.

4.4 RESULTS AND DISCUSSION

4.4.1 THE EXISTENCE AND APPEARANCE OF THE QUENCH PRODUCT

The quench product is the new phase formed by quenching the hot bottom ash into quenching water. In this study, the combination of petrographic thin-section analysis and the intact particle analysis by SEM/EDX were used to determine the microstructure and mineralogical characteristic of representative samples. [Figure 4.1](#) displays a photomicrograph of the freshly quenched bottom ash which contained the quench product on its surface. The quenched product under SEM shows characteristic of rough texture containing numerous aggregates, which later identified as Ca-hydrate phases ([Speiser et al., 2000](#)). Generally, the morphological texture of slag particle is the melt product with the moon texture showing that particle passed metamorphism under high temperature. The melt product may have classified into three types namely vitreous, porous, and microcrystalline ([Pfrang-Stotz and Schneider, 1995](#)). However, all types of the melt product are generally excluded any precipitated phases. In case of the quenched bottom ash, the quench product usually included on its surface, particularly at the concave area where the vesicle opened to the external surface.

By SEM investigation, the quench product appeared on the surface of the melt product distinctively. It could be identified as the extreme fineness of the newly form amorphous and microcrystalline, which ranged from a few μm to several tens of μm . The result was consistent with [Speiser et al. \(2000\)](#) in terms of the precipitate found on the surface of freshly quenched bottom ash appeared to be both microcrystalline and amorphous phases. Nonetheless, in this study, the distribution of microcrystalline could be found occasionally, while, the amorphous phase seemed to be most abundant in the quench product.

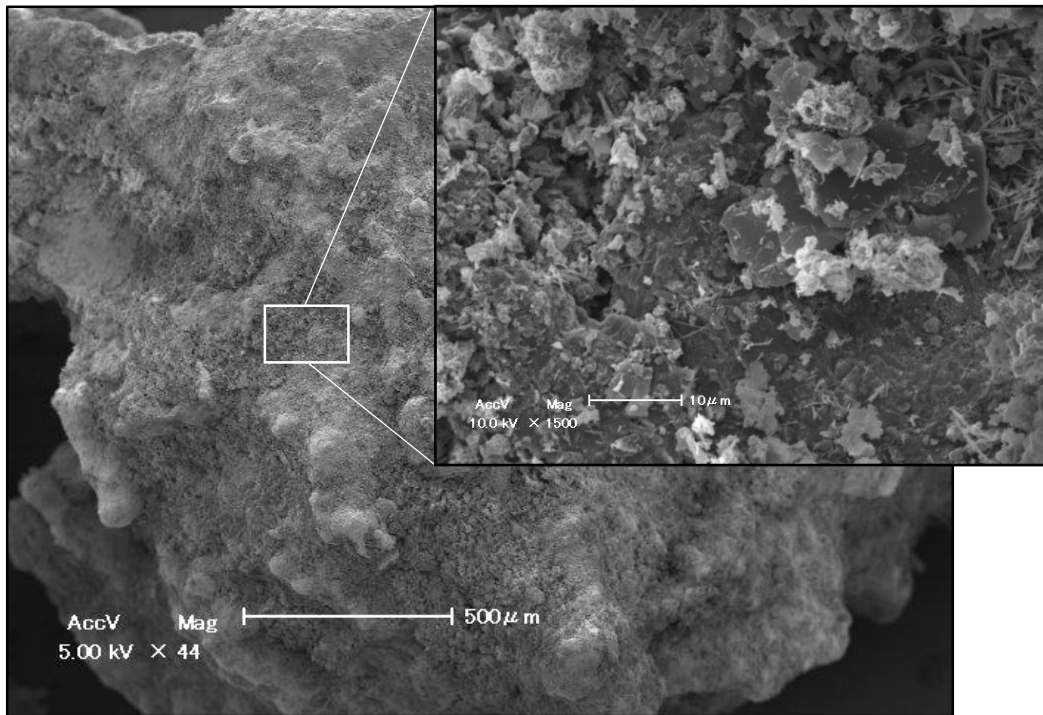


Figure 4.1 The quenched bottom ash under scanning electron microscope shows a rough texture containing the quench product at the outer surface.

The results obtained from petrographic thin section observation indicated that the quenched product was usually bound to the concave of the melt product. [Figure 4.2](#), presents the photomicrograph of the thin section of the quenched bottom ash. Practically, petrographic thin section observation or petrogenesis is extensively used by petrologist to identify the origin of igneous rock. In the field of environmental engineering, it is applied successfully to identify bottom ash by comparing to crystalline rock system ([Eighmy et al., 1994](#); [Eusden et al., 1999](#)). In this investigation, the thin section photomicrograph enabled detail cross-section of the quenched product and bottom ash particle. The quench product exhibited yellowish semitransparent precipitated phases. The loose and fragile characteristics provided the additional active surface to the bottom ash up to seven times of the unquenched bottom ash ([Inkaew et al., 2015](#)). The intensive investigations guided that it was rarely to find the quench product inside the void or cavity if those voids were closed or had a narrow cavity.

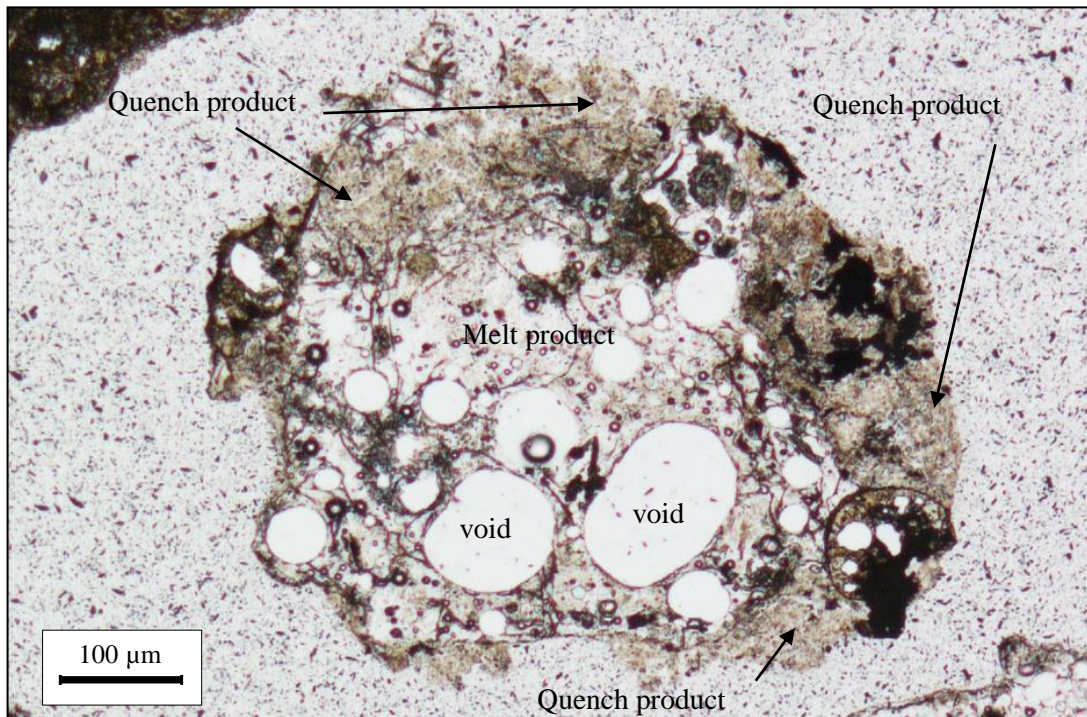


Figure 4.2 The photomicrograph of the thin section of the quenched bottom ash showing the precipitated quench product at the concave of the melt glass particle

4.4.2 MICROSTRUCTURE OF THE QUENCH PRODUCT

Figure 4.3 shows the photomicrograph of the thin section of the quench product under the observation using the petrographic microscope with the crossed Nicol and gypsum plate. It could be seen that the quench product is a heterogeneous admixture of various materials remains after combustion and those neo-formed during/after quenching (Inkaew et al., 2015; Wei et al., 2011; Yang et al., 2014). Specifically, the quench product is mainly exhibited by the hydrate phases embed with tiny pieces of quartz, feldspar, glass, relics, metal, and organic (such as bone). The percent composition of each is not reported here since the distribution of the quench product is uneven. Besides, the thickness of the quench layer may vary from several 10 μm to 1 mm regardless of the melt particle size. Thus the estimate composition of heterogeneous admixture like the quench product may not be representative for reality. Quartz, feldspars, and non-vesicular, angular glass fragments are reported to be refractory phases that survived combustion (Eusden et al., 1999). The tiny pieces of glass in the quench product could be both droplet and irregular shape. The observation indicated that the droplet of glass in the quench product was

commonly in the range of 5-10 μm . The relics in the quench product are refractory mainly dominant by iron and aluminium alloy. These relics were refractory and account for the main sources of redox reactions in the bottom ash. Additionally, the organic substances in the quench product were usually found to be bone. Although bottom ash commonly contains the uncompleted burnt organic materials such as paper, vegetable, fruit peel, etc. (Chandler et al., 1997), it was hardly found cellulose as a part of the quench product in this study.

In the matrix of the quench layer, pieces of mineral such as quartz, arkermanite, hematite was occasionally found. These minerals were mainly being able to find in the melt product. The existing of these minerals in the quench product were fragments that probably precipitated out of the melt particle during cooling (Pfrang-Stotz and Schneider, 1995).

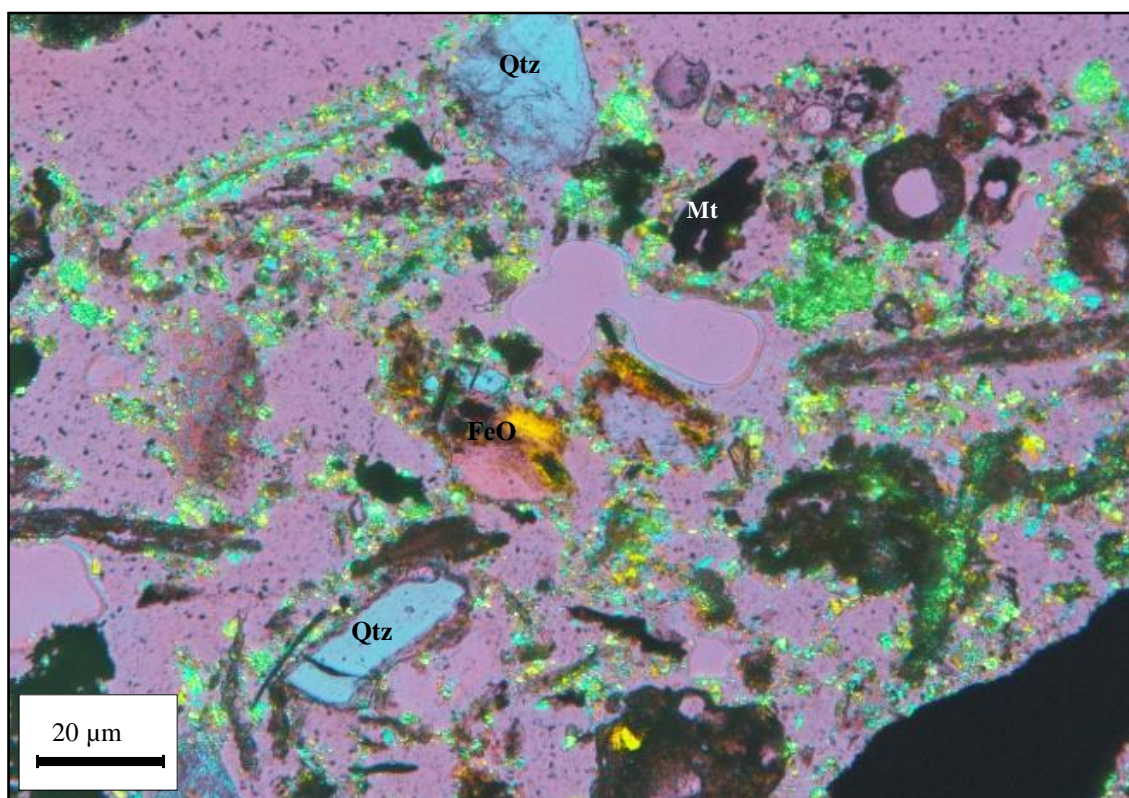


Figure 4.3 Photomicrograph of the quench products with heterogeneous admixture of various materials (using the crossed Nicol and gypsum plate in the observation); Qtz = quartz, FeO=FeO, Mt= Metal alloy.

4.4.3 HYDRATE PHASE IN THE QUENCH PRODUCT

To clarify the chemical composition of hydrate phases on the quench product, the intact quenched bottom ash particle was subjected to SEM/EDX. The results of designated points analyses are given in Table 4.1. Clearly, the quench product composed mainly Ca-hydrate phases with the concentration of Ca in range 27.89-34.88 %. In consistent with Speiser et al. (2000), Ca-hydrate phase in the bottom ash may produce immediately after quenching the hot ash.

From Table 4.1, although new precipitated hydrate shared the common major composition of Ca, Si, and Al, the minor concentration of Na, K, S, Cl, Mg, and F were different. The ions of elements on the hydrates were usually found in quenching water. Therefore, it is possible that the ions of these elements were reabsorbed into hydrate phases during alteration, particularly Cl and S, which partially replaced OH-group in the structure of hydrate phase (Speiser et al., 2000).

There are five types of hydrate morphology reported by Speiser et al. (2001) including; 1) fibrous, 2) ribbon like, 3) tubular, 4) crumbled foils, and 5) rosettes. In this research, needle-like hydrate (Figure 4.4 a)), and fibrous hydrate (Figure 4.4 b)), were found dominantly in particle thin section. However, under intact particle observation by SEM, the most dominant hydrates found were needle-like hydrate and plate-like hydrate (Figure 4.4 c)). The crumble foil and the rosette hydrate phases (Figure 4.4 d)), were found occasionally.

Table 4.1 Chemical composition of the points designated on the quench product.

Element (wt%)	Point of analysis						
	1	2	3	4	5	6	7
O	36.16	31.63	28.69	27.16	19.44	46.17	46.88
Ca	34.4	34.42	34.88	27.89	30.29	34.25	34.78
C	9.26	6.19	4.72	6.87	6.56	10.54	5.92
Si	6.79	4.49	4.6	6.86	6.29	0.89	2.18
Na	5.14	6.34	6.39	5.57	5.37	0.56	4.07
K	2.18	1.44	2.02	1.53	4.02	0.36	1.07
Al	2.13	3.34	3.6	9.09	8.8	0.48	0.6
S	1.86	3.15	4.21	4.29	5.53	1.94	1.14
Cl	1.28	1.3	2.98	3.51	5.77	0.46	0.28
Mg	0.19	3.24	3.04	2.7	3.58	1.95	0.19
F	0.6	4.41	4.34	4.53	4.35	2.41	2.88

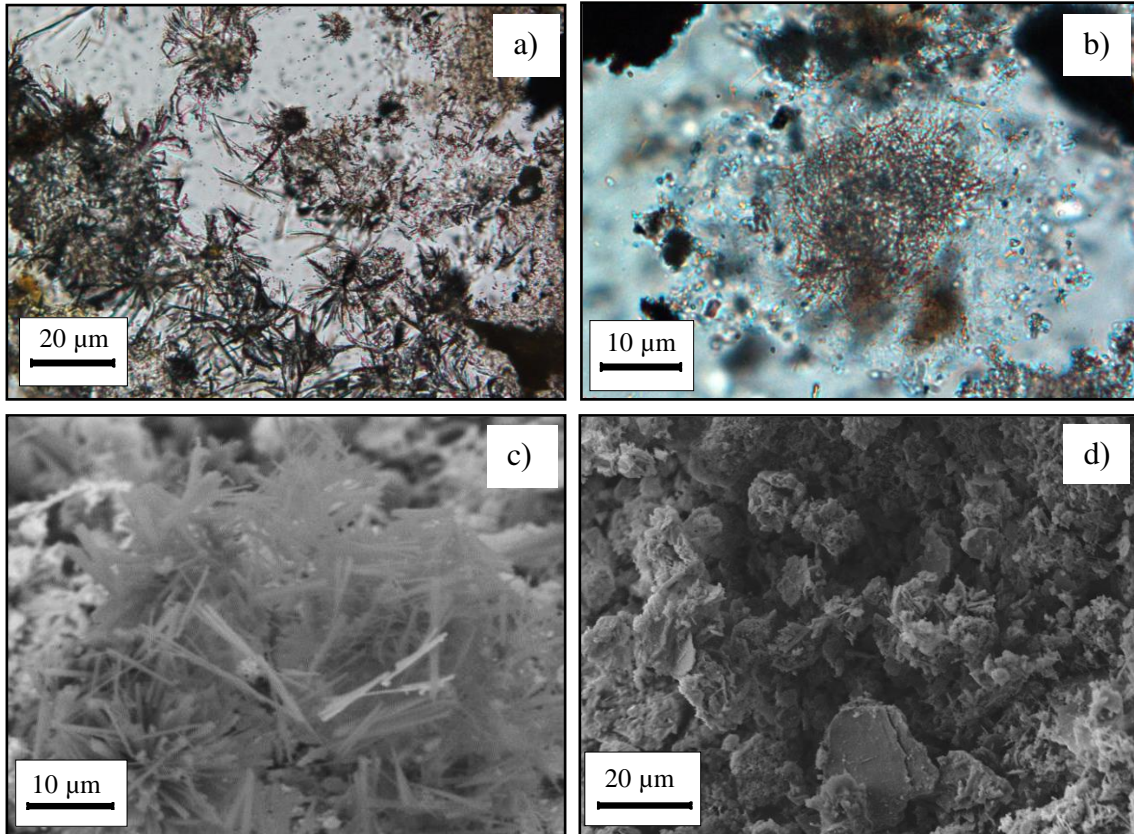


Figure 4.4 Morphologies of hydrate phases observed under petrographic thin section a) needle like amorphous hydrate b) fibrous hydrate, c) plate-like hydrate and d) rosette hydrate phases.

4.4.4 DISTRIBUTION OF THE QUENCH PRODUCT ON BOTTOM ASH SURFACE

From the investigation, the distribution may have classified into four patterns (Figure 4.5); 1) the whole particles composed of the quench product as medium and other materials embedded in (Figure 4.5 a), 2) the quench product as a medium joining two melt particles (Figure 4.5 b), 3) the quench product filled in part to concave or exit pore of the melt product (Figure 4.5 c), 4) only a few portions of the quenched product attached to the melt particle with the very thin layer (Figure 4.5 d).

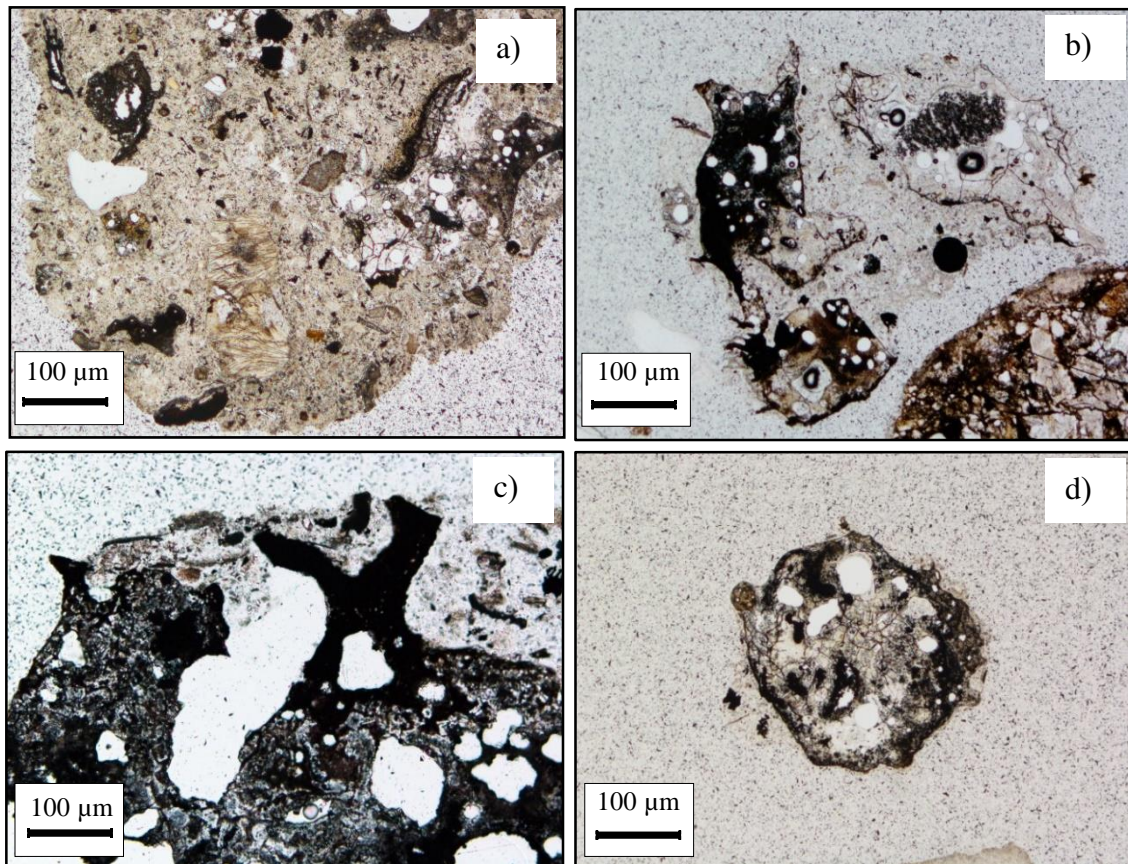


Figure 4.5 Distribution pattern of the quench product; a) the whole particle is the quench product, b) the quench product joins particles together, c) the quench product fills in part to concave or exit pore of the melt product, and d) only a few portions of the quenched product attaches to the melt product.

However, it was not observed that the quench product merge or fusion into the melt product. This means existing of the quench product and binding of the quench product into the melt product may happen dependently. This was quite probably due to the turbulence insides the quenching tank which caused by moving of the drag-chain conveyer or the ram, or the moving of bottom ash particle during the process of discharging.

4.4.5 ORIGIN OF THE QUENCH PRODUCT

Since the unquenched bottom ash and the grate sifting contained variety size of particle range from less than 0.075 mm to over 4.75 mm, it could be predicted that the finer fraction of these ashes might become the quench product by turning into hydrate phases. [Figure 4.6](#) compares the characteristic between the fine fraction of unquenched bottom ash ([Figure 4.6 a](#)) and quenched bottom ash ([Figure 4.6 b](#)). It was found that the fine fraction unquenched bottom ash comprised mainly the particles with the character of incomplete-short and slightly thick shape. The fine fraction of the quenched bottom ash contained both particles similar to those that could be found in the unquenched bottom ash, and the particles of the morphology type as described in section 4.4.3. In the other word, the fine fraction of the quenched bottom ash contained hydrate phases, but the unquenched bottom ash did not.

The conversion of the unquenched bottom ash to the quench product may be described by the alteration of lime and portlandite as [equation 4-1](#) ([Speiser et al., 2000](#)). During incineration, most of calcite or calcite-bearing relic is decomposed to lime, when lime reacts with water then is converted to portlandite which is a hydrate phase.

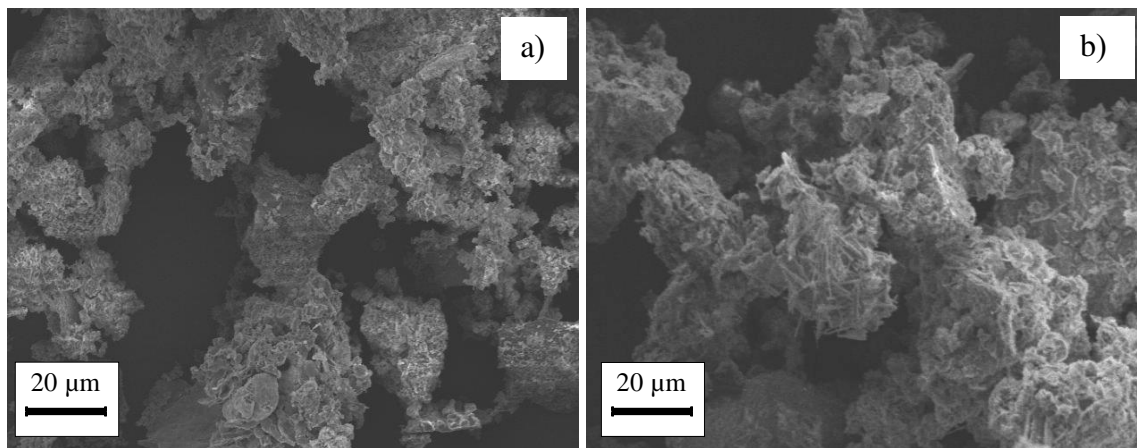
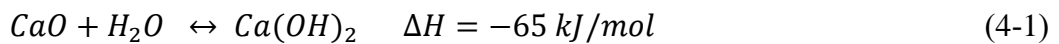
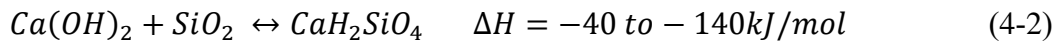


Figure 4.6 photomicrograph of the fine fraction of ash samples a) unquenched bottom ash and b) quenched bottom ash.

However, the crystal of portlandite was rarely to find in this study. This is probably due to portlandite is easily dissolved in quenching water. In terns, the small needles of calcium-rich hydrates are formed out instead of portlandite (Speiser et al., 2000). Due to the composition of observed hydrate phases (Table 4.2) can be identified as Ca-Si-Al hydrate phases or C-S-H-phases, which are known from the cement research. The formation of these phases can be described as equation 4-2.



The C-S-H phases that were usually found during the investigation are shown as Figure 4.7.

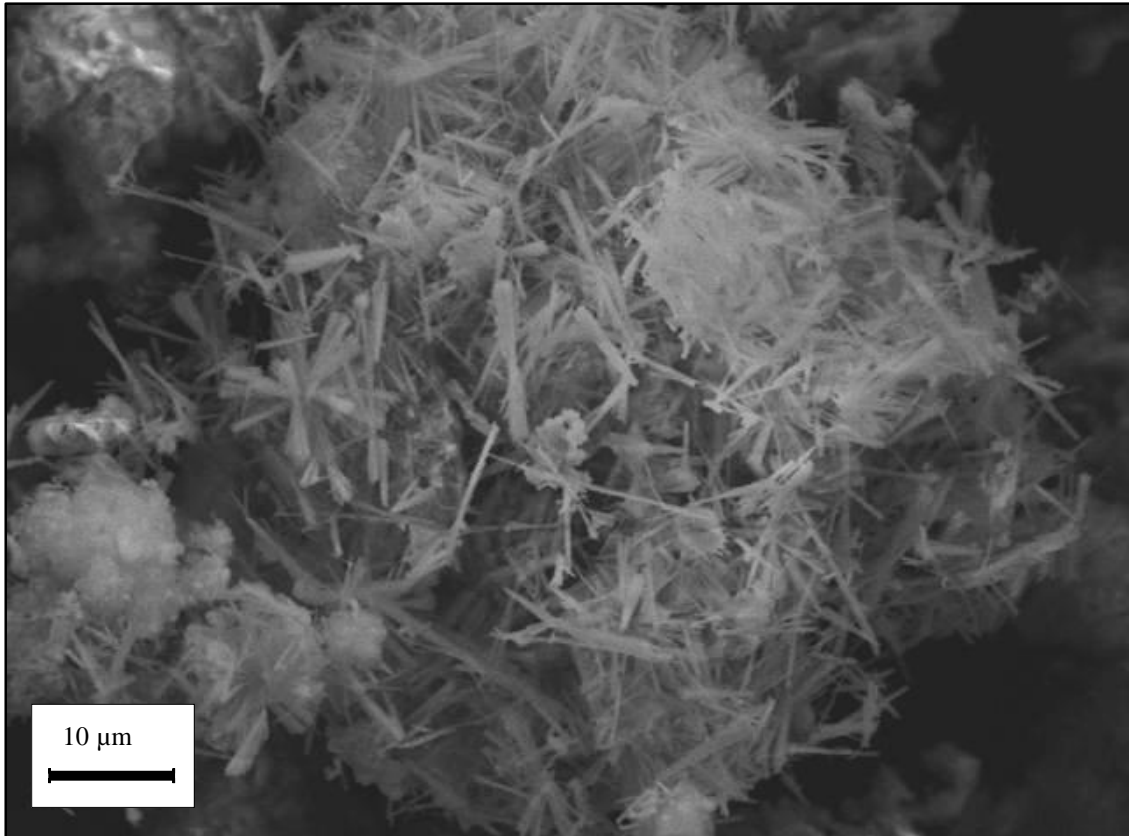


Figure 4.7 The newly-formed microcrystalline of C-S-H phases on the surface layer of the freshly quenched bottom ash.

4.4.6 SUSPENDED SOLID ANALYSIS AND ITS ROLE ON THE QUENCH PRODUCT FORMATION

In order to evaluate the role of suspended solids in the formation of the quench products, the solids in quenching water were filtered, dried and observed under SEM respectively. The suspended solids in quenching water exhibited with a rod of microcrystalline that similar to ettringite which usually found in the aged bottom ash (Piantone et al., 2004). However, the combinative result of XRD (Figure 4.8) indicated that the mineral composition of the suspended solids in the quench bottom ash was calcite. Generally, the needle-like calcite crystal, which might be fiber or dendrite calcite, formed by abnormal growth condition. The shape of crystals can be substantial modified by destructive or constructive diagenetic processes during quenching (Jones and Kahle, 1993).

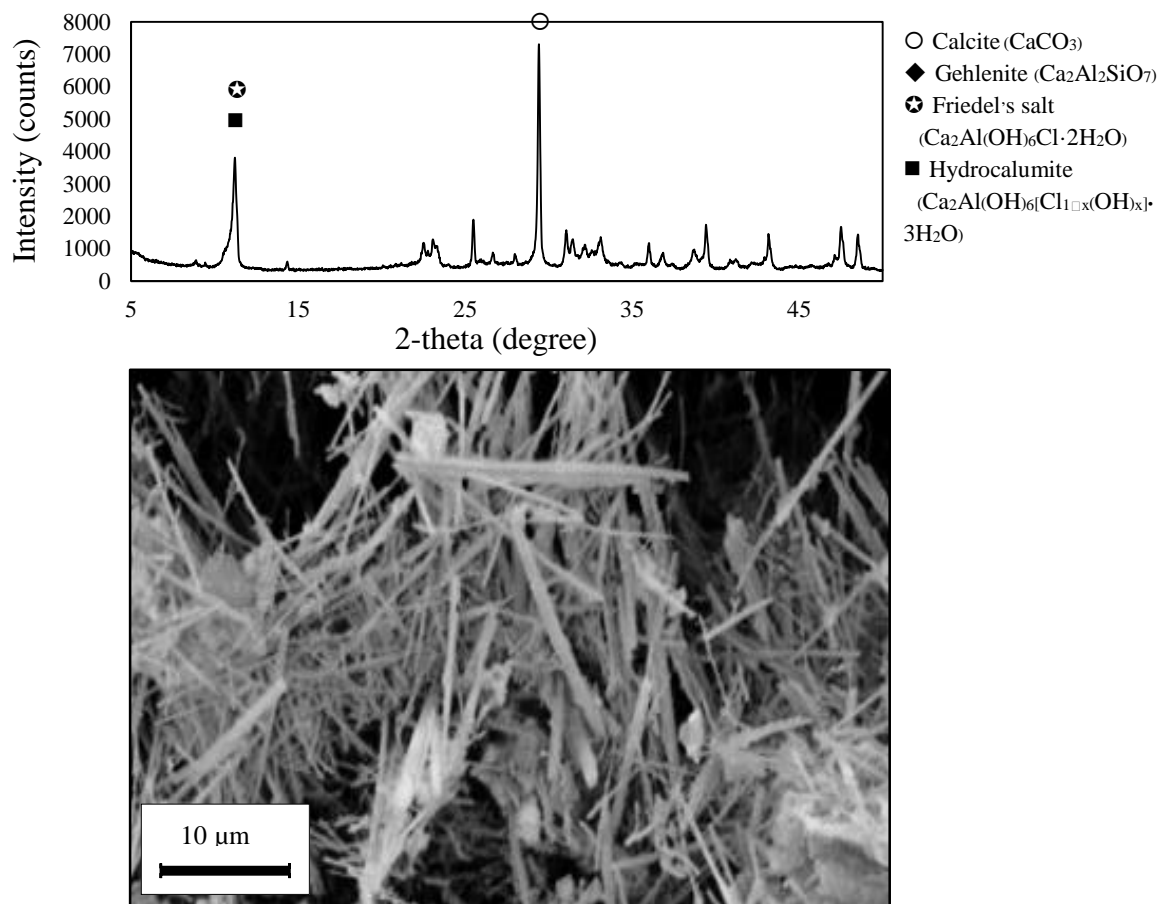


Figure 4.8 X-ray diffraction data with SEM photomicrograph of suspended solids obtained from quenching tank.

As the suspended solids in quenching water was dominated by the needle-like microcrystal of calcite, it might be inferred that these suspended solids were formed by the reaction of slake lime with CO₂ that dissolved in quenching water as described in [equation 4-1](#). [Speiser et al. \(2001\)](#) mentioned that the Ca-hydrate phases, and in the presence of sufficient CO₂ the carbonation phases also, can form cementation shells around the bottom ash particles. It may assume that this cementation shell is the quench product that can cause passivation of the corroded particles and retard subsequent interactions between the bottom ash particle and the leachate water in landfill condition.

4.4.7 DISTRIBUTION OF CHLORINE AND OTHER ELEMENTS ON THE QUENCH PRODUCT

The quench product that is bound into bottom ash particle is the first part that interact with the exposed environment. Since leaching of salts and heavy metals from bottom ash can cause the contamination to soil or water, therefore, the understanding of salts and metals distribution in the bottom ash would help to understand their leaching behavior. The distribution of elements on the quench product was investigated using the intact particle of the quenched bottom ash. The result is given in [Figure 4.9](#).

[Figure 4.9](#) was obtained by using SEM/EDX. With the proper setting of magnification and acceleration voltage, part of quench product appears microcrystalline of hydrate phases. The imagery mapping of EDX was performed to identify element distribution pattern comparing the quench product, and the melt product. The bright spot in photo indicates the distribution of each target element. The red line is given to bordering between the melt product and the quench product. The result indicates that Ca, Si distributes in both the quench product and the melt products.

Clearly, Ca and Si distributes on both the melt product and the quench product eventually. Al and Cl mainly distribute on the quench product. Na distributes densely on the Na-Si hydrate product. The result confirmed that the main part of the quench product are Ca-Al-Si hydrate phases with the binding of Cl, and these phases account for the composition of Cl in the bottom ash. Generally, Cl⁻ and other salts are dissolved into quenching water. The percentage Cl⁻ removal by water washing is up to 82 % with the liquid/solid (L/S) ratio of 10: 1 ([Chandler et al., 1997](#)). However, due to the quenching water in most of the incineration plant is static, the concentration of Cl⁻ in quenching

water increase each times the bottom ash is quenched. It could be considered that quenching water is the secondary source of Cl^- (Ito et al., 2008; Yang et al., 2014), thus the leached out Cl^- could have reabsorbed into the quench product and became insoluble.

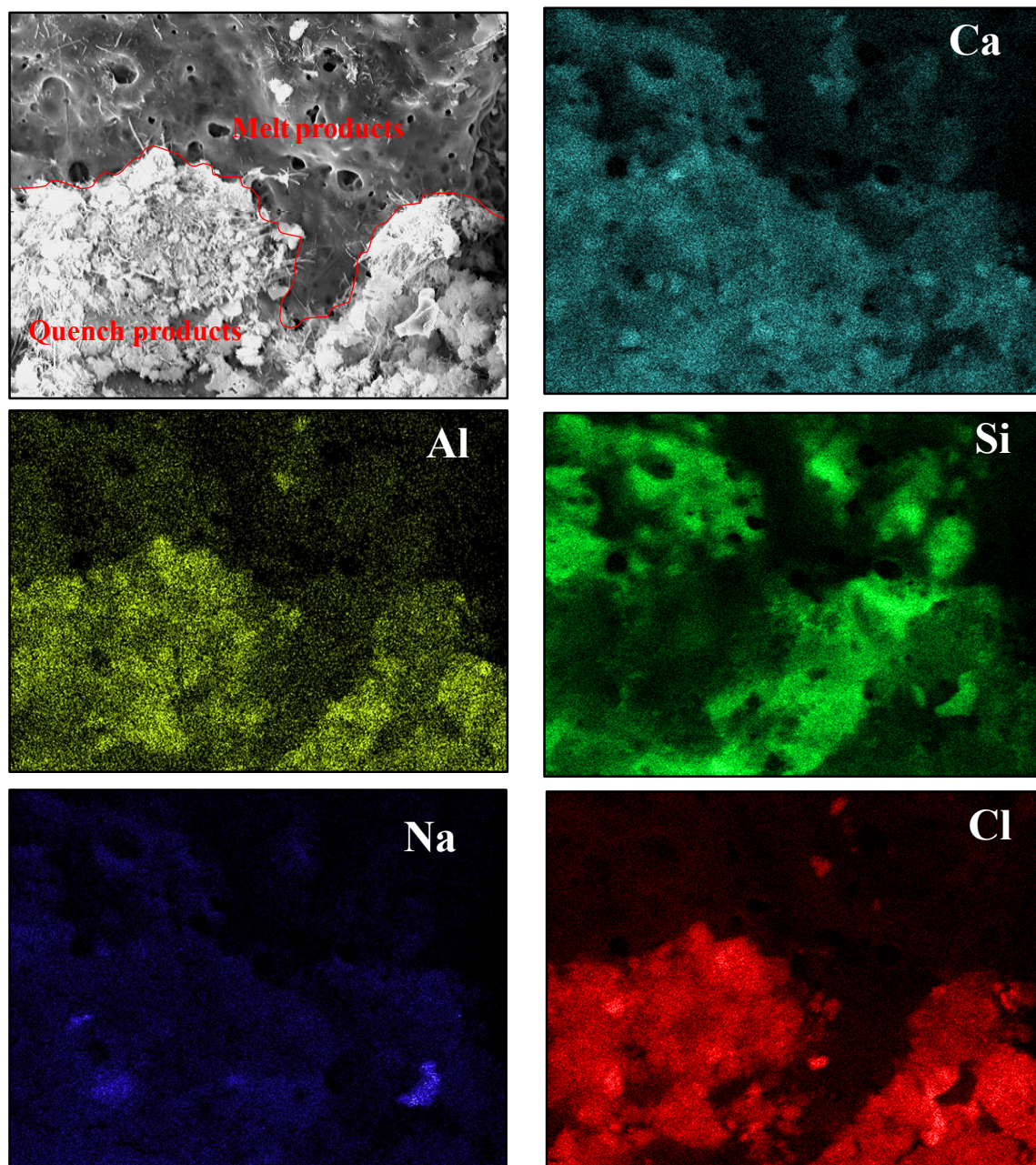


Figure 4.9 Distribution of elements in freshly quenched bottom ash particle.

4.4.8 MINERAL COMPOSITION ON THE BOTTOM ASH WITH REGARD TO PARTICLE SIZE DISTRIBUTION

In order to determine mineral phases that account for Cl distribution with regard to the quench product, the quenched bottom ash was fractionated into diameter class <0.075 mm, 0.075-0.125 mm, 0.125-0.250 mm, 0.250-0.425 mm, 0.425-1.00 mm, 1.00-2.00 mm, 2.00-4.75 mm, and >4.75 mm, and was analyzed by XRD. Figure 4.10 shows the diffractogram of mineral in the bottom ash with different size fractions.

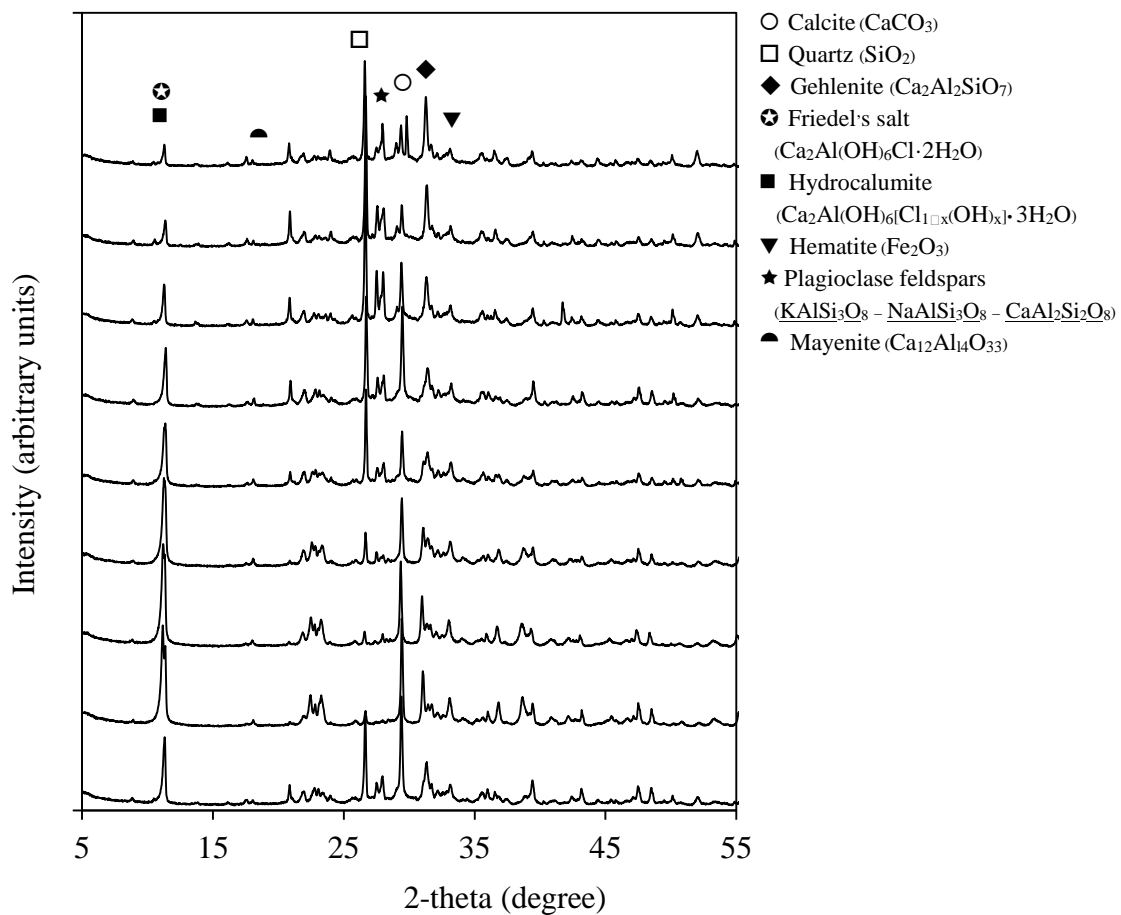


Figure 4.10 the diffraction data of mineral in the bottom ash with different size fractions ranging from less than 0.075 mm to 4.75 mm.

Clearly, distribution of mineral in bottom ash was particle size dependent. Quartz and plagioclase feldspars were mainly in the particle larger than 0.250 mm. This could be expected since these minerals were refractory glass or ceramics (Chimeno et al., 1999).

In opposition, calcite preferable distributed mainly in particles smaller than 2.00 mm. Previously, calcite was reported as an alteration product of plagioclases rich in Ca, and new produced when Ca-bearing mineral decay (Pfrang-Stotz and Schneider, 1995; Speiser et al., 2000). In the present work, it was also found to be the product of carbonation in quenching process. Gehlenite, hematite and mayenite were seemingly distributed eventually in all size fractions. Friedel's salt/hydrocalumite could be found in all particle fractions. Nonetheless, it was size-dependent, the smaller particle size, the higher intensity. Additionally, Friedel's salt/hydrocalumite was the mineral detected by XRD that consisted of Cl.

4.4.9 FORMATION OF FRIEDEL'S SALT IN THE FRESHLY QUENCHED BOTTOM ASH

When the bulk bottom ash is quenched in water, the fine fraction (less than 0.425 mm) is altered to the quench product by hydration. In the same time, Friedel's salt is produced. Friedle's salt can be synthesized in the ash by the wet hydration of Cl⁻ only with the addition of Ca(OH)₂ and Al(OH)₃. Besides, by hydration, more than 90 % of Cl⁻ was converted into the Friedel's salt phase (Ito et al., 2008). The mechanism that Cl⁻ bound into the hydrate phase in the quench product might be described by two routes: 1) via a direct chemical reaction between the tricalciumaluminate (3CaO·Al₂O₃) and CaCl₂ (Birnin-Yauri and Glasser, 1998), or 2) via an ion-exchange between the OH⁻ ions present in the interlayer of the 3CaO·Al₂O₃ hydrates and the free Cl⁻ ions derived from NaCl or other salts in bottom ash. With increasing aqueous Cl⁻ content in quenching water, Friedel's salt becomes essentially Cl⁻ saturated, once saturated, Friedel's salt is no longer able to bind additional Cl⁻ from the quenching water (Birnin-Yauri and Glasser, 1998). Therefore, quenching of bottom ash is the great factor for Friedel's salt formation. In order to recycle the bottom ash as a raw material in cement production, Cl⁻ need to be removed to the required level (i.e 1000 ppm). Based on the investigation in this chapter, there are probably two methods for enhancing bottom ash utilization; 1) preventing the formation of Friedel's salt by separate the fine fraction before quenching, or 2) removing the chlorides from the ash by using circulated water in quenching process. The prevention or the removal of most of Cl⁻ from the ash was also considered as a possibility to minimize

volatile metal oxide formation, thus increasing the thermal stability of bottom ash which benefit for its disposal or its utilization (Wang et al., 2001).

4.5 CONCLUSIONS

In this chapter, the combination of petrographic thin-section analysis and the intact particle analysis by SEM/EDX and XRD were used to determine the microstructure and mineralogical characteristic of the quench product. It was found that the quench product was the new phase formed by quenching, which found to be bound to the melt product surface. It was a rough texture containing numerous aggregates that identified as Ca-hydrate phases embedded with tiny pieces of quartz, feldspars, glass, relics, metal, and organic. The thickness of the quench layer may vary from several 10 μm to mm, regardless of the melts particle size. The uneven distribution may have classified into four patterns 1) the whole particles composed of the quench product as medium and other materials embedded in, 2) the quench product as a medium joining two melt particles, 3) the quench product filled concave or vesicle partly, 4) the quenched product attached to the melt particle with a very thin layer. Besides, it was not observed that the quench product merge or fusion into the melt product. Therefore, the existing of the quench product and binding of the quench product into the melt product may happen dependently. The finer fraction of these ashes may become the quench product by turning into hydrate phases, described by the alteration of lime and portlandite and the formation of Friedel's salt. Besides, it was found that the suspended solids in quenching water was dominated by the needle-liked microcrystal of calcite. The element mapping confirmed that the main part of the quench products was C-S-H hydrate phases with the binding of Cl, and these phases accounts for the composition of Cl in the bottom ash along with Friedel's salt/hydrocalumite. The XRD analysis indicated that Friedel's salt/hydrocalumite could be found in all particle fractions, and it was size-dependent by the smaller particle size, the higher intensity.

In short, the quench product was the heterogeneous material of C-S-H hydrate phases with Friedel's salt that mixed by microcrystal of secondary mineral and tiny pieces of glass, metals and those refractory remain after combustion.

REFERENCES

- Birnin-Yauri, U.A., Glasser, F.P., 1998. Friedel's salt, $\text{Ca}_2\text{Al}(\text{OH})_6(\text{Cl},\text{OH})\cdot 2\text{H}_2\text{O}$: Its Solid Solutions and Their Role in Chloride Binding. *Cem. Concr. Res.* 28, 1713–1723. doi:10.1016/S0008-8846(98)00162-8
- Chandler, A.J., Eighmy, T.T., Hjelmar, O., Kosson, D.S., Sawell, S.E., Vehlow, J., Sloat, H.A. van der, Hartlén, J., 1997. *Municipal Solid Waste Incinerator Residues*. Elsevier.
- Chimeno, J.M., Segarra, M., Fernández, M.A., Espiell, F., 1999. Characterization of the Bottom Ash in Municipal Solid Waste Incinerator. *J. Hazard. Mater.* 64, 211–222. doi: 10.1016/S 0304-3894(98)00246-5
- Eighmy, T.T., Eusden Jr., J.D., Marsella, K., Hogan, J., Domingo, D., Krzanowski, J.E., Stämpfli, D., 1994. Particle Petrogenesis and Speciation of Elements in MSW incineration Bottom Ashes, in: J.J.J.M. Goumans, H.A. van der S. and T.G.A. (Ed.), *Studies in Environmental Science, Environmental Aspects of Construction with Waste Materials Proceeding of the International Conference on Environmental Implications of Construction Materials and Technology Developments*. Elsevier, pp. 111–136.
- Eusden, J.D., Eighmy, T.T., Hockert, K., Holland, E., Marsella, K., 1999. Petrogenesis of Municipal Solid Waste Combustion Bottom Ash. *Appl. Geochem.* 14, 1073–1091. doi: 10.1016/S0883-2927(99)00005-0
- Inkaew, K., Saffarzadeh, A., Shimaoka, T., 2015. Impacts of Water Quenching on MSWI Bottom Ash Characterization, in: *The 2nd Symposium of Asian Regional Branch of International Waste Working Group. Presented at the IWWG-ARB 2015, Institute of waste treatment and reclamation (IWTR), College of Environmental Science and Engineering, Shanghai, China*, pp. 87–100.
- Ito, R., Dodbiba, G., Fujita, T., Ahn, J.W., 2008. Removal of Insoluble Chloride from Bottom Ash for Recycling. *Waste Manag.* 28, 1317–1323. doi:10.1016/j.wasman.2007.05.015
- Jones, B., Kahle, C.F., 1993. Morphology, Relationship, and Origin of Fiber and Dendrite Calcite Crystals. *J. Sediment. Res.* 63, 1018–1031. doi:10.1306/D4267C85-2B26-11D7-864 8000102C1865D
- Kirby, C.S., Rimstidt, J.D., 1993. Mineralogy and Surface Properties of Municipal Solid Waste Ash. *Environ. Sci. Technol.* 27, 652–660. doi:10.1021/es00041a008
- Krzanowski, J.E., Eighmy, T.T., Crannell, B.S., Eusden, J.D., 1998. An Analytical Electron Microscopy Investigation of Municipal Solid Waste Incineration Bottom Ash. *J. Mater. Res.* 13, 28–36. doi:10.1557/JMR.1998.0005
- Pfrang-Stotz, G., Schneider, J., 1995. Comparative Studies of Waste Incineration Bottom Ashes From Various Grate and Firing Systems, Conducted With Respect To Mineralogical and Geochemical Methods of Examination. *Waste Manag. Res.* 13, 273–292. doi:10.1177/07 34242X9501300307

- Piantone, P., Bodéan, F., Chatelet-Snidaro, L., 2004. Mineralogical Study of Secondary Mineral Phases from Weathered MSWI Bottom Ash: Implications for the Modelling and Trapping of Heavy Metals. *Appl. Geochem.* 19, 1891–1904. doi:10.1016/j.apgeochem.2004.05.006
- Saffarzadeh, A., Shimaoka, T., Wei, Y., Gardner, K.H., Musselman, C.N., 2011. Impacts of Natural Weathering on the Transformation/Neof ormation Processes in Landfilled MSWI Bottom Ash: A Geoenvironmental Perspective. *Waste Manag.* 31, 2440–2454. doi:10.1016/j.wasman.2011.07.017
- Speiser, C., Baumann, T., Niessner, R., 2001. Characterization of Municipal Solid Waste Incineration (MSWI) Bottom Ash by Scanning Electron Microscopy and Quantitative Energy Dispersive X-ray Microanalysis (SEM/EDX). *Fresenius J. Anal. Chem.* 370, 752–759. doi:10.1007/s002160000659
- Speiser, C., Baumann, T., Niessner, R., 2000. Morphological and Chemical Characterization of Calcium-Hydrate Phases Formed in Alteration Processes of Deposited Municipal Solid Waste Incinerator Bottom Ash. *Environ. Sci. Technol.* 34, 5030–5037. doi:10.1021/es990739c
- Wang, K.-S., Chiang, K.-Y., Lin, K.-L., Sun, C.-J., 2001. Effects of a Water-Extraction Process on Heavy Metal Behavior in Municipal Solid Waste Incinerator Fly Ash. *Hydrometallurgy* 62, 73–81. doi:10.1016/S0304-386X(01)00186-4
- Wei, Y., 2011. Geoenvironmental Study of MSWI Bottom Ash with Emphasis on Secondary Mineralization and Behavior of Heavy Metals. Kyushu University, Fukuoka, Japan.
- Wei, Y., Shimaoka, T., Saffarzadeh, A., Takahashi, F., 2011. Mineralogical characterization of municipal solid waste incineration bottom ash with an emphasis on heavy metal-bearing phases. *J. Hazard. Mater.* 187, 534–543. doi:10.1016/j.jhazmat.2011.01.070
- Yang, S., Saffarzadeh, A., Shimaoka, T., Kawano, T., 2014. Existence of Cl in Municipal Solid Waste Incineration Bottom Ash and Dechlorination Effect of Thermal Treatment. *J. Hazard. Mater.* 267, 214–220. doi:10.1016/j.jhazmat.2013.12.045
- Zevenbergen, C., Wood, T.V., Bradley, J. p., Van Der Broeck, P. f. c. w., Orbons, A. j., Van Reeuwijk, L. p., 1994. Morphological and Chemical Properties of MSWI Bottom Ash with Respect to the Glassy Constituents. *Hazard. Waste Hazard. Mater.* 11, 371–383. doi:10.1089/hwm.1994.11.371

CHAPTER 5

MODELING THE FORMATION MECHANISM OF THE QUENCH PRODUCT ON THE SURFACE OF MSWI BOTTOM ASH

CHAPTER 5

MODELING THE FORMATION MECHANISM OF THE QUENCH PRODUCT ON THE SURFACE OF MSWI BOTTOM ASH

5.1 ABSTRACT

The quenched bottom ash consists of metastable materials generated after quenching and it changes toward equilibrium in the environment. In this chapter, changes in the bottom ash morphology and mineral composition under experimental quenching conditions were investigated to clarify the mechanisms behind the formation of the quench product/layer around the bottom ash particle. In the experiments, the unquenched bottom ashes were heated to 300 °C, immediately quenched by warm water, filtered, and dried. Particle size distribution analyses, intact particle and thin-section observation, X-ray diffractometry, and scanning electron microscope/energy dispersive X-ray spectroscopy were conducted on the quenched bottom ash samples. The result indicated that after quenching, the morphology and mineralogy of the bottom ash changed significantly. The quenched bottom ash was dominated by the quench product that was characterized by amorphous and microcrystalline C-S-H phases, which bounded as a layer. This layer also enclosed tiny minerals, glasses, ceramics, metals, and organic materials as unburned residues. The dominant mineral phases produced by quenching process and detected by XRD were calcite, Friedel's salt, hydrocalumite and portlandite. The formation of quench product was controlled by the fine fraction of the bottom ash (particle size <0.425 mm). From the observations, a conceptual model of the ash-water reactions and formation of the quench product in the bottom ash was proposed.

5.2 INTRODUCTION

In many industrialized countries, incineration, along with recycling and waste disposal, has long been an important part to the waste management system. MSWI offers an attractive benefit, including destroying pathogens and toxins, reducing mass and volume

of waste, and providing an alternative energy source. After incineration, however, a considerable amount of solid residues remains as bottom ash, fly ash, and boiler ash. The bottom ash accounts for about 80 % of the total residue (Chimeno et al., 1999).

After combustion, bottom ash is discharged by an ash discharger, now commercially available in both dry and wet types. The former is a new technology either operated without water or using only a small amount of water as a semi-dry system. The latter combines water reservoirs into a quenching system, which helps cool the bottom ash, reduce dust, reduce the size of large clinker, and separate incompletely burnt materials (Chandler et al., 1997). The wet discharge is the dominant technology applied in most waste-to-energy plants worldwide (Bourtsalas, 2013). In Japan, there were 1,172 incineration plants by 2013 (Ministry of the Environment, 2013), only six of which used the dry discharge system (Bourtsalas, 2013). Therefore, most of the bottom ash is traditionally quenched by water before being discharged.

Water quenching has been determined to have a great impact on bottom ash characteristics (Chandler et al., 1997). Inkaew et al. (2015) found that water quenching influenced bottom ash by changing particle size; increasing specific surface area; changing morphology by producing the quench products; reducing pH; altering the chemical composition; and enhancing the formation of portlandite, hydrocalumite, and Friedel's salt. The main difference between unquenched/air-cooled and quenched bottom ash was determined to be the quench products present in the latter.

Generally, the unquenched bottom ash contains two main products that are combined together; refractory and melt. Refractory materials refer to ceramics, metals, or other substances that were inherited from waste and retain their original characteristics after combustion. Melt products are slag materials that consist mainly of glass and mineral phases that formed during incineration (Eusden et al., 1999; Saffarzadeh et al., 2006). In quenched bottom ash, the quench products are generated by the physico-chemical reaction between ash and water. These products have been defined as quench layer/phase (Saffarzadeh et al., 2011) or fragile (Wei et al., 2011) because of their spatial distribution within the bottom ash particles, and their fragile characteristics compared with those of melt products. Hydrate and carbonate phases have been reported as the main components of quench products (Saffarzadeh et al., 2011; Wei et al., 2011; Yang et al., 2014). Because quench products provide active pores and a substantial specific surface area to the bottom

ash (Inkaew et al., 2015), they are assumed to be the chief host for chemical reactions during weathering. Additionally, quench product plays a crucial role in the accumulation and distribution of chloride compounds (Inkaew et al., 2015; Yang et al., 2014). Therefore, the formation of the quench product may be considered as the negative affected induced by quenching due to the active property and the chloride content of the ash prevent its utilization in construction and cement production.

Although some differences between unquenched and quenched bottom ash have been clarified, the formation of quench products and the mechanisms behind quenching are still unclear. The quench product formation process is important to understand the agglomeration of quenched bottom ash, which directly controls the ash characteristics and chemical reactions when exposed to the surrounding environment. In this study, the formation of quench products in freshly quenched bottom ash was investigated through lab-scale quenching experiments. The aims of this work were 1) to determine the characteristics of quench products after quenching, 2) to investigate the reactions during the quenching process, and 3) to propose a conceptual model for the formation of quench products and the agglomeration of quenched bottom ash particles.

5.3 MATERIALS AND METHODS

5.3.1 MATERIALS

The bottom ash used for this study was collected from a waste-to-energy MSWI plant in Kurume city, Japan. The plant uses a multistage grate furnace and contains three parallel processing lines with a total capacity of 300 t/day. The collected municipal solid waste was initially separated in the households and then sent through the incinerator without any further separation or treatments, except mechanical mixing in the waste pit by a crane. Approximately 60 kg of unquenched bottom ash was taken from the top of the burnt-out grate during routine maintenance. Refractory metals, glasses, and ceramics were screened out using 9.5 mm mesh. The freshly quenched bottom ash was also sampled from the exit of the quenching tank as a reference sample. It was air-dried to remove moisture and then freeze-dried for 24 h. The dried samples were kept in an air-tight container for further experiments. About 20 l of quenching water was collected from the quenching tank of the incineration plant in order to be used in the lab-scale tests. The

water temperature inside the quench tank was recorded during sampling that was about 65 °C in average.

5.3.2 EXPERIMENTS

Due to the unquenched bottom ash was sampled at the ambient temperature and was transferred to the laboratory, some mineralogical rearrangement under ambient conditions may occur. Therefore, before quenching experiment, the unquenched bottom ash was heated in a muffle furnace. The heating temperature was set to 300 °C to match the approximate temperature of the ash which is discharged from the combustion chamber (Eusden et al., 1999). The dwell time was set as 1 h to ensure that the bottom ash reached the same condition as that of the incinerator. Subsequently, the heated bottom ash was carefully quenched in a 5-liter beaker that was filled with warm water (65 °C) as shown in Figure 5.1. The system was allowed to mimic the estimated residence time of the ash inside the quenching tanks of 5 min. The experimental conditions are shown in Table 5.1. To obtain additional information about quenching liquid/solid ratio, the quenching experiment were performed by setting the liquid/solid ratio to 15 and 50 respectively, the quenching temperature were set to 65 °C and residence time of 5 min. For the influence of quenching residence time, the temperature of system was also set to 65 °C with liquid/solid ratio to 15. Only the quenching residence time was varied to 1, 2, 3, 4, and 8 h respectively. After quenching, samples were dried for particle size distribution, surface morphology, thin-section, and mineral composition analyses.

5.3.3 ANALYTICAL METHODOLOGIES AND APPARATUS

Particle size distribution of the bulk sample was determined using standard sieves class of 0.075, 0.125, 0.250, 0.425, 1.00, 2.00, and 4.75 mm to evaluate particle size distribution before and after quenching. Several particles were carefully picked out under the stereo microscope to prepare standard petrographic thin sections. The thin sections were observed using a petrographic polarized microscope (BX51-33MB, Olympus) in different optical modes (plane polarized light, PPL; cross polarized light, XPL; and reflected light, RL). The morphological properties and chemical composition of the intact particles and thin sections were determined using scanning electron microscopy (SEM) coupled with quantitative energy-dispersive X-ray spectroscopy (EDX) in backscattered

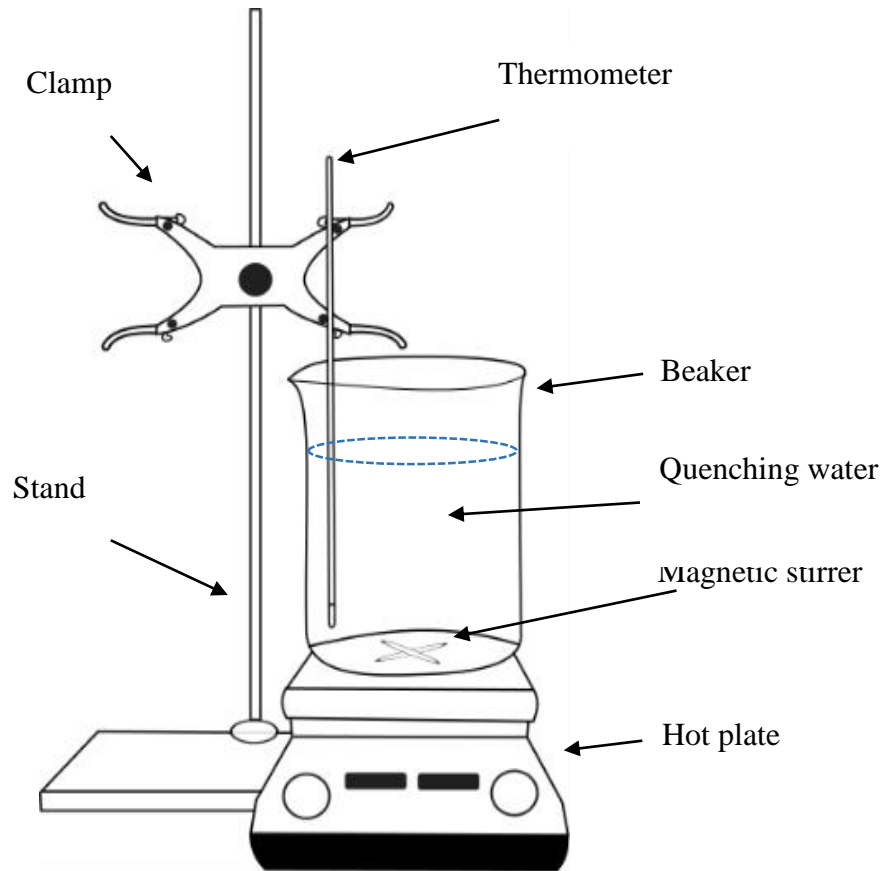


Figure 5.1 Schematic diagram of the experimental quenching setup.

Table 5.1 Experimental condition and treatment.

Treatment	Bottom ash	Quenching water
Scenario 1	Bulk bottom ash 100 g.	Filtrate quenching water 1.5 l
	Bulk bottom ash 100 g.	Tab water 1.5 l
Scenario 2	Bottom ash 1.00-2.00 mm 10 g.	Non-filtrate quenching water 1.5 l
	Bottom ash 1.00-2.00 mm 10 g.	Tab water 1.5 l
Scenario 3	Bottom ash <0.425 mm	Filtrate quenching water 1.5 l
	Bottom ash <0.425 mm	Tab water 1.5 l

electron (BSE) mode. The bulk samples were ground using automatic ball milling prior to bulk mineralogical and chemical composition analyses. To identify the existing crystalline phases, powder X-ray diffraction (XRD) analysis was conducted in a diffractometer (Rigaku Multiflex) using CuK α radiation at 30 kV and 40 mA. Phase identification was carried out using PDXL (Integrated X-ray powder diffraction, Rigaku) software. Semi-quantitative bulk chemical analysis of the powdered samples was completed using an X-ray fluorescence spectrometer (XRF, Rigaku RIX3100). Loss on ignition (LOI) of each sample was measured at 440 °C for 4 h, and the obtained value was input into EZ scan software (Rigaku). Liquid samples were analyzed for pH, oxidation-reduction potential (ORP), and electric conductivity (EC) using probe sensors connected to a digital meter (Horiba LAQUA). The suspended solids in liquid samples were analyzed using the gravimetric method. Additionally, ion concentration in the liquid phase was determined using ion chromatography (Deonex DX120).

5.4 RESULTS

5.4.1 CHARACTERIZATION OF BOTTOM ASH BEFORE QUENCHING

The unquenched bottom ash was fractionated through stainless steel mesh screens of 0.075, 0.125, 0.250, 0.425, 1.00, 2.00, and 4.75 mm to evaluate particle size distribution before quenching. [Figure 5.2](#) shows the cumulative percent passing curve according to size of the unquenched bottom ash. Particle size distribution of bottom ash residues may be influenced by waste input, combustion conditions, and the mechanical system inside the furnace ([Chandler et al., 1997](#); [Chimenos et al., 1999](#); [Phongphiphat et al., 2011](#)). The unquenched bottom ash contained particles with diameter sizes ranging from less than 0.075 mm to over 4.75 mm (from powder-like particles to coarse aggregates), with 50 % of the ash composed of particles finer than 0.7 mm. The uniformity coefficient (C_u), defined as the ratio of the particle diameter at the 60 % fine fraction (D_{60}) to the diameter at the 10 % fine fraction (D_{10}), was 5.55, indicating good gradation ([ASTM D2487-06](#)). Thus, the unquenched bottom ash can be considered a well-graded material that can be readily compacted to a density favorable for most engineering purposes (e.g., road construction, construction materials etc.) ([Chandler et al., 1997](#)).

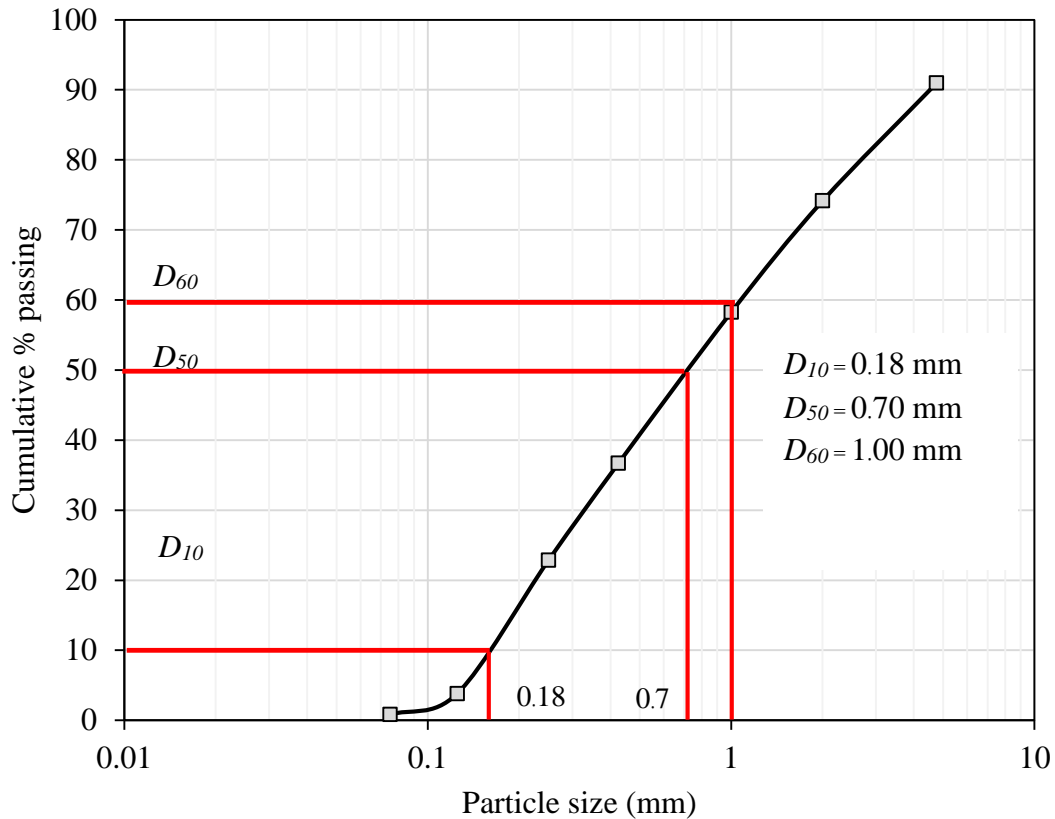


Figure 5.2 Particle size distribution of unquenched bottom ash before quenching.

The chemical composition of the unquenched bottom ash in terms of major and minor constituents by percent weight and trace constituents in ppm is shown in [Table 5.2](#). The composition is provided in the oxide form, as most of the elements were converted into oxide compounds during XRF measurements. Light elements, including oxygen and carbon, cannot be individually analyzed by XRF. From [Table 5.2](#), the major oxides, accounting for approximately 70 % of the weight, were calcium, silicon, and aluminum oxides, while the minor constituents presented considerably low concentrations. These results are consistent with those of [Li et al. \(2004\)](#) in terms of constituents, whose bottom ash also came from the top of the grates of an incinerator. However, the percentage of individual elements slightly differed, probably because of variance in the original waste composition and the incinerator operational conditions ([Rendek et al., 2007](#)). The samples were also found to contain relatively high trace metal concentrations of Zn and Ba as well as, Cu, Cr, Pb, Cd and Ni. This might raise concerns about the potential hazards of using

the unquenched ash as a resource. Thus, the ash may require additional treatment prior to use (Bayuseno and Schmahl, 2010).

Table 5.2 Chemical composition of the unquenched bottom ash determined by XRF.

Composition	This study	Ref. (Li et al., 2004)
Major and minor element (wt.%)		
CaO	44.63	27.93
SiO ₂	22.64	32.83
Al ₂ O ₃	12.21	4.37
Fe ₂ O ₃	4.47	3.39
MgO	3.10	5.40
Na ₂ O	2.09	3.18
K ₂ O	0.85	2.42
P ₂ O ₅	3.70	5.03
TiO ₂	2.17	0.78
MnO	0.10	0.13
LOI*	0.45	5.97
Cl	2.32	2.80
S	0.46	n.d.**
F	0.04	n.d.
Trace element (ppm)		
Zn	3,856	2,809
Ba	1,464	n.d
Cu	1,101	858.2
Cr	446	366.6
Pb	443	660.6
Cd	101	23.29
Ni	94	178.2

Remark: * LOI = loss on ignition, ** n.d. = not detected

According to its mineralogy shown in [Table 5.3](#), the unquenched bottom ash consisted of a variety of minerals, including silicates, carbonates, oxides, aluminates, and salts. Among these minerals, calcite, quartz, gehlenite, hematite, and lime were readily identified through a traditional search match procedure with high relative intensities. Accordingly, most of the above mineral phases have often been identified in previous studies as major components in bottom ash ([Bayuseno and Schmahl, 2010](#); [Wei et al., 2011](#); [Zevenbergen et al., 1994](#)). In addition to those mentioned minerals, the presence of lime particularly indicates the non-hydrated condition of the calcium oxide directly obtained from the combustion. Lime in bottom ash has been shown to be the product of calcium carbonate calcination at furnace temperatures ([Chimenos et al., 1999](#)).

Table 5.3 Mineral composition in the unquenched bottom ash identified by XRD.

Mineral name	Chemical formula	Unquenched bottom ash
<i>carbonate</i>		
Calcite	CaCO ₃	++++
Magnesite	MgCO ₃	++
<i>silicate</i>		
Quartz	SiO ₂	+++
Gehlenite	Ca ₂ Al ₂ SiO ₇	+++
Hardystonite-Arkermanite	Ca ₂ (Mg,Zn)Si ₂ O ₇	+
Larnite	Ca ₂ SiO ₄	++
Plagioclase feldspars	KAlSi ₃ O ₈ -NaAlSi ₃ O ₈ -CaAl ₂ Si ₂ O ₈	++
<i>oxide</i>		
Lime	CaO	+++
Hematite	Fe ₂ O ₃	++
Mayenite	Ca ₁₂ Al ₁₄ O ₃₃	+
Tricalcium aluminate	3CaO·Al ₂ O ₃	++
<i>salt</i>		
Halite	NaCl	++
Sylvite	KCl	+

Remark: ++++: highly abundant, +++: abundant, ++: low abundant, +: possible.

5.4.2 CHARACTERIZATION OF QUENCHING WATER

Table 5.4 shows the basic characteristic of liquid samples used in this chapter. According to Table 5.4, the quenching water was highly alkaline with a pH in excess of 13, high EC, and high solids and ion concentrations (particularly Na^+ , K^+ , SO_4^{2-} , and Cl^-), while the tap water was neutral (pH 7), low EC and no solids. The concentration of measured ions, such as Cl^- , Na^+ , K^+ , SO_4^{2-} , Mg^+ , NO_3^{-2} and F^- in the tap water were less than 15 mg/l. The analyses indicate that quenching water is an anti-oxidizing agent with negative oxidation reduction potential. The high concentration of ions in the quenching water represents great availability of ions for hydrate precipitation. Since the binding capacity of Cl^- to hydrate phase could be happened rapidly (Florea and Brouwers, 2012), and quenching water accumulated extreme concentrations of Cl^- up to 2,605 g/l (Table 5.4), it might be possible that Cl^- may re-absorb into bottom ash. Thus, if quenching water is used frequently without treatment, it might be considered a secondary source for chloride ions in bottom ash (Ito et al., 2008)

Table 5.4 Basic characteristic of liquid samples used in this study.

Parameter	units	Quenching water	Tap water
pH		13.34	7.50
ORP	mV	-279	-46
Electrical conductivity	ms/cm	75.67	0.06
Suspended solids	g/l	1.90	n.d.
Dissolve solids	g/l	75.17	n.d.
Cl^-	mg/l	26,053.95 ± 45.68	10.54 ± 0.06
Na^+	mg/l	19,842.72 ± 26.41	9.82 ± 0.04
K^+	mg/l	10,557.86 ± 13.38	1.51 ± 0.04
SO_4^{-2}	mg/l	6,726.14 ± 11.35	7.45 ± 0.06
Ca^+	mg/l	96.52 ± 5.71	12.66 ± 0.40
F^-	mg/l	70.36 ± 0.72	0.32 ± 0.00
Mg^+	mg/l	n.d.	2.41 ± 0.03
NO_3^{-2}	mg/l	n.d.	0.97 ± 0.01

Remark: n.d. = not detected

5.4.3 ALTERATION OF BOTTOM ASH DURING QUENCHING

At the incineration plant, the quenching phenomenon is difficult to observe directly because the quenching system is connected to the furnace in a closed system. Therefore, a laboratory-scale experiment, as shown in [Figure 5.3](#), was conducted to investigate the reaction between ash and water and the phenomenon inside the water quenching system.

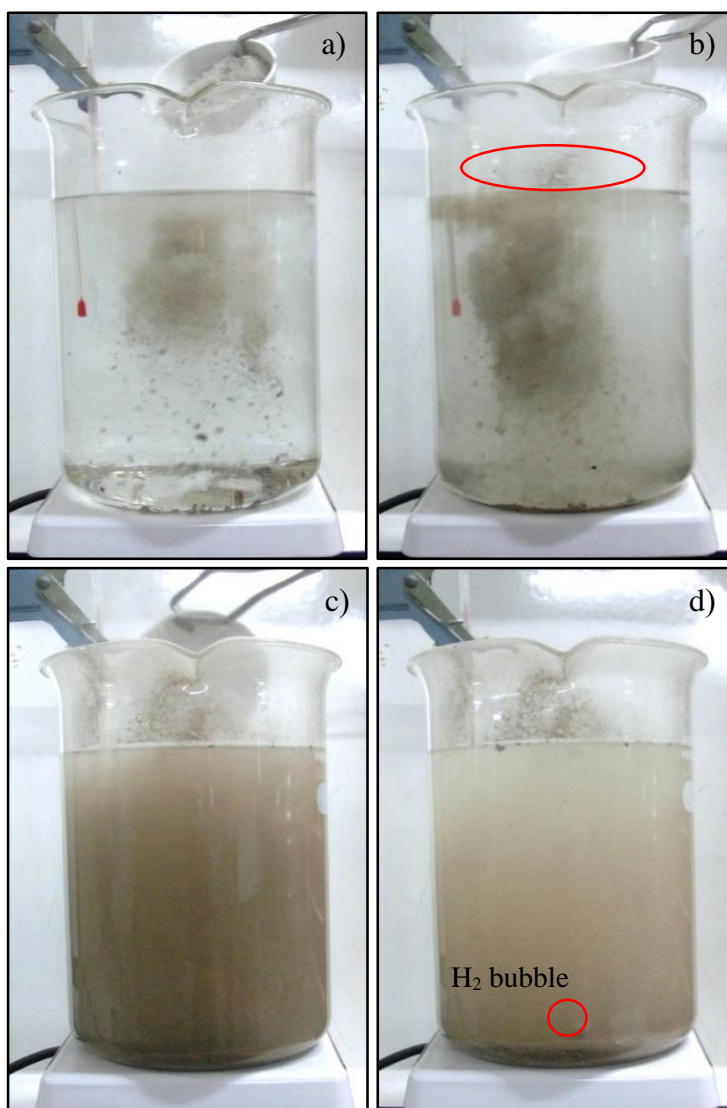
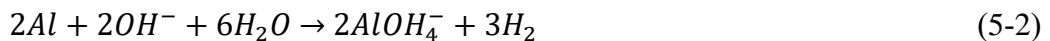


Figure 5.3 Interaction between bottom ash and water during quenching experiment; a) bottom ash submerged into water, b) floating of bottom ash caused by buoyant force c) settling of bottom ash at the bottom of beaker, and d) hydrogen gas evolution.

When the hot bottom ash dropped and was immersed in water (Figure 5.3 a)), particles were essentially moved under the influence of gravity and turbulence. At the same time, heat transfer between the solid and liquid phases occurred along with other phenomena. When the bottom ash came into contact with water, the soluble salts, sulfate, and oxides immediately began to dissolve, resulting in the accumulation of cations and anions, such as Na^+ , K^+ , Ca^{2+} , Mg^{2+} , SO_4^{2-} , and Cl^- , in the quenching water (Table 5.4). The solubility of these ions from the bottom ash is generally controlled by surface reactions via diffusion and ion exchange (Bendz et al., 2007). Some of the bottom ash flew back and floated on the surface because of the buoyant force caused by a difference in pressure between the hot ash and quenching water (Figure 5.3 b)). Simultaneously, some of the bottom ash turned into suspended solids, particularly in the form of fine particulates. Within a minute, most of the bottom ash settled to the bottom of the quenching vessel because of gravity and was then ready for discharge (Figure 5.3 c)). During quenching, the insoluble phases were precipitated. The precipitation could not be observed by the naked eye in this quenching study. However, precipitation of micro-crystalline and amorphous substances clearly occurred in the bottom ash surface based on microscopic investigation (see section 5.5). Along with hydration, oxidation of metals or alloys in the bottom ash also occurred and led to the generation of gaseous phases (Figure 5.3d)), particularly hydrogen (Arm and Lindeberg, 2006; Heuss-Aßbichler et al., 2010; Sabbas et al., 2003). The generation of hydrogen gas from metal aluminum in the bottom ash can be described by the following equations:



In addition, hydration was found to occur in the bottom ash with exposure to quenching water. The dominant hydration process in the bottom ash is known as hydration of quicklime and the formation of portlandite, as described in equation 5-3. However, portlandite is highly sensitive to carbonation process and can be considerably converted to more stable phase of calcite at the presence of dissolved or atmospheric CO_2 during or right after quenching process as shown in equation 5-4.



Through quenching, carbonation can particularly occur at the air-water interface. Of note was the precipitation of calcite scum on the sidewall of the quenching tank (Figure 5.4) of the incineration plant that can be an evidence for the above processes. However, since carbonation is accompanied by a decrease of ash pH from over 12 to approximately 8, this reaction enhanced releasing of heavy metal from the ash. In some plants, the bottom ash is left to be mature for 1-3 months as the promising technique for ash treatment to meet the regulation (Chimenos et al., 2000; Van Gerven et al., 2005). Thus, disposal of the quenched ash may offer a greater advantage over dry disposal in the view of environmental concern of heavy metal.



Figure 5.4 Accumulation of calcite scum on the side-wall of the quenching tank in the real incineration facility. The width of the calcite band shown in the photograph is around 5 cm.

5.4.4 CHARACTERIZATION OF THE QUENCHED BOTTOM ASH

5.4.4.1 MORPHOLOGY

Generally, the morphological characteristics of bottom ash particles depend both on particles' exposure conditions and chemical composition (Zevenbergen et al., 1994). In the wet discharge system, bottom ash morphology is affected by the exposure to quenching water and agglomeration during discharge. Therefore, the intact freshly quenched bottom ash particles are usually coated by finer particles, causing the fragile zone or the so-called quench product/layer that is not found in the air-cooled or unquenched bottom ash, as previously mentioned. To investigate the formation of this layer, bottom ash particles with diameters of 2.00-4.75 mm were subjected to quenching with tap water and non-filtrated quenching water. Besides, the bulk bottom ash (bottom ash containing a mixture of different particle sizes) was also quenched in tap water and filtered quenching water.

Figure 5.5 illustrates the microscopic images from the thin section of the quenched bottom ash particles treated under different quenching scenarios. The observations revealed extremely fine crystallites and amorphous solids on the outer surface of the melt (slag) products when the bulk bottom ash was quenched (Figure 5.5 a) and Figure 5.5 c)), regardless of quenching water quality. No layer of the quench products appeared on the melt product surface when the 2.00-4.75 mm slags were quenched with either non-filtered quenching water or tap water (Figure 5.5 b) and Figure 5.5 d)). The thickness of the quench products varied from about 10 μm to 1 mm. These findings confirmed the assumption that the formation of quench products in the bottom ash is controlled by the fine fraction of bottom ash. Thus, if the fine bottom ash is separated from the remainder of the ash before quenching, the quench layer with complex surface morphology can hardly be developed around the melt phase.

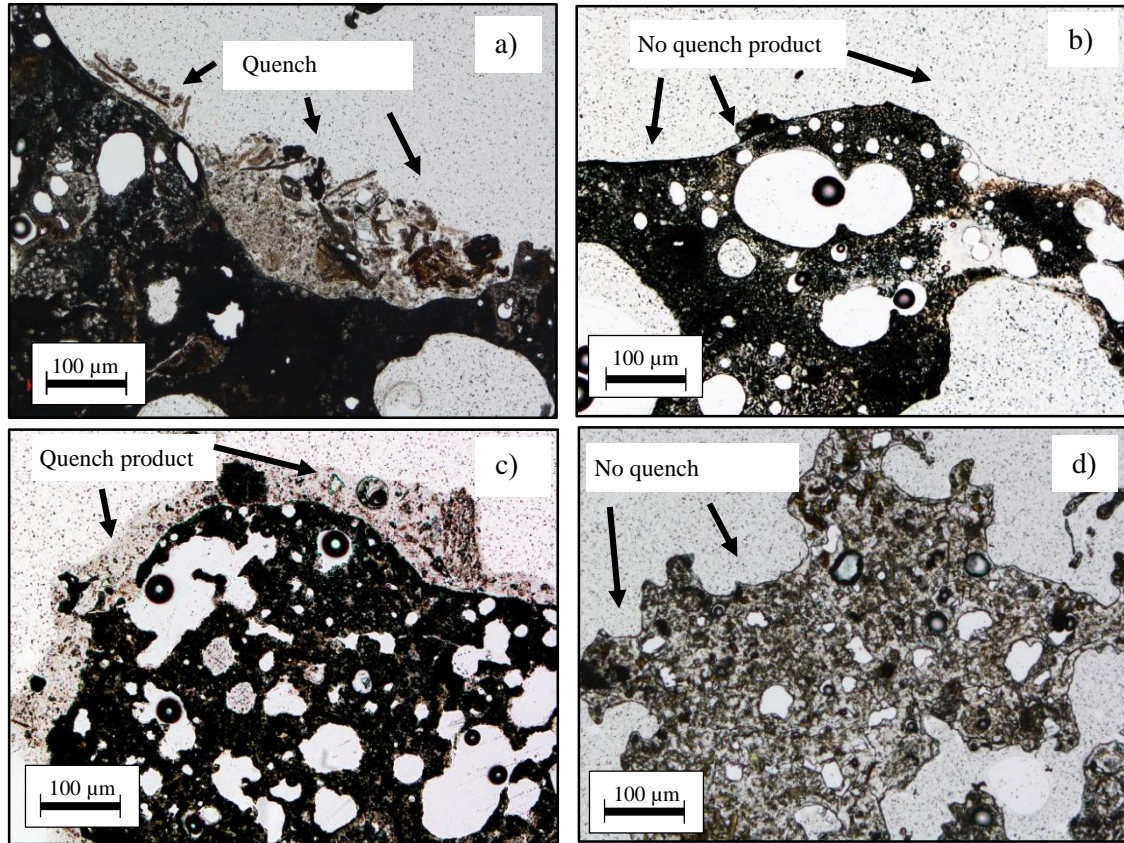


Figure 5.5 Photomicrographs of quenched bottom ash with different quenching scenarios: a) bulk bottom ash quenched with tap water, b) bottom ash (particle size between 2.00-4.75mm) quenched with tap water, c) bulk bottom ash quenched with filtered quenching water, and d) bottom ash (particle size between 2.00-4.75mm) quenched with non-filtered quenching water.

Figure 5.6 shows the microscopic characteristics of the quench products under different light modes. The quench products contained a mixture of heterogeneous materials, including opaque and non-opaque glass/melt products; tiny pieces of metal and ceramics; and microcrystalline, amorphous, organic, and other unidentified materials. Under plane polarized light (PPL), the components of the quench products essentially exhibited transparency (Figure 5.6 a)), but under cross polarized light (XPL), they presented various optical behaviors (Figure 5.6 b)). Under XPL, the organic and metallic components were opaque. Under reflected light mode (RL), most of constituents displayed similar features; however, the metallic components could be distinguished by their metallic luster (Figure 5.6 c)). Intensive investigation found that the quench product was primarily a neo-formation of

amorphous/micro-crystalline calcium silicate (C-S-H) hydrate and oxide, which behaved as a medium for the pieces of minerals, crystal, metal, glass, ceramic, and organic and inorganic materials that remained after combustion.

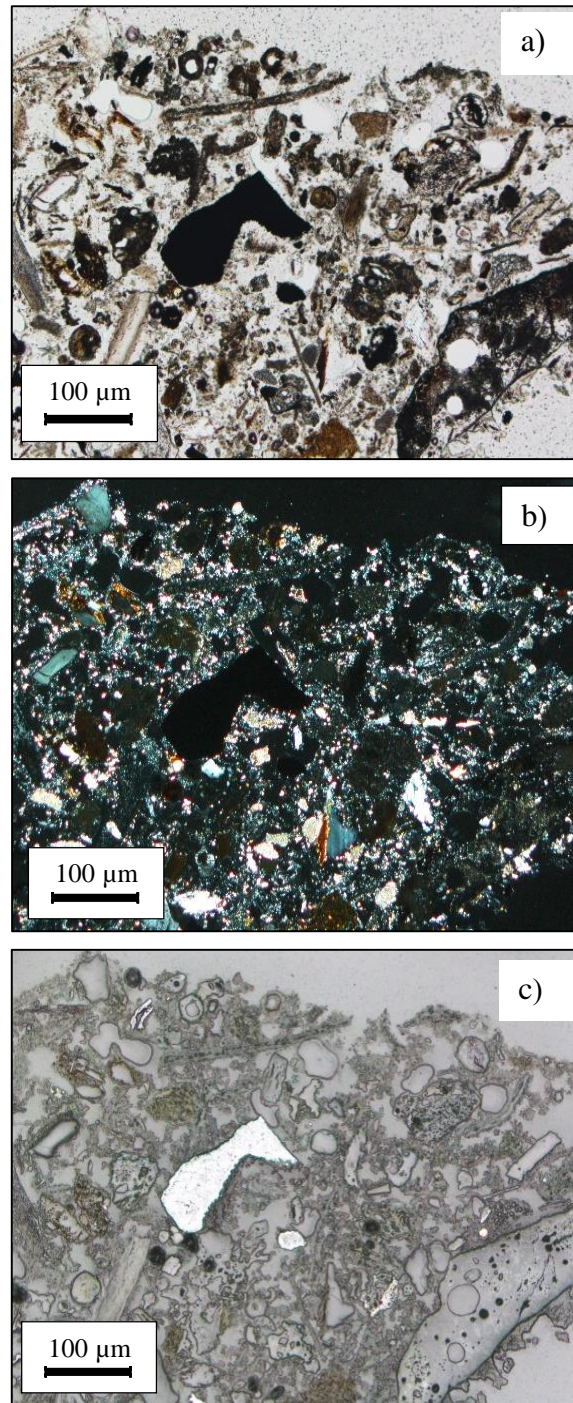
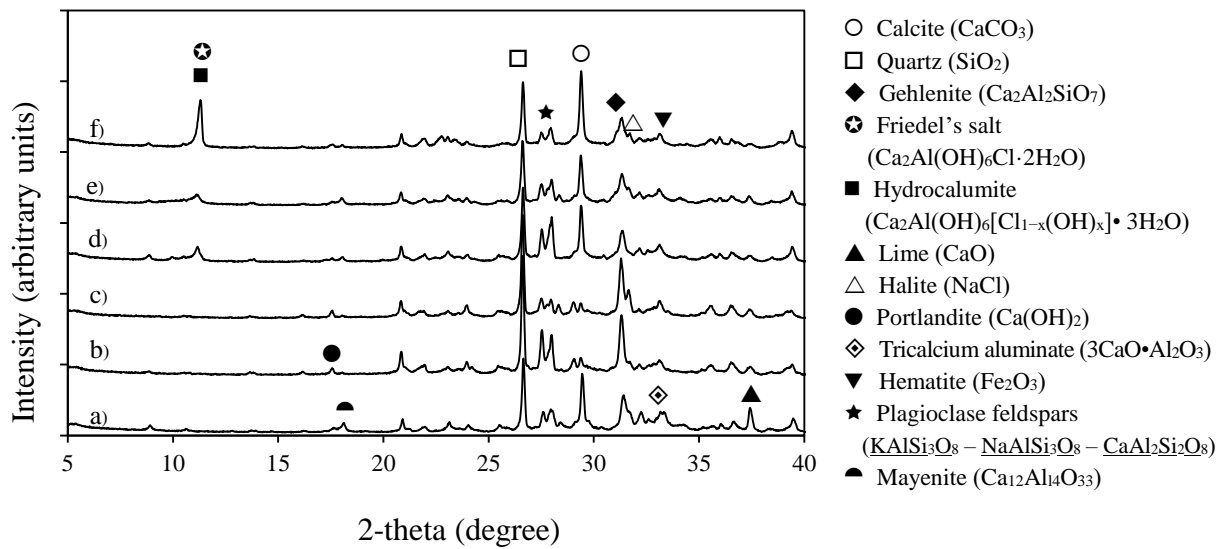


Figure 5.6 The quench product with heterogeneous admixture under different light modes; a) PPL, b) XPL, and c) RL.

5.4.4.2 MINERAL COMPOSITION

The crystalline phases detected in various samples are compared in [Figure 5.7](#). The main crystalline phases qualitatively identified were quartz, calcite, Friedel's salt, hydrocalumite, and gehlenite, while minor phases included hematite, halite, plagioclase feldspar, and possibly mayenite. Clearly, water quenching produces new crystalline phases, particularly Friedel's salt and hydrocalumite, not found in the original unquenched bottom ash. Friedel's salt has previously been identified in bottom ash products of incineration as a major insoluble salt and has a negative influence on the properties of construction materials when recycled ([Ito et al., 2008](#)). Hydrocalumite is a polymer derivative of Friedel's salt ([Vieille et al., 2003](#)), and some researchers have found hydrocalumite instead of Friedel's salt ([Bayuseno and Schmahl, 2010](#)). In this work, as can be seen in [Figure 5.7](#), Friedel's salt and hydrocalumite both are present at 2Θ , 11.5. Since bottom-ash quenching provides an adequate amount of Ca-Al and Cl-rich compounds to the system, it is possible that both Friedel's salt and hydrocalumite existed in the quenched sample as dominant hydration products. Hydration in bottom ash is known to occur in the formation of new phases, such as portlandite, ettringite, hydrocalumite, and gypsum ([Bayuseno and Schmahl, 2010](#); [Speiser et al., 2000](#)). However, in this study, portlandite, ettringite, and gypsum could not be detected by XRD, probably because the amounts of these minerals were lower than the XRD detection limit or the quenching time was insufficient to enhance the minerals formation, as occurred in the aged bottom ash. Another possibility is that portlandite formed and then immediately converted to calcite via carbonation ([Equation 4](#)).



- a) unquenched bottom ash
 b) bottom ash particle size 2.00-4.75 mm quenched in tap water,
 c) bottom ash particle size 2.00-4.75 mm quenched in non-filtrated quenching water,
 d) bulk bottom ash quenched in tap water,
 e) bulk bottom ash quenched in filtrated quenching water,
 f) reference freshly quenched bottom ash.

Figure 5.7 X-ray diffraction data of sample after quenching experiment compared to unquenched bottom ash and reference freshly quenched bottom ash from the same incineration plant.

Considering to the influence of liquid/solid ratio and residence time of quenching on mineralogy of the ash, it was found that although the liquid/solid ratios of quenching system were different, the mineral composition of the quenched ash which detected by XRD were fairly similar (Figure 5.8). In contrary, the residence time of quenching appeared to have a greater influenced on the quenched ash mineralogy than the liquid/solid ratio. Figure 5.9 presents the XRD pattern of the ashes that were quenched with different residence time. It could be seen that the peak of Friedel's salt/Hydrocalumite between 1 and 8 h were different apparently. However, due to the quenching residence time in practical operation is slightly short (about 1-5 min), it is possible that the mineral composition of the ash may be similar even the liquid/solid ratio of quenching system is different.

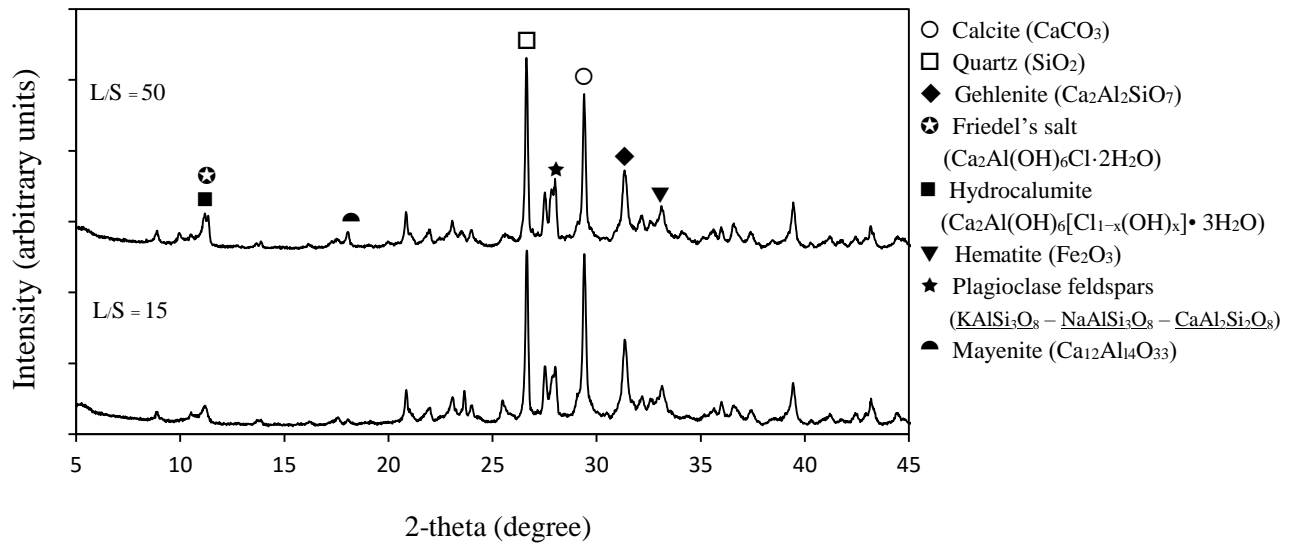


Figure 5.8 X-ray diffraction data of samples after quenching with different liquid/solid ratio.

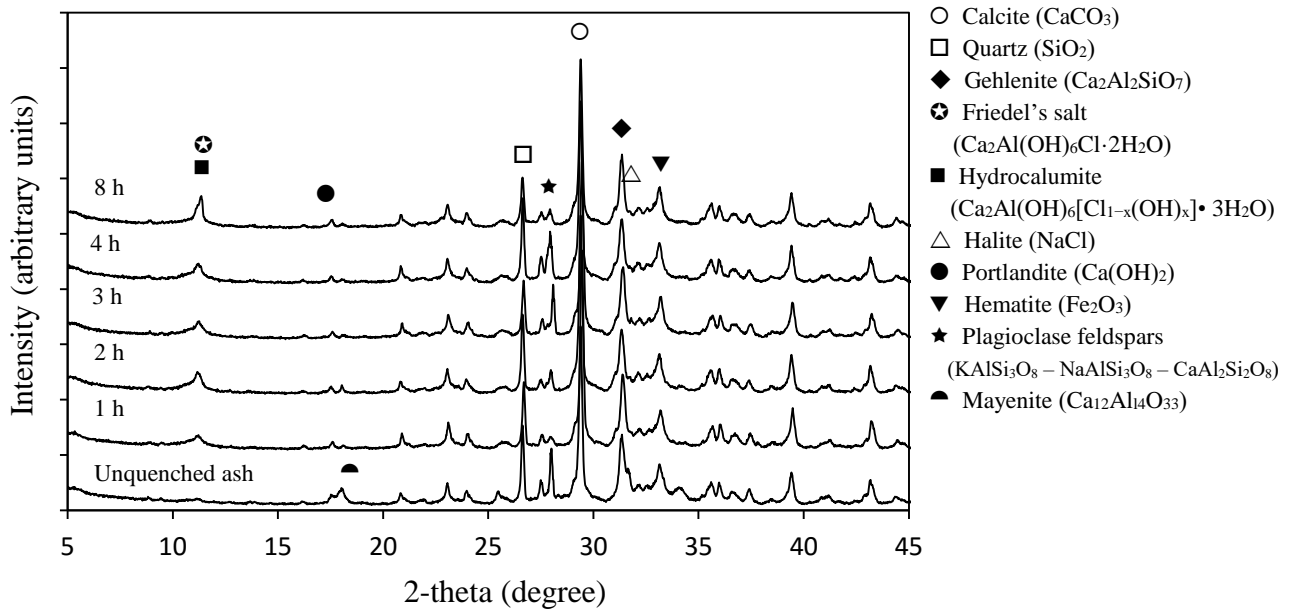


Figure 5.9 X-ray diffraction data of samples after quenching with different residence time.

5.4.5 FACTORS CONTROLLING THE FORMATION OF THE QUENCH PRODUCT

There are three major factors that control the formation of quenched bottom ash, including fine fraction of bottom ash particles; quenching water; and physico-chemical changes, such as de-watering during discharge and drying, precipitation of hydrate phases, hardening, and cementation effect, which exerted by the precipitated carbonate layer during carbonation. Based on the particle size distribution analysis (Figure 5.10), particles between 0.125 and 0.425 mm may have been responsible for the formation of the quench product by assembling into coarser particles, as the proportion of particles in this size range decreased drastically in the quenched ash after quenching. When fine bottom ash with a diameter less than 0.425 mm underwent quenching, its mineral composition changed, and it became quench products through the formation of new hydrate phases, such as Friedel's salt, hydrocalumite (Figure 5.11), and other microcrystalline and amorphous phases. Later, the fine particles that had transformed into quench products were bound together to form coarser particles.

The experiments revealed that the quench products were attached to the rigid core (melt phase) of the quenched bottom ash after quenching. Evidence of this process was observed during the quenching test when the bottom ash was discharged from the system. As described in section 5.4.3, when the bulk sample dropped into water, each particle sank freely. Some finer particles that initially stuck to the coarser particle surface via static force (Chimenos et al., 1999) were later removed out by water. The ashes that settled in the bottom of the quenching tank were then discharged completely. During discharge, bottom ash was extracted from the quenching water, resulting in a moisture content of about 20-46% by weight. Through extraction, the finer particle and the coarser particle were mixed and attached to the coarser particles.

The attachment between bottom ash particles can be divided into two stages. In the early stage, during discharge, the thin film of saturated quenching water (capillary bridge) in the ash is assumed to cause the adhesion between particles via capillary force (Balakin et al., 2015). In the second stage, when the ash becomes dry, the formation of new phases causes the stronger adhesion between particles. Near the vicinity of the melt phases, newly formed hydrate phases usually appear, particularly between metallic

particles (Figure 5.12). These hydrate phases may act as binding agents for the quench product. In addition, hardening of the previously mentioned cement phases, such as C-S-H hydrate, contained in bottom ash accounts for the strong bond between the quench products and the melt particles. To confirm the influence of cementation/carbonation on hardening of the quenched bottom ash, freeze-drying (which prevented carbonation) and air-drying were performed after quenching. The results (Figure 5.10) show that the average mass of the retained bottom ash with particles larger than 2 mm increased after quenching in the air-dried sample. This finding reflects a stronger bond between particles in the quenched bottom ash exposed to carbonation via air-drying compared to the freeze dried bottom ash.

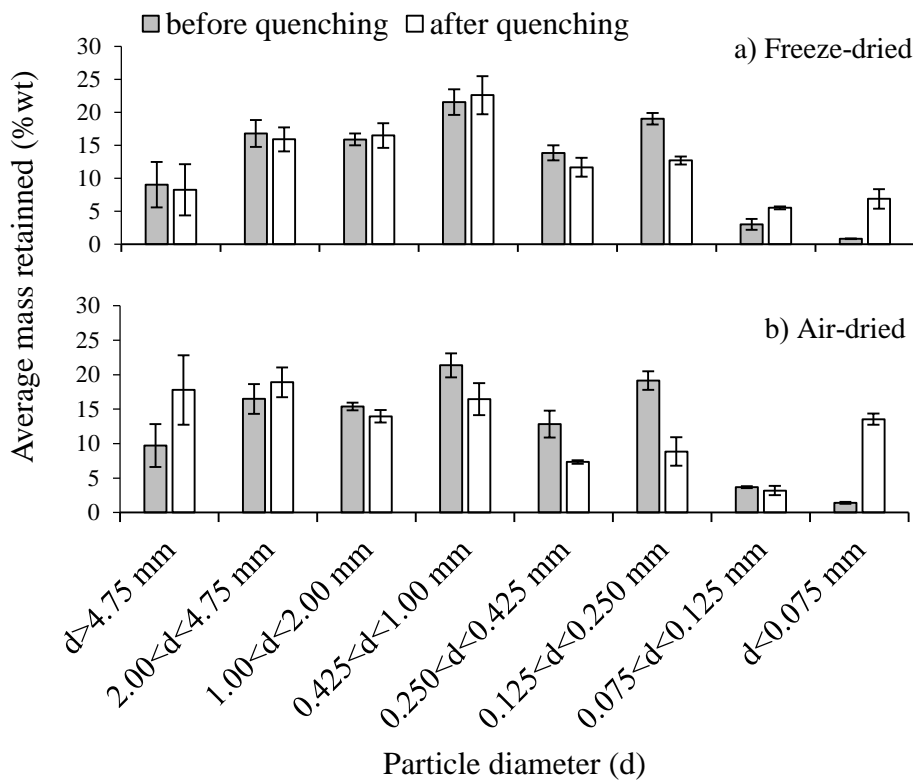


Figure 5.10 Percentage weight of bottom ash particles retained on sieve before and after quenching comparing between 2 drying method; a) freeze-dried and b) air dried.

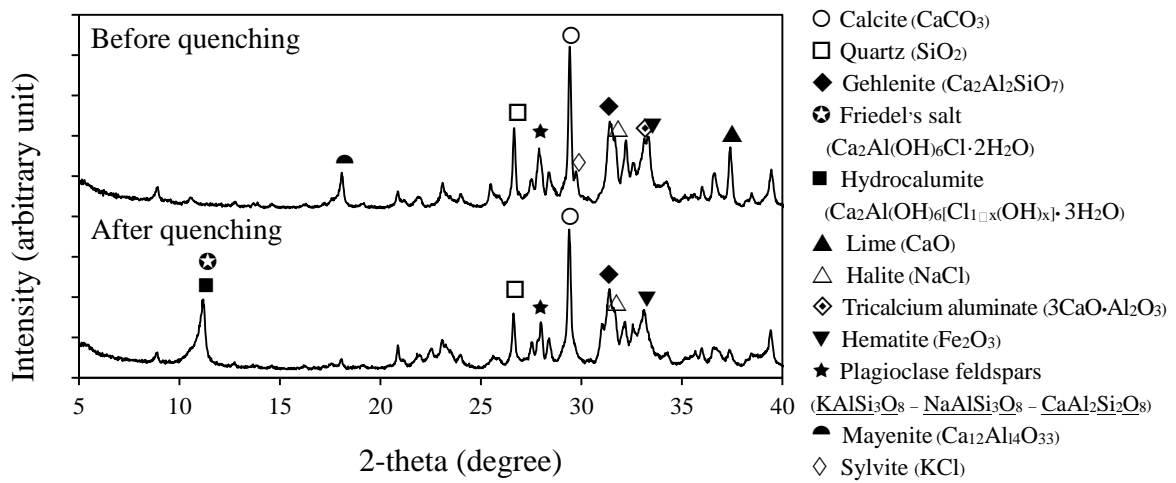


Figure 5.11 X-ray diffractogram of bottom ash particles with diameter smaller than 0.425 mm comparing before and after quenching.

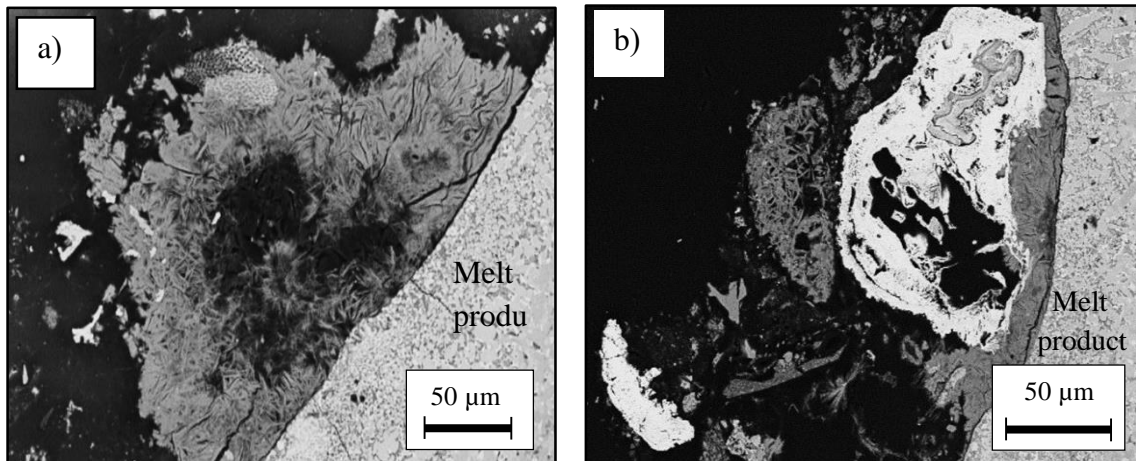


Figure 5.12 Backscattered electron images show Ca-rich dendritic hydrate phases that precipitated near a) the vicinity of the melt product and b) an aluminum relic.

5.4.6 PROPOSED MODEL FOR FORMATION MECHANISM OF THE QUENCH PRODUCT ON BOTTOM ASH

To simplify the reactions involved in the quenching process and the formation of the quench product, a conceptual model for these phenomena was developed (Figure 5.11). The model was created based upon observations and a literature review of possible reactions (Arm and Lindeberg, 2006; Balakin et al., 2015; Bendz et al., 2007; Chimenos et al., 2000; Heuss-Aßbichler et al., 2010; Meima and Comans, 1997; Saffarzadeh et al., 2011; Speiser et al., 2000). The chemical alteration of bottom ash caused by quenching can be divided into two stages. The first stage includes dissolution of major soluble salts via diffusion (Figure 5.11 a), precipitation of hydrate phases, and oxidation of metallic aluminum (Figure 5.11 b). This stage begins immediately after the bottom ash is immersed in the quenching water (Meima and Comans, 1997; Speiser et al., 2000). As the bottom ash reaches the bottom of the quenching system, it is simultaneously discharged. The chemical reactions from the first stage continue until equilibrium is obtained. When the bottom ash is discharged, the second stage begins. This stage involves the agglomeration of bottom ash via capillary bridge (Figure 11 c), carbonation via pore water, and hardening of hydration phases such as C-S-H hydrate via drying. (Figure 11 d). The capillary bridge is an important phenomenon that causes powder-liked materials agglomeration. It occurs at the particle surface with capillary force between particles in the presence of moisture or liquid as a bridge (Balakin et al., 2015). The capillary bridge between bottom ash particles occurs by the saturated quenching water after discharge, it also plays the role of a medium for surface reactions such as carbonation, metallic aluminum oxidation, etc. For hardening; this process takes place in the hydration product gradually after the ash was discharged. The strong bond between the hydration product and the rigid core is believed to be bonded during the course of drying. Since the quenching process does not provide completely stable conditions for the bottom ash, thus further aging continues in the disposal environment.

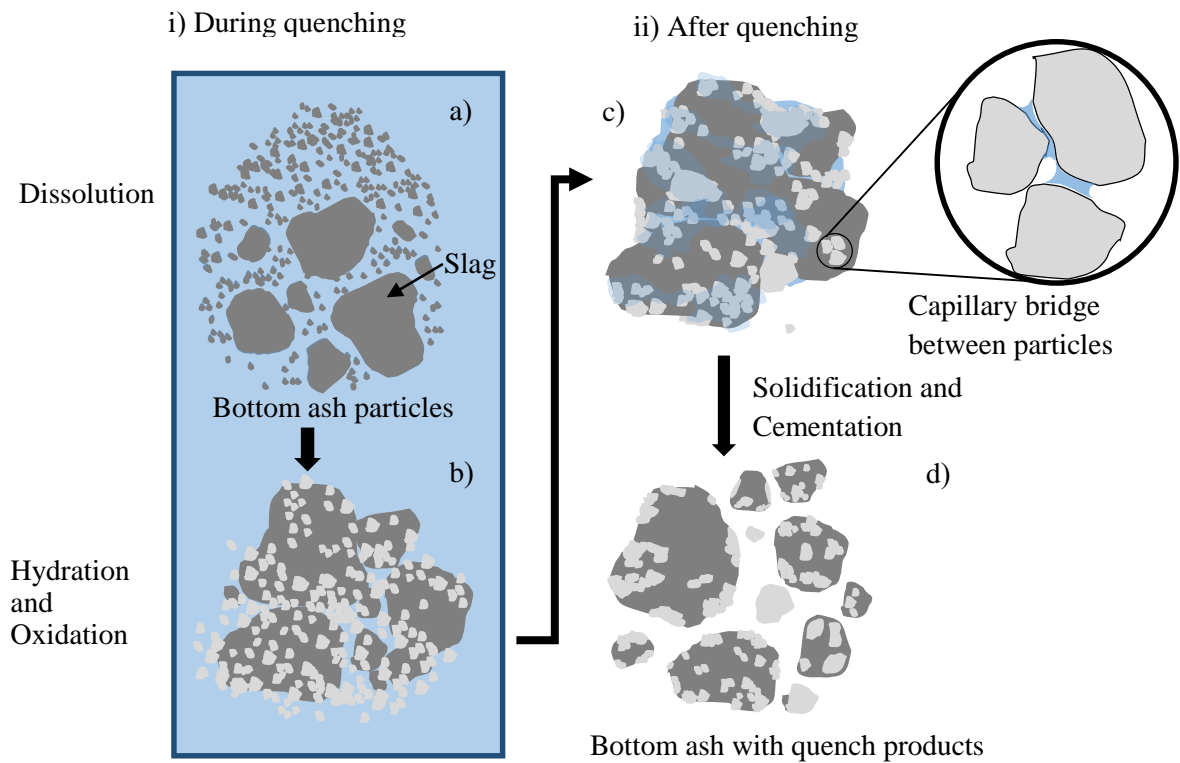


Figure 5.11 A schematic conceptual model describing various stages in the formation of the quench products in bottom ash particles: a) dissolution of major soluble salts, b) precipitation of hydrate phases, and oxidation of metals, c) agglomeration of bottom ash particles via capillary-bridging, and d) hardening and solidification stage.

5.5 CONCLUSIONS

Quenching process has a great influence on bottom ash characterization, particularly inducing the formation of the quench products on the ash surface. In order to obtain the basis information about mechanism involved in the quench product formation, the laboratory scale quenching was simulated. In this chapter, the formation of quench products on bottom ash was investigated through quenching experiments. The unquenched bottom ash was heated and quenched with quenching water in different scenarios. Along with visual observation during the experiments, particle size analysis, microscopic analysis, and XRD helped illuminate the phenomena and the influence of the

quenching process on bottom ash. Based on the results from this study, the conclusions are summarized below:

1. The unquenched bottom ash was composed of particles with diameters ranging from less than 0.075 to over 4.75 mm (from powder-like particles to coarse aggregates). About 50% of the ash typically consisted of particles finer than 0.7 mm.
2. The major oxides in the unquenched bottom ash, accounting for approximately 70% of the weight, included calcium, silica and aluminum oxides, while the minor constituents presented considerably less concentrations.
3. After quenching, the morphology and mineralogy of the bottom ash changed significantly through the formation of the quench product, characterized by amorphous or microcrystalline C-S-H phases that embedded tiny minerals, glasses, ceramics, metals, and organic materials remaining after combustion.
4. The quenching process produced new hydrate crystalline phases, particularly Friedel's salt and hydrocalumite, not found in the original unquenched bottom ash.
5. The factors that controlled the formation of the quenched bottom ash included fine bottom ash particles (0.125-0.425 mm); quenching water; and physiochemical changes, such as de-watering, precipitation of hydrate phases, hardening, and cementation/ carbonation.
6. A conceptual model of the formation of the quench product and agglomeration of the quenched bottom ash was proposed. The chemical changes in the bottom ash caused by quenching can be divided into two stages. The first stage includes dissolution of major soluble salts via diffusion, precipitation of hydrate phases, and oxidation of both ferrous and non-ferrous metals. The second stage involves the agglomeration of bottom ash via water-bridging, carbonation via pore water, and hardening of cement phases.

REFERENCES

- Arm, M., Lindeberg, J., 2006. Gas Generation in Incinerator Ash. Proc. WASCON 6, 629–637.
- ASTM D2487-06, Standard Practice for Classification of Soils for Engineering Purposes (Unified Soil Classification System), 2006. ASTM international, West Conshohocken, PA, www.astm.org.
- Balakin, B.V., Shamsutdinova, G., Kosinski, P., 2015. Agglomeration of Solid Particles by Liquid Bridge Flocculants: Pragmatic Modelling. Chem. Eng. Sci. 122, 173–181. doi:10.1016/j.ces.2014.09.003
- Bayuseno, A.P., Schmahl, W.W., 2010. Understanding the Chemical and Mineralogical Properties of the Inorganic Portion of MSWI Bottom Ash. Waste Manag. 30, 1509–1520. doi:10.1016/j.wasman.2010.03.010
- Bendz, D., Tüchsen, P.L., Christensen, T.H., 2007. The Dissolution Kinetics of Major Elements in Municipal Solid Waste Incineration Bottom Ash Particles. J. Contam. Hydrol. 94, 178–194. doi:10.1016/j.jconhyd.2007.05.010
- Bourtsalas, A., 2013. Review of WTE Ash Utilization Processes Under Development in north west Europe. URL <http://www.seas.columbia.edu/earth/wtert/sofos/WTEBA.pdf> (accessed 8.17.15).
- Chandler, A.J., Eighmy, T.T., Hjelmar, O., Kosson, D.S., Sawell, S.E., Vehlow, J., Sloop, H.A. van der, Hartlén, J., 1997. Municipal Solid Waste Incinerator Residues. Elsevier.
- Chimenos, J.M., Fernández, A.I., Nadal, R., Espiell, F., 2000. Short-term Natural Weathering of MSWI Bottom Ash. J. Hazard. Mater. 79, 287–299. doi:10.1016/S0304-3894(00)00270-3
- Chimenos, J.M., Segarra, M., Fernández, M.A., Espiell, F., 1999. Characterization of The Bottom Ash in Municipal Solid Waste Incinerator. J. Hazard. Mater. 64, 211–222. doi:10.1016/S0304-3894(98)00246-5
- Eusden, J.D., Eighmy, T.T., Hockert, K., Holland, E., Marsella, K., 1999. Petrogenesis of Municipal Solid Waste Combustion Bottom Ash. Appl. Geochem. 14, 1073–1091. doi:10.1016/S0883-2927(99)00005-0
- Florea, M.V.A., Brouwers, H.J.H., 2012. Chloride Binding Related to Hydration Products: Part I: Ordinary Portland Cement. Cem. Concr. Res. 42, 282–290. doi:10.1016/j.cemconres. 2011.09.016
- Heuss-Aßbichler, S., Magel, G., Fehr, K.T., 2010. Abiotic Hydrogen Production in Fresh and Altered MSWI-Residues: Texture and Microstructure Investigation. Waste Manag 30, 1871–1880. doi:10.1016/j.wasman.2010.02.015
- Inkaew, K., Saffarzadeh, A., Shimaoka, T., 2015. Impacts of Water Quenching on MSWI Bottom ash Characterization, in: The 2nd Symposium of Asian Regional Branch of International Waste Working Group. Presented at the IWWG-ARB 2015, Institute of waste treatment and reclamation (IWTR), College of Environmental Science and Engineering, Shanghai, China, pp. 87–100.

- Ito, R., Dodbiba, G., Fujita, T., Ahn, J.W., 2008. Removal of Insoluble Chloride from Bottom Ash for Recycling. *Waste Manag.* 28, 1317–1323. doi:10.1016/j.wasman.2007.05.015
- Li, M., Xiang, J., Hu, S., Sun, L.-S., Su, S., Li, P.-S., Sun, X.-X., 2004. Characterization of Solid Residues from Municipal Solid Waste Incinerator. *Fuel* 83, 1397–1405. doi:10.1016/j.fuel.2004.01.005
- Meima, J.A., Comans, R.N.J., 1997. Overview of Geochemical Processes Controlling Leaching Characteristics of MSWI Bottom ash, in: J.J.J.M. Goumans, G.J.S. and H.A. van der S. (Ed.), *Studies in Environmental Science, Waste Materials in Construction Putting Theory into Practice Proceedings of the International Conference on the Environment and Technical Implications of Construction with Alternative Materials.* Elsevier, pp. 447–457.
- Ministry of the Environment, 2013. Waste Treatment in Japan. URL http://www.env.go.jp/.recycle/waste_tech/ippan/h25/data/disposal.pdf (accessed 10.5.15).
- Phongphiphat, A., Ryu, C., Finney, K.N., Sharifi, V.N., Swithenbank, J., 2011. Ash Deposit Characterisation in a Large-Scale Municipal Waste-to-Energy Incineration Plant. *J. Hazard. Mater.* 186, 218–226. doi:10.1016/j.jhazmat.2010.10.095
- Rendek, E., Ducom, G., Germain, P., 2007. Influence of Waste Input and Combustion Technology on MSWI Bottom Ash Quality. *Waste Manag., Wascon 2006 6th International Conference: Developments in the re-use of mineral waste* 27, 1403–1407. doi:10.1016/j.wasman.2007.03.016
- Sabbas, T., Poletini, A., Pomi, R., Astrup, T., Hjelmar, O., Mostbauer, P., Cappai, G., Magel, G., Salhofer, S., Speiser, C., Heuss-Assbichler, S., Klein, R., Lechner, P., 2003. Management of Municipal Solid Waste Incineration Residues. *Waste Manag.* 23, 61–88. doi:10.1016/S0956-053X(02)00161-7
- Saffarzadeh, A., Shimaoka, T., Motomura, Y., Watanabe, K., 2006. Chemical and Mineralogical Evaluation of Slag Products Derived from the Pyrolysis/Melting Treatment of MSW. *Waste Manag.* 26, 1443–1452. doi:10.1016/j.wasman.2005.12.005
- Saffarzadeh, A., Shimaoka, T., Wei, Y., Gardner, K.H., Musselman, C.N., 2011. Impacts of Natural Weathering on the Transformation/Neof ormation Processes in Landfilled MSWI bottom Ash: A Geoenvironmental Perspective. *Waste Manag.* 31, 2440–2454. doi:10.1016/j.wasman.2011.07.017
- Speiser, C., Baumann, T., Niessner, R., 2000. Morphological and Chemical Characterization of Calcium-Hydrate Phases Formed in Alteration Processes of Deposited Municipal Solid Waste Incinerator Bottom Ash. *Environ. Sci. Technol.* 34, 5030–5037. doi:10.1021/es990739c
- Van Gerven, T., Van Keer, E., Arickx, S., Jaspers, M., Wauters, G., Vandecasteele, C., 2005. Carbonation of MSWI-Bottom Ash to Decrease Heavy Metal Leaching, in View of Recycling. *Waste Manag.* 25, 291–300. doi:10.1016/j.wasman.2004.07.008
- Vieille, L., Rousselot, I., Leroux, F., Besse, J.-P., Taviot-Guého, C., 2003. Hydrocalumite and Its Polymer Derivatives. 1. Reversible Thermal Behavior of Friedel’s Salt: A Direct Observation by Means of High-Temperature in Situ Powder X-ray Diffraction. *Chem. Mater.* 15, 4361–4368. doi:10.1021/cm031069j

- Wei, Y., Shimaoka, T., Saffarzadeh, A., Takahashi, F., 2011. Mineralogical Characterization of Municipal Solid Waste Incineration Bottom Ash with an Emphasis on Heavy Metal-Bearing Phases. *J. Hazard. Mater.* 187, 534–543. doi:10.1016/j.jhazmat.2011.01.070
- Yang, S., Saffarzadeh, A., Shimaoka, T., Kawano, T., 2014. Existence of Cl in Municipal Solid Waste Incineration Bottom Ash and Dechlorination Effect of Thermal Treatment. *J. Hazard. Mater.* 267, 214–220. doi:10.1016/j.jhazmat.2013.12.045
- Zevenbergen, C., Wood, T.V., Bradley, J. p., Van Der Broeck, P. f. c. w., Orbons, A. j., Van Reeuwijk, L. p., 1994. Morphological and Chemical Properties of MSWI Bottom Ash with Respect to the Glassy Constituents. *Hazard. Waste Hazard. Mater.* 11, 371–383. doi:10.1089/hwm.1994.11.371

CHAPTER 6

CONCLUSIONS

CHAPTER 6

CONCLUSIONS

6.1 CONCLUSIONS

The incineration has been widely accepted as one of the robust technologies for handling municipal solid waste. This technology not only provides the hygienic condition to waste but also reduces a large volume of waste by converting MSW into ashes. As the major by-product from incineration, it is disposed at the landfill commonly. From the past decades, several attempts have been made to characterize the bottom ash and used as a new resource for the exclusive purpose, however, only a few amount are used due to its characteristic that heterogeneous, contains heavy metal and chloride, and remains active under exposure condition. Since the weathering of the bottom ash is initially activated by quenching, this study is attempted to explore the influence of the quenching process on the characterization of the bottom ash and the mechanism behind the formation of the quench product on the surface of bottom ash. To achieve the objectives, two approaches have been used; the investigation on representative samples obtained from the incineration plants and the lab-scale quenching experiment.

In this study, the physical, chemical and mineralogical characteristic of the materials involved in quenching system, including grate sifting, unquenched bottom ash and quenched bottom ash were investigated. The difference between the characteristics of the unquenched bottom ash and the quenched bottom ash were evaluated as the influence of quenching process. The microstructure and mineralogy of the quench product is then investigated as the major influence caused by quenching. Finally, the lab-scale quenching experiments were done to explore the phenomena during quenching, and the mechanical model of the formation of the quench product was proposed.

The bottom ash is a mixture of the grate sifting and the unquenched bottom ash (grate ash). The investigation indicated that characteristic of each were heterogeneous. The physical characteristic of the grate sifting was slightly similar to the unquenched bottom ash; however, it was dominant with the fraction less than 1 mm which accounted to about 60-70 % of the total fraction. The morphology of the grate sifting and the

unquenched bottom ash showed the characteristic of the melt product, which consisted mainly of vitreous phases in which embedded crystalline and refractory materials. In contrast, the quenched bottom ash was prevalent with the external layer which later identified as the quench product, and it was dominant in particle larger than 1 mm. The chemical composition of the grate sifting, the unquenched bottom ash and the quenched bottom ash was mainly composed of CaO, SiO₂, Al₂O₃, and Fe₂O₃ in the total range about 70-80 % of all compositions. However, the grate sifting and the unquenched bottom ash had lesser moisture content, higher pH (over 12), and higher concentrations of CaO, P₂O₅, MgO, Na₂O, K₂O, and Cl, when compared to quenched bottom ash. On the other hand, the quenched bottom ash was dominated by pH lower than 12, higher moisture content, higher LOI, and higher concentrations of Al₂O₃, Fe₂O₃, Ba, Pb, and As than grate sifting and unquenched bottom ash. The results guided that grate sifting might be the additional source of Al, Fe, Ba, Pb, and As in the quenched bottom ash. In the view of mineral composition, it was found that all samples were exhibited mainly with calcite, quartz, and gehlenite. The mineral that could be found only in the unquenched bottom ash and the grate sifting was lime, while the mineral that could be found only in the quenched bottom ash was Friedel's salt.

The comparative investigation on particle size distribution, morphological observations, specific surface area analyses, pH analyses, mineral and chemical composition analyses between the unquenched and the freshly quenched bottom ash lead to the fact that water quenching obviously impacts on the bottom ash product. The results showed that after quenching the particle size distribution of the bottom ash changed, and the size of particles with a diameter larger than 0.425 mm became bigger by coating of finer particles. As a consequence, specific surface area of bottom ash product increased up to seven times. During quenching several chemical reactions occurred and led to changing of bottom ash pH, chemical and mineral composition. The predominant reactions were dissolution and precipitation of various phases that led to decreasing of pH value and the formation of hydrate phases. It is found that water quenching process enhances the formation of portlandite, Friedel's salt and hydrocalumite. These hydrate phases distributed mainly on the quench product on the surface of quenched bottom ash particle.

Microstructure characterization revealed the quench product commonly distributes on the surface of the melt products, particularly at the concave area of particle .

The thickness of the quench product is variable from 10 μm to 1 mm. The quench product was identified as the mixture of tiny pieces of metal and glassy melt particles, fragment or cluster of minerals, organic matter and those remain after combustion on the matrix of amorphous and Ca rich hydrate phases (C-S-H phases). The most dominant hydrate microcrystals in the quench product were needle-like or platy microcrystals that usually formed nests rather than individual distributed throughout the mixture. The investigation data led that the existence of quench product highly correlated the presence of insoluble chlorides (Friedel's salt/hydrocalumite) in the quenched bottom ash.

Via the simulated quenching experiment, the same characteristic of the quench product as the reference samples that obtain from the large-scale quenching were achieved. Regarding to the results, it is confirmed that the quenching process produced new hydrate crystalline phases, particularly Friedel's salt and hydrocalumite, which is not found in the original unquenched bottom ash. The factors that controlled the formation of the quenched bottom ash included fine bottom ash particles (0.125-0.425 mm) moisture/quenching water, and physiochemical changes, such as de-watering, precipitation of hydrate phases, hardening, and cementation/carbonation. Based on the experimental observation, a conceptual model of the formation of the quench product and agglomeration of the quenched bottom ash was proposed that the chemical changes in the bottom ash caused by quenching can be divided into two stages. The first stage includes dissolution of major soluble salts from the bottom ash via diffusion, precipitation of hydrate phases and oxidation of both ferrous and non-ferrous metals. These chemical alterations convert the ash particles that smaller than 0.425 mm to the quench product. In the second stage, later the quench product is agglomerated or attached to the bigger particle (the melt product) via water-bridging, carbonation in the pore water, and hardening of cement phases.

6.2 OUTLOOK AND RECOMMENDATION

Water quenching is a key process that influences the characteristics of quenched bottom ash. To manage bottom ash effectively, the stability of the ash chemical and physical properties must be maintained (Sabbas et al., 2003; Tang et al., 2015). In this research work, valuable information on the phenomena that occur during bottom ash

quenching and the formation of the quench product was obtained. The quenched bottom ash was drastically altered through quenching, particularly during the formation of the quench product, which mainly consisted of Ca-rich hydrate phases with the accumulation of insoluble chloride. Since the hydration product causes volumetric expansion of the ash during aging (Bayuseno and Schmahl, 2010), and chloride content causes corrosion in the reinforced concrete (Ito et al., 2008), using the freshly quenched bottom ash in construction may require more attention or additional treatment.

In this study, the influence of the quenching process on metal absorption/leaching behavior was not included because it has already been reported (Marchese and Genon, 2011). However, different washing ratios and residence times will lead to the release of different metals, which may directly affect bottom ash mineralogy and quench layer formation. Therefore, further experiments should investigate different quenching times and longer residence times between hydration product and quench phase formation. Additionally, the application of geochemical modeling to quenching process observations may help improve the understanding about the characteristics of the ash, particularly regarding leaching of salt and heavy metals.

Since the quench product originates from fine ash residues (<0.425 mm), removing these fractions prior to quenching may help to reduce insoluble salt formation and Cl content in bottom ash by preventing the formation of hydration product. The proposed option may include the use of a dry discharger or the separation of the fine fraction from the ash prior to quenching; however, these techniques might raise the costs of the system. In addition, because hydration products, such as Friedel's salt and hydrocalumite, are unstable Ca-Al compounds in bottom ash, they readily change and release chloride through carbonation reactions with CO₂. The idea of using an ash discharger as a reactor for enhancing bottom ash utilization via carbonation or hydrogen oxidation may also be promising; even so, further research is required.

REFERENCES

- Bayuseno, A.P., Schmahl, W.W., 2010. Understanding the Chemical and Mineralogical Properties of the Inorganic Portion of MSWI bottom ash. *Waste Manag.* 30, 1509–1520. doi:10.1016/j.wasman.2010.03.010
- Ito, R., Dodbiba, G., Fujita, T., Ahn, J.W., 2008. Removal of Insoluble Chloride from Bottom Ash for Recycling. *Waste Manag.* 28, 1317–1323. doi:10.1016/j.wasman.2007.05.015
- Marchese, F., Genon, G., 2011. Effect of Leaching Behavior by Quenching of Bottom Ash from MSW Incineration. *Waste Manag. Res. J. Int. Solid Wastes Public Clean. Assoc. ISWA* 29, 39–47. doi:10.1177/0734242X10387848
- Sabbas, T., Poletini, A., Pomi, R., Astrup, T., Hjelmar, O., Mostbauer, P., Cappai, G., Magel, G., Salhofer, S., Speiser, C., Heuss-Assbichler, S., Klein, R., Lechner, P., 2003. Management of Municipal Solid Waste Incineration Residues. *Waste Manag.* 23, 61–88. doi:10.1016/S0956-053X(02)00161-7
- Tang, P., Florea, M.V.A., Spiesz, P., Brouwers, H.J.H., 2015. Characteristics and Application Potential of Municipal Solid Waste Incineration (MSWI) Bottom Ashes from Two Waste-to-Energy Plants. *Constr. Build. Mater.* 83, 77–94. doi:10.1016/j.conbuildmat.2015.02.033